CHEMISTRY OF RUTHENIUM DERIVATIVES OF THE

2-DIPHENYLPHOSPHINOQUINOLINE LIGAND

by

WERNER KARL SCHAUERTE B.Sc.(Hons), (Rhodes)

A thesis submitted in partial fulfillment of the requirements for the degree of Master of Science in the Faculty of Science, University of Natal, Pietermaritzburg

Department of Chemistry

University of Natal

Pietermaritzburg

January 1993

DECLARATION

I hereby certify that this research is the result of my own investigation which has not already been accepted in substance for any degree and is not being submitted in candidature for any other degree.
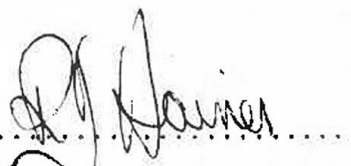
Signed: ....

W K SCHAUERTE

I hereby certify that this statement is correct.

Signed: ....

PROFESSOR R J HAINES

(Supervisor)

Signed: ....

PROFESSOR J S FIELD

(Co-supervisor)

Department of Chemistry

University of Natal

Pietermaritzburg

January 1993

ACKNOWLEDGEMENTS

LIST OF ABBREVIATIONS AND SYMBOLS

ampy	deprotonated form of 2-amino-6-methylpyridine
Analar	analytical grade reagent
apy	deprotonated form of 2-aminopyridine
AsPPh$_3$	triphenylarsine
bipy	2,2'-bipyridine
cod	1,5-cyclooctadiene
CO$_2$Me	methoxy carbonyl
CP	chemically pure
dppe	bis(diphenylphosphino)ethane
dppm	bis(diphenylphosphino)methane
{^{1}H}	proton noise decoupled
Hampy	2-amino-6-methylpyridine
Hapy	2-aminopyridine
HBF$_4 \cdot$OEt$_2$	tetrafluoroboric acid - diethyl ether complex
HSquin	quinoline-2-thiol
HSpy	pyridine-2-thiol
M$^+$	molecular ion
MeO	methoxy
Me$_3$NO$\cdot$H$_2$O	trimethylamine-N-oxide
NaPh$_2$CO	sodium benzophenoneketyl
NCMe	acetonitrile
NEt$_3$	trimethylamine
NMR	nuclear magnetic resonance
OPh$_2$Pquin	oxidized form of 2-diphenylphosphinoquinoline
Ph$_2$CO$^-$	benzophenoneketyl radical anion
PMe$_3$	trimethylphosphine
PPh$_3$	triphenylphosphine

PPh_2H	diphenylphosphine
Ph_2Ppy	2-diphenylphosphinopyridine
Ph_2Pquin	2-diphenylphosphinoquinoline
ppm	parts per million
[PPN]	bis(triphenylphosphine)imminium cation
quin	quinoline
Spy	deprotonated form of pyridine-2-thiol
Squin	deprotonated form of quinoline-2-thiol
THF	tetrahydrofuran
TLC	thin layer chromatography

SUMMARY

Chapter One serves as an introduction to the work described in this thesis. Methods which may be employed to achieve a selective, stoichiometric and efficient substitution of the carbonyl groups in $[Ru_3(CO)_{12}]$ are first reviewed. The reactions of the 2-diphenylphosphinopyridine (Ph_2Ppy), 2-aminopyridine (Hapy) and 2-thiolpyridine (Hspy) ligands with $[Ru_3(CO)_{12}]$ are surveyed, these ligands being closely related to the 2-diphenylphosphinoquinoline (Ph_2Pquin) ligand whose reactions with $[Ru_3(CO)_{12}]$ are described in Chapter Three. The reactions of substituted quinolines in general with $[Ru_3(CO)_{12}]$ and with other clusters are also discussed. Finally, conclusions are drawn as to how the Ph_2Pquin ligand might be expected to react with $[Ru_3(CO)_{12}]$.

Chapter Two describes the synthesis and characterization of the novel 2-diphenylphosphosphinoquinoline (Ph_2Pquin) ligand. The ligand is prepared from the reaction of 2-chloroquinoline with lithium diphenylphosphide and isolated as a cream-coloured air-stable solid. The $^{31}P\{^1H\}$ NMR spectrum of the ligand, recorded in $CDCl_3$, exhibits a sharp singlet at -2.82 ppm relative to H_3PO_4.

Chapter Three begins with a description of the substitution reactions of $[Ru_3(CO)_{12}]$ with the 2-diphenylphosphinoquinoline ligand. The mono-, di- and tetrasubstituted products $[Ru_3(\eta^1-Ph_2Pquin)(CO)_{11}]$ (2), $[Ru_3(\eta^1-Ph_2Pquin)_2(CO)_{10}]$ (4) and $[Ru_3(\mu-\eta^2-Ph_2Pquin)_2(CO)_8]$ (5) may all be obtained by suitable choice of reaction conditions. Heating of compound (2) results in the dephenylation of the Ph_2Pquin ligand to afford $[Ru_3\{\mu-\eta^2-C(O)(C_6H_5)\}\{\mu_3-\eta^2-P(C_6H_5)(C_9H_6N)\}(CO)_9]$ (3) whose structure was determined by X-ray crystallography. The $P(C_6H_5)(C_9H_6N)$ fragment in (3) caps the triangle of ruthenium atoms allowing the cluster to undergo

a variety of transformations without fragmentation. Removal of the bridging acyl group is achieved by addition of [PPN][BH$_4$] to afford [PPN][Ru$_3${μ_3-η^2-P(C$_6$H$_5$)(C$_9$H$_6$N)}(CO)$_9$] (8) or by addition of molecular hydrogen with gentle heating to afford [Ru$_3$(μ-H){μ_3-η^2-P(C$_6$H$_5$)(C$_9$H$_6$N)}-(CO)$_9$] (7) the structure of the latter being confirmed X-ray crystallographically. Substitution of a carbonyl group in (3) by a second mole equivalent of Ph$_2$Pquin proceeds smoothly to afford [Ru$_3${μ-η^2-C(O)-(C$_6$H$_5$)}{μ_3-η^2-P(C$_6$H$_5$)(C$_9$H$_6$N)}(η^1-Ph$_2$Pquin)(CO)$_8$] (6); deacylation of the latter by addition of molecular hydrogen affords [Ru$_3$(μ-H){μ_3-η^2-P(C$_6$H$_5$)(C$_9$H$_6$N)}(Ph$_2$Pquin)(CO)$_8$] (9) which can also be obtained by addition of Ph$_2$Pquin to cluster (7). Of most significance, is the substitution of a carbonyl group in (3) by diphenylphosphine (PPh$_2$H). The hydrogen bound to the phosphorus atom of this ligand readily transfers to the bridging acyl group, the end product of this reaction being [Ru$_3${μ_3-η^2-P(C$_6$H$_5$)(C$_9$H$_6$N)}(μ-PPh$_2$)(μ-CO)$_2$(CO)$_6$] (11) the triangular face of which is capped by the P(C$_6$H$_5$)(C$_9$H$_6$N) fragment and one edge of which is further bridged by the diphenylphosphido group as confirmed X-ray crystallographically. Interestingly, cluster (11) adds carbon monoxide with a concomitant opening of a metal-metal bond to afford [Ru$_3${μ_3-η^2-P(C$_6$H$_5$)(C$_9$H$_6$N)}(μ-PPh$_2$)(CO)$_9$] (12). The reaction is easily reversed by reduction of the CO pressure and thus provides a rare example of the facile opening and closing of a metal-metal bond in a cluster molecule without cluster fragmentation. Chapter Three concludes with a summary of the reactions described in the chapter.

CONTENTS

CHAPTER ONE

SUBSTITUTION REACTIONS OF TRIRUTHENIUM DODECACARBONYL

1.1 INTRODUCTION

The research described in this thesis is mainly concerned with the synthesis of the hitherto unreported 2-diphenylphosphinoquinoline ligand (Ph$_2$Pquin) and its substitution reactions with [Ru$_3$(CO)$_{12}$]. This chapter serves as an introduction to that work.
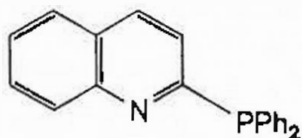
Figure 1.1: The Ph$_2$Pquin Ligand   Figure 1.2: [Ru$_3$(CO)$_{12}$]
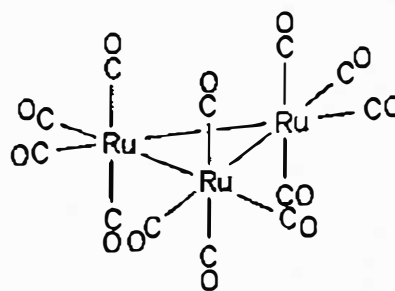
In Section 1.2 the problem of achieving a selective, stoichiometric and efficient substitution of carbonyl group(s) in [Ru$_3$(CO)$_{12}$] is noted, and the various methods employed to overcome this problem are described. Sections 1.3, 1.4 and 1.5 review reactions with [Ru$_3$(CO)$_{12}$] of the 2-diphenylphosphinopyridine (Ph$_2$Ppy), 2-aminopyridine (Hapy) and 2-thiol-pyridine (HSpy) ligands respectively; all three ligands are closely related to the Ph$_2$Pquin ligand in that they contain two donor atoms (P, N or S) linked by the carbon atom in the 2-position of a pyridine ring.
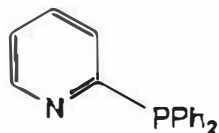
Figure 1.3: The Ph$_2$Ppy Ligand
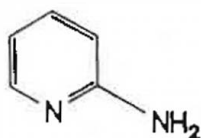
Figure 1.4: The Hapy Ligand   Figure 1.5: The HSpy Ligand
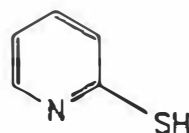
Section 1.6 summarizes the limited information available on the reactions of substituted quinolines in general with [Ru$_3$(CO)$_{12}$] and other clusters. Finally in Section 1.7 conclusions are drawn from the previous discussion of the co-ordination chemistry of the Ph$_2$Ppy, Hapy and HSpy ligands as to how the 2-diphenylphosphinoquinoline ligand itself might be expected to react with [Ru$_3$(CO)$_{12}$].

1.2 THERMAL AND CATALYTIC METHODS FOR THE SUBSTITUTION OF CARBONYL GROUPS IN [Ru$_3$(CO)$_{12}$]

By the early 1980's many mononuclear tertiary phosphine and arsine

complexes of ruthenium were known. However, the chemistry of simple substituted derivatives of $[Ru_3(CO)_{12}]$ such as $[Ru_3(CO)_{12-n}L_n]$ (with, for example, L = Group VB donor ligand) was very limited.[1] The major reason for this difference was the reactivity of the parent carbonyl cluster. The elevated temperatures used in the reactions of the Group VB donor ligands with $[Ru_3(CO)_{12}]$ lead to polysubstitution, ligand transformation after complexation, or both. Thus thermal reactions of $[Ru_3(CO)_{12}]$ with tertiary phosphines afford the well known trisubstituted complexes $[Ru_3(CO)_9(PR_3)_3]$ with mono- and disubstituted products being obtained only under special conditions such as under a carbon monoxide atmosphere or by use of very bulky phosphine ligands.

What was required was a method of selectively and stoichiometrically substituting the CO ligands of the $[Ru_3(CO)_{12}]$ cluster. Bruce *et al.* had noted the enhanced reactivity towards nucleophiles of organometallic radical anions, specifically those obtained from binuclear cobalt carbonyl derivatives.[2] They then showed that the radical anion generated from $[Ru_3(CO)_{12}]$ and sodium benzophenoneketyl $(NaPh_2CO)$, which they presumed to be $[Ru_3(CO)_{12}]^{\overline{\cdot}}$, reacted smoothly with Group VB and isocyanide donor ligands to give substituted products of the desired stoichiometry.[3]

For example, reaction of $[Ru_3(CO)_{12}]$ with triphenylphosphine using the benzophenoneketyl radical anion $(Ph_2CO^{\overline{\cdot}})$ as catalyst affords mono-, di- and trisubstituted products selectively and in high yield, depending only on reagent ratios. Similar results were obtained from the reaction of triphenylarsine with $[Ru_3(CO)_{12}]$; thus, while reactions in refluxing hexane yield only the disubstituted complex $[Ru_3(CO)_{10}(AsPh_3)_2]$,[4,5] the radical anion initiated reaction allows the selective formation of mono- or disubstituted products. Radical anion initiated reactions of

[Ru$_3$(CO)$_{12}$] with bis(diphenylphosphino)methane (dppm) selectively afford [Ru$_3$(μ-dppm)(CO)$_{10}$] or [Ru$_3$(μ-dppm)$_2$(CO)$_8$], the equivalent thermal reactions on the other hand affording only the latter complex,[6] or a mixture of the two,[7] with the phosphinidine complex [Ru$_3$(μ_3-PPh$_3$)(μ-CHP-Ph$_2$)(CO)$_7$(dppm)] (formed by the oxidative addition of the ligand to the Ru$_3$ cluster) also forming as an impurity. Indeed, the formation of the phosphinidine complex is completely avoided in the radical initiated reaction.

Bruce *et al.* have proposed an electron-transfer catalyzed mechanism[3,8] for these radical ion initiated reactions by comparison with other organometallic[2,9,10] and organic[11] systems. The following equations outline the proposed mechanism:

$$[Ru_3(CO)_{12}] + Ph_2CO^{\overline{\cdot}} \longrightarrow [Ru_3(CO)_{12}]^{\overline{\cdot}} + Ph_2CO \qquad \text{Equation 1.1}$$

$$[Ru_3(CO)_{12}]^{\overline{\cdot}} + L \longrightarrow [Ru_3(CO)_{11}L]^{\overline{\cdot}} + CO \qquad \text{Equation 1.2}$$

$$[Ru_3(CO)_{11}L]^{\overline{\cdot}} + [Ru_3(CO)_{12}] \longrightarrow [Ru_3(CO)_{11}L] + [Ru_3(CO)_{12}]^{\overline{\cdot}} \qquad \text{Equation 1.3}$$
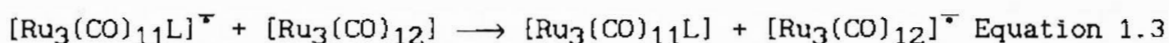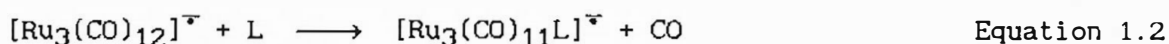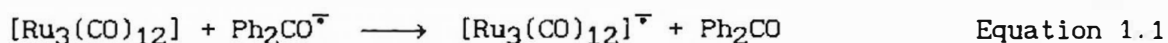
The mechanism relies on the radical anion [Ru$_3$(CO)$_{12}$]$^{\overline{\cdot}}$ being more susceptible to nucleophilic attack than the parent cluster. This is probably due to the extra electron entering a Ru–Ru antibonding orbital thereby facilitating cleavage of a Ru–Ru bond and so generating a labile seventeen-electron metal centre. Following a brief electrochemical study of [Ru$_3$(CO)$_{12}$] which showed that the radical anion [Ru$_3$(CO)$_{12}$]$^{\overline{\cdot}}$ has a very short lifetime,[12] Robinson *et al.*[10] suggested that the substitution did not involve an electron-transfer catalyzed mechanism but occurred by some other route. However, no alternative mechanism was proposed.

It should be noted that although mono-, di- and trisubstitution of the carbonyl groups in $[Ru_3(CO)_{12}]$ can be brought about by addition of catalytic amounts of $Ph_2CO^{\bullet}$, efficiencies decrease with higher substitution. This is expected since reduction of the cluster to the corresponding labile radical anion is rendered more difficult when a CO is replaced by a poorer Π-acceptor ligand, for example by a PR_3 (R = alkyl or aryl group) ligand which is, in fact, strongly electron donating. Steric and statistical factors also tend to discourage higher substitution.

Having isolated a number of selectively substituted clusters of the type $[Ru_3(CO)_{12-n}L_n]$ (L = Group VB donor ligand, n = 1 - 4), Bruce et al.[7] were able to relate certain features of the $\nu(CO)$ absorptions in the infrared spectra of these clusters to the degree of substitution. For the monosubstituted complexes there are three or four strong absorptions between 1985 and 2055 cm^{-1} and a medium to weak absorption between 2090 and 2100 cm^{-1}. The frequencies of the absorptions decrease as the basicity of the ligand increases. For n = 2 there is again a high frequency absorption between 2070 and 2090 cm^{-1} but with two bands between 1965 and 2050 cm^{-1}; the profiles of the latter bands indicate they may contain three or more absorptions. As expected, there is a general decrease in frequency on introduction of a second ligand. For trisubstituted complexes the trends are less clear with the spectra being less well resolved. The major bands are as for n = 2 with the high frequency band occurring between 2050 and 2085 cm^{-1}. For n = 4, the overall pattern is shifted to the lower frequency by some 20 cm^{-1} relative to the trisubstituted complexes. This reflects the movement of electron density from the phosphorus ligands via the metal atom orbitals into the CO antibonding orbitals. The high frequency band is absent in the n = 4 case. Indeed, the most useful feature of these infrared

spectra is the high frequency band whose appearance changes sufficiently to allow for monitoring of the growth and decay of a particular complex, especially for the mono- or disubstituted species.

Catalytic substitution reactions of $[Ru_3(CO)_{12}]$ are not limited to those initiated by radical anions. In their attempt to trace the stepwise transformation of $[Ru_3(CO)_{12}]$ into hydrido-halogen derivatives,[13] Kaesz and Lavigne[14] observed that the cluster reacts with bis(triphenylphosphine)imminium chloride [PPN][Cl] to afford [PPN][$Ru_3(\mu-Cl)(CO)_{10}$].

$[Ru_3(CO)_{12}]$ + [PPN][Cl] $\longrightarrow$ [PPN][$Ru_3(\mu-Cl)(CO)_{10}$] + 2CO   Equation 1.4
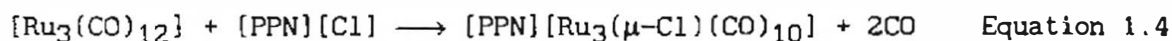
This reaction parallels the known reactions of $[PPN][NO_2]$[15] and [PPN]-[acetate][16] with $[Ru_3(CO)_{12}]$ which afford PPN salts of anions of the formula $[Ru_3(\mu-Nu)(CO)_{10}]^-$ (Nu = CH_3COO^- or NO_2). These reactions involve the replacement of CO under mild conditions[14] which suggests that labilization of a carbonyl ligand occurs in some intermediate such as $[Ru_3(\eta-(CO)-Nu)(CO)_{11}]^-$.[17,18] Such an intermediate was isolated for Nu = CH_3O^-.[19]

Kaesz and Lavigne[14] investigated the reaction shown in Equation 1.4 using various bis(triphenylphosphine)imminium salts and in the presence of various donor ligands. They discovered that [PPN]acetate is an excellent catalyst for the selective substitution of one carbonyl group in $[Ru_3(CO)_{12}]$ by PPh_3 with yields and rates matching those for radical anion initiated reactions.[7] Further work showed, however, that di- and trisubstitution are not catalyzed by this salt. Another example of a similar catalyst is [PPN][CN] which catalyzes instantaneous disubstitution of $[Ru_3(CO)_{12}]$ in the presence of excess PPh_3 and also promotes substitution by ligands of lower nucleophilicity (such as $AsPh_3$) as well

as by bridging ligands such as dppm.

Catalytic methods function by generating reactive intermediates *in situ* which react almost instantaneously with the ligands present. An alternative approach is to prepare stable intermediates which may be isolated and which allow for ligand displacement under mild conditions in subsequent reactions. Lewis *et al.*[20] first used such methods in the preparation of osmium decacarbonyl species but subsequently extended their work to ruthenium carbonyl clusters. For example, they showed that $[Ru_3(CO)_{12}]$ reacts with one or two mole equivalents of trimethyl-amine-N-oxide in the presence of acetonitrile to yield $[Ru_3(CO)_{11}(NCMe)]$ or $[Ru_3(CO)_{10}(NCMe)_2]$ respectively.[21] These complexes may be isolated by thin layer chromatography.

Reaction of the mono- and bis-acetonitrile species with PPh_3[21] selectively affords the mono- and disubstituted complexes as expected, the reaction simply involving the displacement of the labile aceto-nitrile groups by the incoming ligands. Also of interest are the reactions of $[Ru_3(CO)_{10}(NCMe)_2]$ with quinoline (quin) and 2,2'-bipyri-dine (bipy) which afford $[HRu_3(CO)_{10}(quin)]$ and $[Ru_3(CO)_{10}(bipy)]$ respectively.[22]

1.3 REACTIONS OF THE 2-DIPHENYLPHOSPHINOPYRIDINE LIGAND WITH $[Ru_3(CO)_{12}]$

In their efforts to introduce site specificity within the ruthenium triangle, Bonnet *et al.*[23] reacted 2-diphenylphosphinopyridine (Ph_2Ppy) (a potentially edge-bonding ligand) with $[Ru_3(CO)_{12}]$. By using sodium benzophenoneketyl[7] or $[PPN][CN]$[14] as catalysts it was possible to isolate the monosubstituted complex $[Ru_3(CO)_{11}(\eta^1-Ph_2Ppy)]$; here the

ligand bonds through just the phosphorus atom to one ruthenium atom. Thus the catalysts promote co-ordination of the Ph_2Ppy ligand to a ruthenium atom via the phosphorus atom leaving the nitrogen atom unco-ordinated. However, upon being passed through a silica gel column or being stirred in THF at 40°C for two hours, $[Ru_3(CO)_{11}(\eta^1-Ph_2Ppy)]$ converts to the acyl complex $[Ru_3\{\mu-\eta^2-C(O)(C_6H_5)\}\{\mu_3-\eta^2-(C_6H_5)(C_5H_4N)\}-(CO)_9]$. This is an unusual reaction and at first it was not clear why the intermediate $[Ru_3(CO)_{10}(\mu-\eta^2-Ph_2Ppy)]$ containing an edge-bridging Ph_2Ppy ligand could not be isolated. The authors proposed the following scheme by way of explanation:
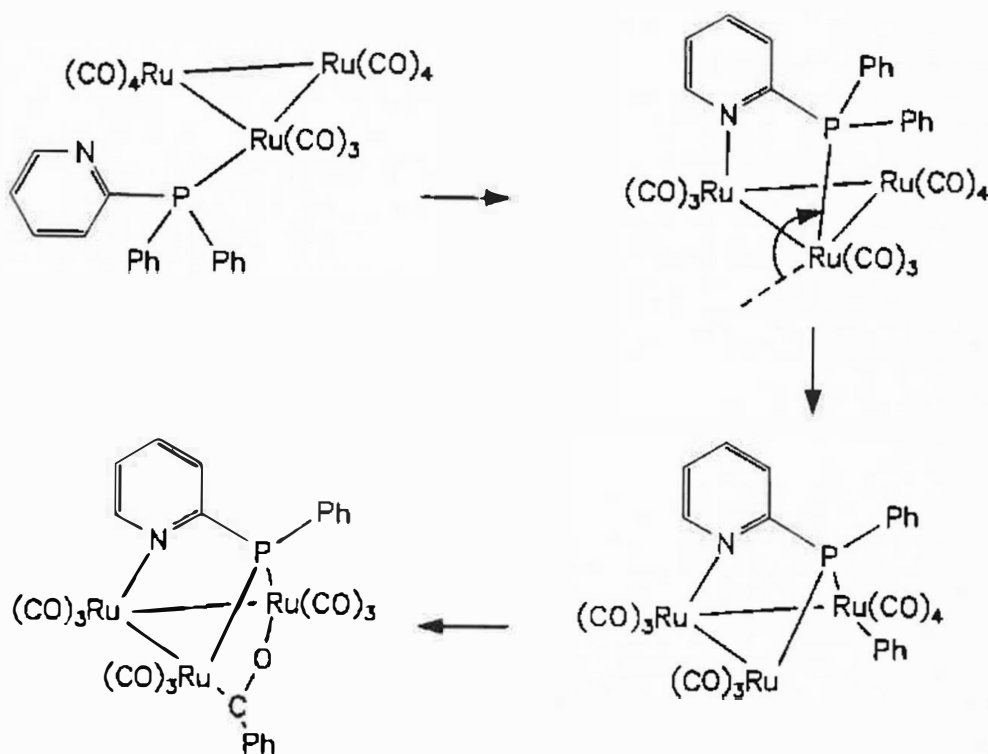
Scheme 1.1: Proposed pathway for generation of the acyl complex[23]

It was noted that nitrogen ligands show a tendency to co-ordinate at

axial sites in trimetal clusters.[24] In this case such co-ordination would force the phosphorus atom into an axial position (see Scheme 1.1). This is known to be highly favourable for P-C bond cleavage at two metal centres.[25] This accounts for the mild conditions under which cleaving occurs here (as opposed to other examples in the literature).[26] The formation of the acyl group probably proceeds via a σ-bond phenyl intermediate.[27-29] Reductive elimination of benzene would have been favoured if a hydride ligand had been available.[25,30] In this case, however, the phenyl group undergoes migratory CO insertion to yield the acyl group.[31,32]

The complex $[Ru_3\{\mu-\eta^2-C(O)(C_6H_5)\}\{\mu_3-\eta^2-P(C_6H_5)(C_5H_4N)\}(CO)_9]$ belongs to the family of reactive doubly-bridged species $[Ru_3\{\mu-X\}\{\mu-\eta^2-C(O)R\}-(CO)_{10}]$ (X = H or halogens; R = alkyl group).[33,34] The face capping group prevents fragmentation[34] of the cluster but does not limit its
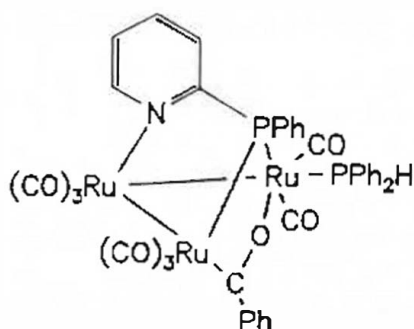
Figure 1.6: *cis* isomer of $[Ru_3\{\mu-\eta^2-C(O)(C_6H_5)\}\{\mu_3-\eta^2-P(C_6H_5)(C_5H_4N)\}(CO)_8(PPh_2H)]$ PPh_2H is *cis* relative to the acyl oxygen and *cis* relative to the bridgehead phosphorus
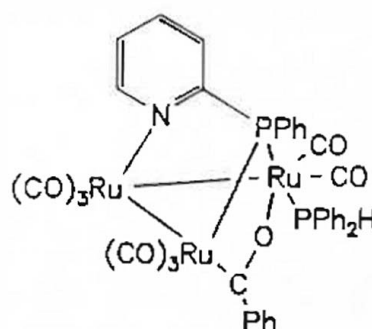
Figure 1.7: *trans* isomer of $[Ru_3\{\mu-\eta^2-C(O)(C_6H_5)\}\{\mu_3-\eta^2-P(C_6H_5)(C_5H_4N)\}(CO)_8(PPh_2H)]$ PPh_2H is *cis* relative to the acyl oxygen and *trans* relative to the bridgehead phosphorus

reactivity. For example, the cluster reacts with both PPh_2H and PPh_3 to afford complexes of the type $[Ru_3\{\mu-\eta^2-C(O)(C_6H_5)\}\{\mu_3-\eta^2-P(C_6H_5)-(C_5H_4N)\}(CO)_8(L)]$ (L = PPh_2H or PPh_3). The substitutions are stereo-specific with the incoming ligand always occupying a site which is *cis* to the oxygen of the acyl group (Figures 1.6, 1.7 and 1.8). The diphenylphosphine derivative exists in two isomeric forms, one in which the incoming phosphorus atom is *cis* relative to the bridged phosphorus atom and the other where it is *trans*. Spectroscopic data, in particular infrared data, for $[Ru_3\{\mu-\eta^2-C(O)(C_6H_5)\}\{\mu_3-\eta^2-P(C_6H_5)(C_5H_4N)\}(CO)_8(PPh_2H)]$ and $[Ru_3\{\mu-\eta^2-C(O)-(C_6H_5)\}\{\mu_3-\eta^2-P(C_6H_5)(C_5H_4N)\}(CO)_8(PPh_3)]$ indicate that the geometry of the parent complex has been retained.[23] The X-ray analysis of the triphenylphosphine derivative (see below) also shows that the bond angles and interatomic distances are very similar to those in the parent complex *i.e.* there is no significant disturbance to the cluster geometry even though the triphenylphosphine ligand is rather bulky.
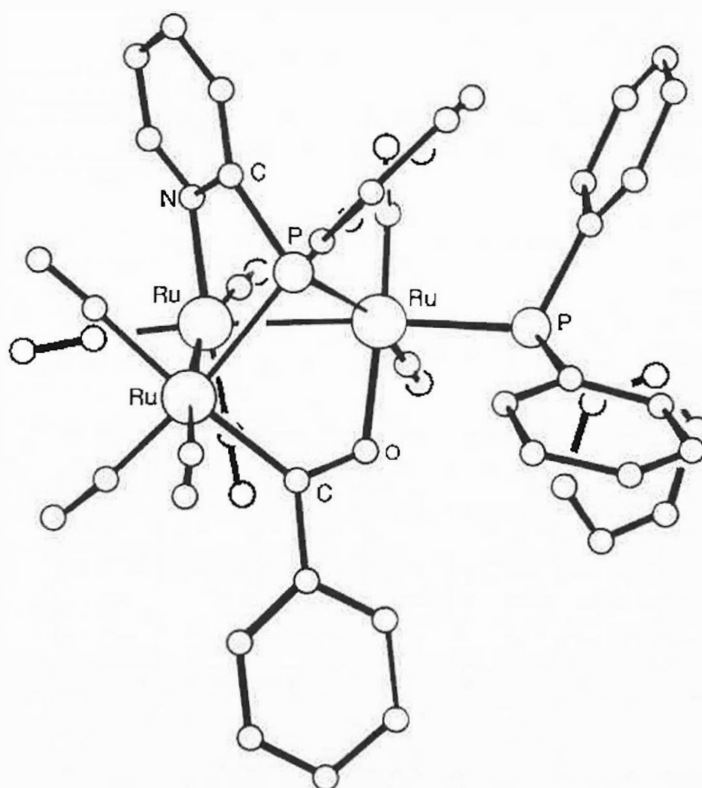
Figure 1.8

Structure of $[Ru_3\{\mu-\eta^2-C(O)(C_6H_5)\}\{\mu_3-\eta^2-P(C_6H_5)(C_5H_4N)\}(CO)_8(PPh_3)]$[23]

Bonnet *et al.* were interested in the catalytic activity of transition metal cluster compounds. The above complexes offered an opportunity to study the reductive elimination of organic molecules from metal clusters,[35] a step at which many clusters fail to complete their catalytic cycle.[36] This work is relevant to this kind of study since it shows how face capping ligands can stabilize triruthenium clusters, allowing further reaction to take place without cluster degradation. Bonnet *et al.*[35] found that reaction of the acyl complex $[Ru_3\{\mu-\eta^2-C(O)-(C_6H_5)\}\{\mu_3-\eta^2-P(C_6H_5)(C_5H_4N)\}(CO)_9]$ with H_2 yields the neutral hydrido cluster $[Ru_3(\mu-H)\{\mu_3-\eta^2-P(C_6H_5)(C_5H_4N)\}(CO)_9]$ and benzene as the sole organic product while reaction with $[PPN][BH_4]$ affords the anionic cluster $[Ru_3\{\mu_3-\eta^2-P(C_6H_5)(C_5H_4N)\}(CO)_9]^-$ with benzaldehyde as the sole
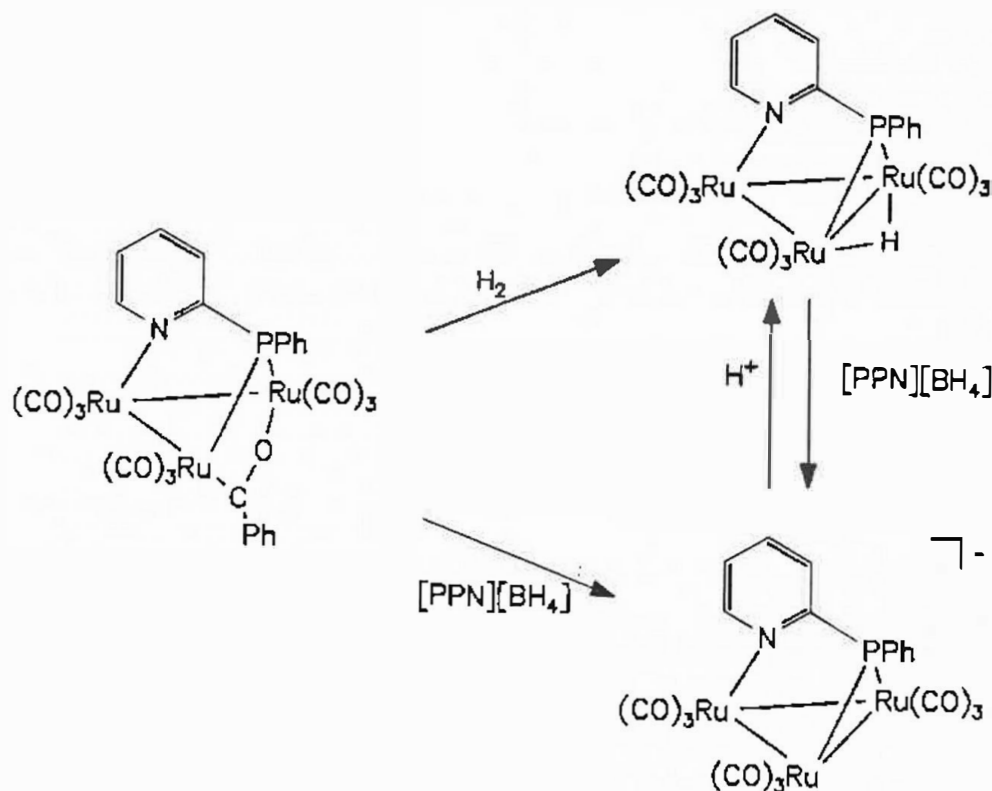
Scheme 1.2: Transformations on the Surface of the
$[Ru_3\{\mu-\eta^2-C(O)(C_6H_5)\}\{\mu_3-\eta^2-P(C_6H_5)(C_5H_4N)\}(CO)_9]$ Cluster[35]

organic product. The deprotonation of the hydride complex is readily effected to afford the anionic species which can be readily reconverted to the neutral hydrido cluster by addition of H^+. These reactions are summarized in Scheme 1.2.

The authors[35] proposed that the co-ordinated PPh_2H ligand in the substituted complex $[Ru_3\{\mu-\eta^2-C(O)(C_6H_5)\}\{\mu_3-\eta^2-P(C_6H_5)(C_5H_4N)\}(CO)_8-(PPh_2H)]$ could transfer a hydrogen atom to the acyl group via oxidative addition of the P-H bond to the metal, followed by reductive C-H coupling[37] to afford benzaldehyde and a new cluster complex. Indeed, thermolysis of the above complex generates a new complex $[Ru_3\{\mu_3-\eta^2-P(C_6H_5)(C_5H_4N)\}(\mu-PPh_2)(\mu-CO)_2(CO)_6]$ and benzaldehyde as expected. As the authors have noted, the intramolecular oxidative addition of a P-H bond to the metal involves the addition of two electrons, while reductive elimination of a C-H bond and deco-ordination of the acyl group involves the loss of four electrons. The resulting unsaturation is balanced by formation of a Ru-Ru bond.
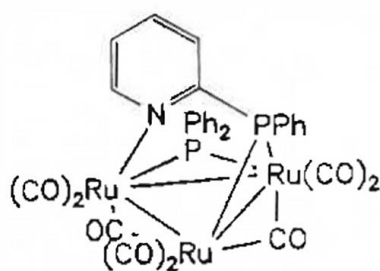
Figure 1.9: $[Ru_3\{\mu_3-\eta^2-P(C_6H_5)(C_5H_4N)\}(\mu-PPh_2)(\mu-CO)_2(CO)_6]$

The different circumstances under which the elimination of either benzene or benzaldehyde takes place were noted by the authors.[35] For benzene to be the organic product, dissociative loss of CO must precede

oxidative addition of hydrogen to the metal.[38] This must then be followed by de-insertion of the acyl group from the co-ordinatively unsaturated species.[39] On the other hand, nucleophilic attack of H^- on the cluster probably occurs via an associative path in which the unsaturated intermediate and migratory de-insertion are avoided. The H^- may well attack directly at the electropositive carbon of the acyl group.[35] It is thus clear that sequential attack of H^- (and H^+) on a cluster may well afford different organic products to those obtained from attack by molecular hydrogen even though the final cluster complexes may be identical.

The complex $[Ru_3\{\mu_3-\eta^2-P(C_6H_5)(C_5H_4N)\}(\mu-PPh_2)(\mu-CO)_2(CO)_6]$ shows a high degree of reactivity towards both CO and phosphine ligands. It reacts reversibly with CO to afford the open fifty-electron cluster $[Ru_3\{\mu_3-\eta^2-P(C_6H_5)(C_5H_4N)\}(\mu-PPh_2)(CO)_9]$. In contrast, reaction with PPh_3 results in simple substitution of one CO ligand to afford $[Ru_3\{\mu_3-\eta^2-P(C_6H_5)(C_5-$

The phenyl substituents on P^* have been omitted for clarity.

Figure 1.10

Structure of $[Ru_3\{\mu_3-\eta^2-P(C_6H_5)-(C_5H_4N)\}(\mu-PPh_2)(CO)_9]$[35]

Figure 1.11

Structure of $[Ru_3\{\mu_3-\eta^2-P(C_6H_5)(C_5-H_4N)\}(\mu-PPh_2)(\mu-CO)_2(CO)_5(PPh_3)]$[35]

$H_4N)\}(\mu\text{-}PPh_2)(\mu\text{-}CO)_2(CO)_5(PPh_3)]$. It is remarkable that the replacement of the CO ligand by PPh_3 causes no significant modification to the geometry of the cluster while addition of a CO ligand causes the bridging carbonyls to shift to terminal positions as well as the opening up of one Ru-Ru edges to a non-bonding distance.

When the incoming ligand is PPh_2H, the substituted derivative is not isolated but is rapidly converted into the complex $[Ru_3(\mu\text{-}H)\{\mu_3\text{-}\eta^2\text{-}P(C_6H_5)(C_5H_4N)\}(\mu\text{-}PPh_2)_2(CO)_6]$ which exists in two isomeric forms differing in the distribution of the $\mu\text{-}PPh_2$ and $\mu\text{-}H$ groups over the two available Ru-Ru edges.
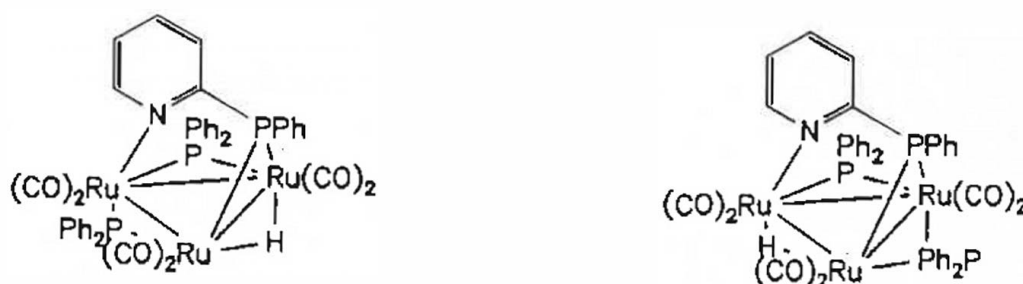
Figure 1.12

The two isomers of $[Ru_3(\mu\text{-}H)\{\mu_3\text{-}\eta^2\text{-}P(C_6H_5)(C_5H_4N)\}(\mu\text{-}PPh_2)_2(CO)_6]$

The high reactivity of $[Ru_3\{\mu_3\text{-}\eta^2\text{-}P(C_6H_5)(C_5H_4N)\}(\mu\text{-}PPh_2)(\mu\text{-}CO)_2(CO)_6]$ towards both CO and phosphines makes it a member of the family of electronically saturated metal clusters for which a facile and reversible metal-metal edge opening can be observed under mild conditions in the presence of nucleophiles.[40-45] Several features may account for its enhanced reactivity. Firstly, the presence of two bridging phosphido groups leads to a highly distorted geometry at each of the metal centres; in fact all three metal centres are heptaco-ordinated. Such a strained structure can only be stabilized in part through carbonyl

bridges and may be involved in a tautomeric equilibrium with an open species containing only terminal carbonyl ligands. This open species can be trapped by addition of CO or phosphine ligands.

The formation of a complex such as $[Ru_3\{\mu_3-\eta^2-P(C_6H_5)(C_5H_4N)\}(\mu-PPh_2)(\mu-CO)_2(CO)_5(PPh_3)]$ from the reaction of $[Ru_3\{\mu_3-\eta^2-P(C_6H_5)(C_5H_4N)\}-(\mu-PPh_2)(CO)_6]$ and PPh_3 may also involve an open adduct as an intermediate which then loses CO. It should also be noted that the co-ordination site of the PPh_3 ligand in $[Ru_3\{\mu_3-\eta^2-P(C_6H_5)(C_5H_4N)\}(\mu-PPh_2)(\mu-CO)_2(CO)_5(PPh_3)]$ is the one which is not associated with the open edge in $[Ru_3\{\mu_3-\eta^2-P(C_6H_5)(C_5H_4N)\}(\mu-PPh_2)(CO)_9]$ (see Figures 1.10 and 1.11).

1.4 REACTIONS OF 2-AMINOPYRIDINES WITH [Ru$_3$(CO)$_{12}$]

While it is well known that nitrogen may act as a donor atom to transition metals, Cabeza et al.[46] reported in 1990 that few studies had been made of substitution reactions of $[Ru_3(CO)_{12}]$ with N-donor ligands.[47-59] This is probably because high temperatures are required which may cause changes in the cluster framework[48-52] as well as degradation to metallated fragments.[51-57] They found that the reaction of $[Ru_3(CO)_{12}]$ with excess 2-aminopyridine (Hapy) affords $[Ru_3(\mu-H)(\mu_3-\eta^2-apy)(CO)_9]$ as
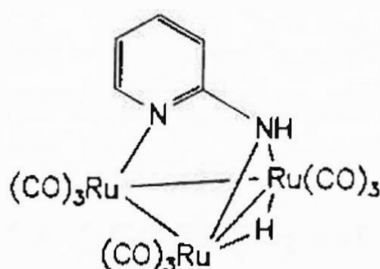
Figure 1.13: The $[Ru_3(\mu-H)(\mu_3-\eta^2-apy)(CO)_9]$ Cluster

the sole product, the intermediate [Ru$_3$(μ-H)(μ-η^2-apy)(CO)$_{10}$] not being detected.

Cabeza et al.[46] also carried out reactions with other aminopyridines to determine whether substituents on the pyridine ring or on the aminic nitrogen affect the reactions. They found that as long as the aminic nitrogen bears at least one hydrogen atom the resulting complexes are all similar to [Ru$_3$(μ-H)(μ_3-η^2-apy)(CO)$_9$] (see Figure 1.13). On the other hand, in the reaction of the 2-(dimethylamino)pyridine ligand with [Ru$_3$(CO)$_{12}$] the product contains the ligand in an edge-bridging, rather than a capping mode.

It has been shown[60,61] that the cluster [Ru$_3$(μ-H)(μ_3-η^2-ampy)(CO)$_9$], which is obtained from the reaction of 2-amino-6-methylpyridine (Hampy) with [Ru$_3$(CO)$_{12}$], is very stable towards fragmentation at high temperatures, probably because of the presence of the triply-bridging ampy ligand. Cabeza et al.[62] used this complex as a starting material to synthesize a series of phosphido-bridged clusters. For example, it reacts with one or two equivalents of PPh$_2$H to afford the substituted clusters [Ru$_3$(μ-H)(μ_3-η^2-ampy)(CO)$_8$(PPh$_2$H)] and [Ru$_3$(μ-H)(μ_3-η^2-ampy)-(CO)$_7$(PPh$_2$H)$_2$] respectively. The CO ligands replaced were those cis to both the NH fragment and the hydride. When a solution of [Ru$_3$(μ-H)(μ_3-η^2-ampy)(CO)$_8$(PPh$_2$H)] in THF is refluxed the complex [Ru$_3$(μ-H)(μ_3-η^2-ampy)(μ-PPh$_2$)(μ-CO)$_2$(CO)$_6$] is obtained while the thermal transformations of [Ru$_3$(μ-H)(μ_3-η^2-ampy)(CO)$_7$(PPh$_2$H)$_2$] affords a mixture of two isomers of [Ru$_3$(μ-H)(μ_3-η^2-ampy)(μ-PPh$_2$)$_2$(CO)$_6$]. The two isomers differ only in the distribution of the PPh$_2$ and μ-H ligands over the available Ru-Ru edges. Scheme 1.3 summarizes the above reactions.

It can be seen from the above discussion that the reaction of the 2-

amino-6-methylpyridine ligand (Hampy) with [Ru$_3$(CO)$_{12}$] leads to the for-

mation of a capped species [Ru$_3$(μ-H)(μ_3-η^2-ampy)(CO)$_9$] whose chemistry

is analogous to that obtained for the capped cluster [Ru$_3$\{μ-η^2-C(O)(C$_6$-

H$_5$)\}\{μ_3-η^2-P(C$_6$H$_5$)(C$_5$H$_4$N)\}(CO)$_9$] discussed in Section 1.3.
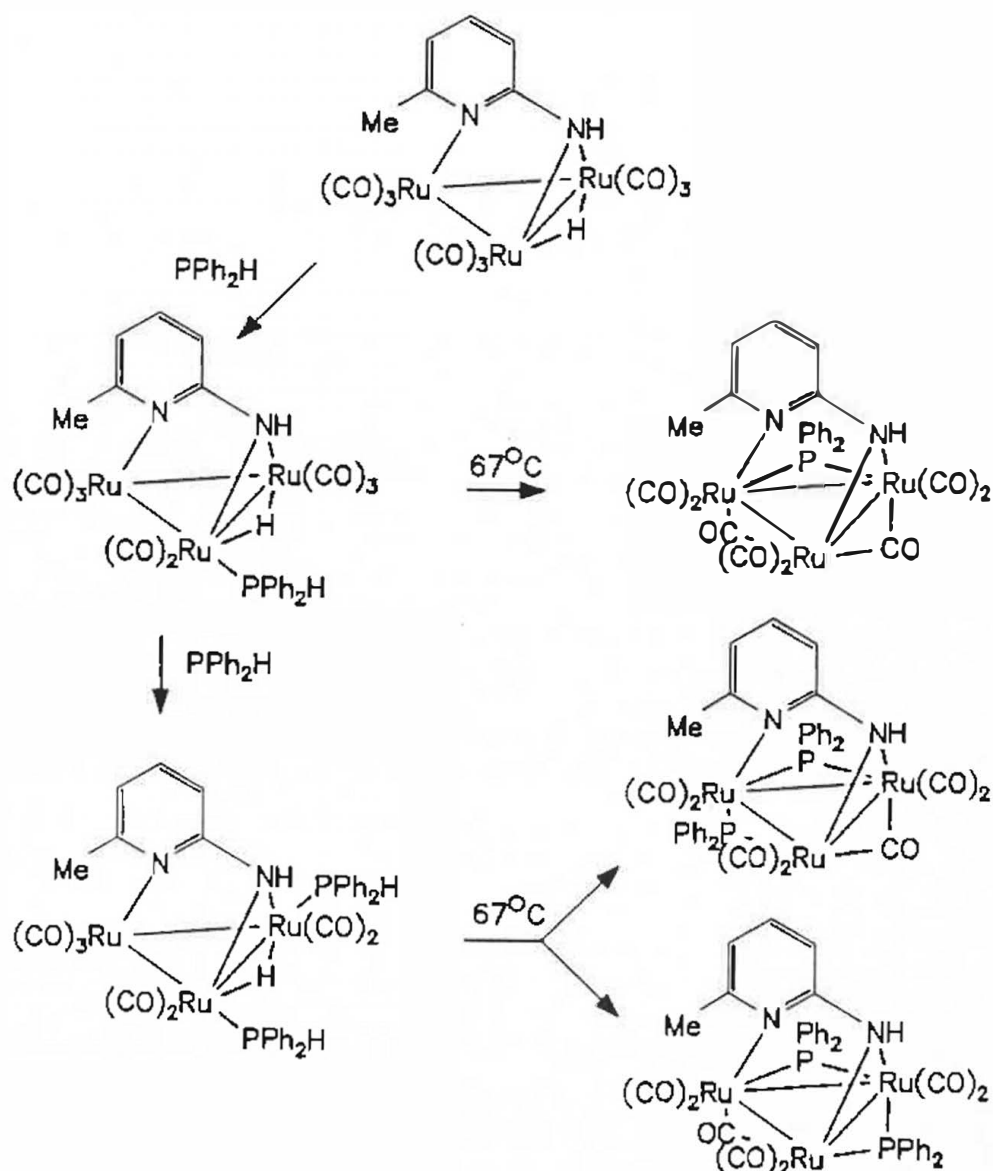
Scheme 1.3: Reactions of [Ru$_3$(μ-H)(μ_3-η^2-ampy)(CO)$_9$] with PPh$_2$H

The cluster $[Ru_3(\mu-H)(\mu_3-\eta^2-ampy)(CO)_9]$ does not react with either tri-ethylamine or potassium methoxide indicating a very low acidity of the hydride and NH hydrogen atoms. It is easily protonated with $HBF_4 \cdot OEt_2$ affording the cationic dihydride $[Ru_3(\mu-H)_2(\mu_3-\eta^2-ampy)(CO)_9][BF_4]$. Treatment of the latter with triethylamine affords $[Ru_3(\mu-H)(\mu_3-\eta^2-ampy)(CO)_9]$, while reaction with potassium methoxide only affords a small amount of the original cluster. The major products are two isomers of $[Ru_3(\mu-H)_2(\mu_3-\eta^2-ampy)(CO_2Me)(CO)_8]$, the isomer obtained being dependent on which of the two CO groups bonded to the $Ru(\mu-H)_2$ unit is attacked (see Scheme 1.4). Cabeza et al.[61] have suggested that the carbon atoms of these two groups carry a higher positive charge than the carbon atoms of the other two CO ligands and are consequently more susceptible to nucleophilic attack by the methoxide ions. Scheme 1.4, below, summarizes these reactions.
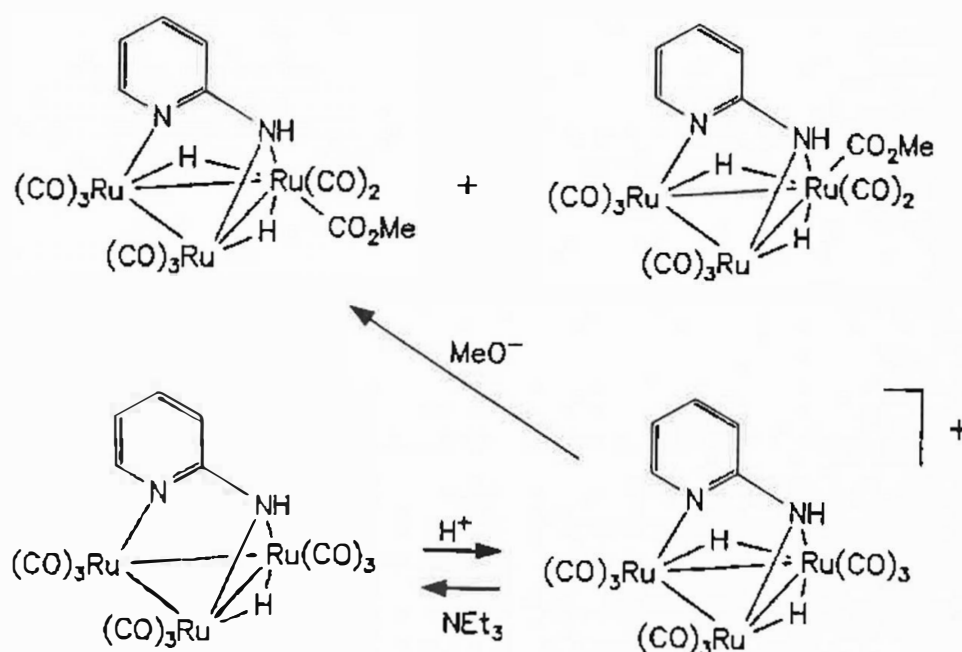
Scheme 1.4: Protonation/deprotonation reactions
involving the cluster $[Ru_3(\mu-H)(\mu_3-\eta^2-ampy)(CO)_9]$

The reactions of $[Ru_3(\mu\text{-H})(\mu_3\text{-}\eta^2\text{-ampy})(CO)_9]$ and $[Ru_3(\mu\text{-H})_2(\mu_3\text{-}\eta^2\text{-ampy})\text{-}$
$(CO)_9][BF_4]$ with PPh_3 afford $[Ru_3(\mu\text{-H})(\mu_3\text{-}\eta^2\text{-ampy})(CO)_8(PPh_3)]$ and $[Ru_3\text{-}$
$(\mu\text{-H})_2(\mu_3\text{-}\eta^2\text{-ampy})(CO)_8(PPh_3)][BF_4]$ respectively. As before,[62] the
substituted CO ligands were those *cis* to the amino group and *cis* to one
hydride. Protonation of $[Ru_3(\mu\text{-H})(\mu_3\text{-}\eta^2\text{-ampy})(CO)_8(PPh_3)]$ leads to the
formation of a different isomer of the cationic dihydride $[Ru_3(\mu\text{-H})_2\text{-}$

Scheme 1.5: Protonation/deprotonation reactions
involving the cluster $[Ru_3(\mu\text{-H})(\mu_3\text{-}\eta^2\text{-ampy})(CO)_8(PPh_3)]$

$(\mu_3-\eta^2\text{-ampy})(CO)_8(PPh_3)][BF_4]$, protonation taking place at the edge containing the ruthenium bonded to the PPh_3 ligand as would be expected, since this is the most basic edge of the ruthenium triangle. An unexpected feature of this reaction is the formation of a different isomer, caused by the migration of the PPh_3 ligand from a *cis* position relative to the hydride that spans the amido-bridged Ru-Ru bond in $[Ru_3(\mu-H)(\mu_3-\eta^2\text{-ampy})(CO)_8(PPh_3)][BF_4]$ to a position *trans* to the same hydride in $[Ru_3(\mu-H)_2(\mu_3-\eta^2\text{-ampy})(CO)_8(PPh_3)]$. Indeed, Cabeza *et al.* found no precedents for such a migration. They proposed that the higher basicity of the Ru-Ru(PPh_3) edge is the driving force for this isomerization, the *trans* isomer being more stable. Scheme 1.5 outlines these reactions.

1.5 REACTIONS OF PYRIDINE-2-THIOL WITH $[Ru_3(CO)_{12}]$

Cabeza *et al.*[63] have reacted pyridine-2-thiol (HSpy) with $[Ru_3(CO)_{12}]$ affording the polymer $[\{Ru(\mu_3-\eta^2\text{-Spy})(CO)_2)_n]$. However, when a shorter reaction time or milder conditions are used together with a 1:1 reactant ratio, the complex $[Ru_3(\mu-H)(\mu_3-\eta^2\text{-Spy})(CO)_9]$ is obtained. Here the Spy anion functions as a triply bridging ligand capping the triruthenium triangle as was previously found by Lugan *et al.* in the anionic cluster $[PPN][Ru_3(\mu_3-\eta^2\text{-Spy})(CO)_9]$.[64] Recently, Hardcastle and co-workers[65] have determined the crystal structure of $[Ru_3(\mu-H)(\mu_3-\eta^2\text{-Spy})(CO)_9]$.
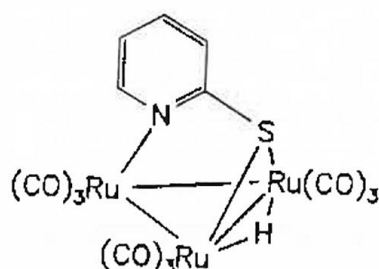
Figure 1.14: The $[Ru_3(\mu-H)(\mu_3-\eta^2\text{-Spy})(CO)_9]$ Cluster

The authors suggested that the polymer is formed via intermediates such as $[Ru_3(\mu-H)(\mu_3-\eta^2-Spy)(HSpy)(CO)_8]$, $[Ru_3(\mu-H)_2(\mu_3-\eta^2-Spy)(\mu-Spy)(CO)_7]$ and $[Ru_3(\mu-H)(\mu_3-\eta^2-Spy)(CO)_9]$ and that since only the latter cluster is observed, the former two clusters must be highly reactive towards the HSpy and possibly other ligands.

The authors[63] also reacted $[Ru_3(\mu_3-\eta^2-Spy)(CO)_9]$ with PPh$_3$ and bis(diphenylphosphino)methane (dppm) to determine whether or not the Ru-S and Ru-N bonds could be broken by reactions with phosphine ligands. These reactions afforded $[Ru_3(\mu-H)(\mu_3-\eta^2-Spy)(CO)_8\{PPh_3\}]$ and $[Ru_3(\mu-H)(\mu_3-\eta^2-Spy)(CO)_7(dppm)]$ respectively. In both cases the CO ligands displaced were those *cis* to both the sulphur atom and the hydride. It is clear that the bonds between the Spy ligand and the ruthenium atom of $[Ru_3(\mu_3-\eta^2-Spy)(CO)_9]$ are less easily broken than are some of the Ru-CO bonds.

1.6 REACTIONS OF SUBSTITUTED QUINOLINES WITH $[Ru_3(CO)_{12}]$ AND OTHER CLUSTERS

A literature survey of the reactions of 2-substituted quinolines with $[Ru_3(CO)_{12}]$ indicated that only one such reaction has been reported. Hardcastle and co-workers[65] reacted the quinoline-2-thiol ligand (HSquin) with $[Ru_3(CO)_{12}]$ to afford $[Ru_3(\mu-H)(Squin)(CO)_9]$ which was characterized spectroscopically. The cluster was obtained only in low yield (3%) and was not studied further. Reaction of HSquin with $[Re_2X_4(dppm)_2]$ (X = Cl, Br) affords the clusters $[Re_2X_4(dppm)_2(HSquin)]$.[66] The infrared spectra of these clusters show no bands which could be attributed to the ν(S-H) vibration of a co-ordinated thiol ligand. This implies that the thiol group is deprotonated and that the ligand is present in its zwitterionic form.[67] These clusters undergo a reversible one electron oxidation to afford $[Re_2X_4(dppm)_2(HSquin)]^+$ which is

followed by elimination of HX to yield [Re$_2$X$_3$(μ-dppm)$_2$(μ-Squin)]$^+$ containing a bridging Squin ligand.
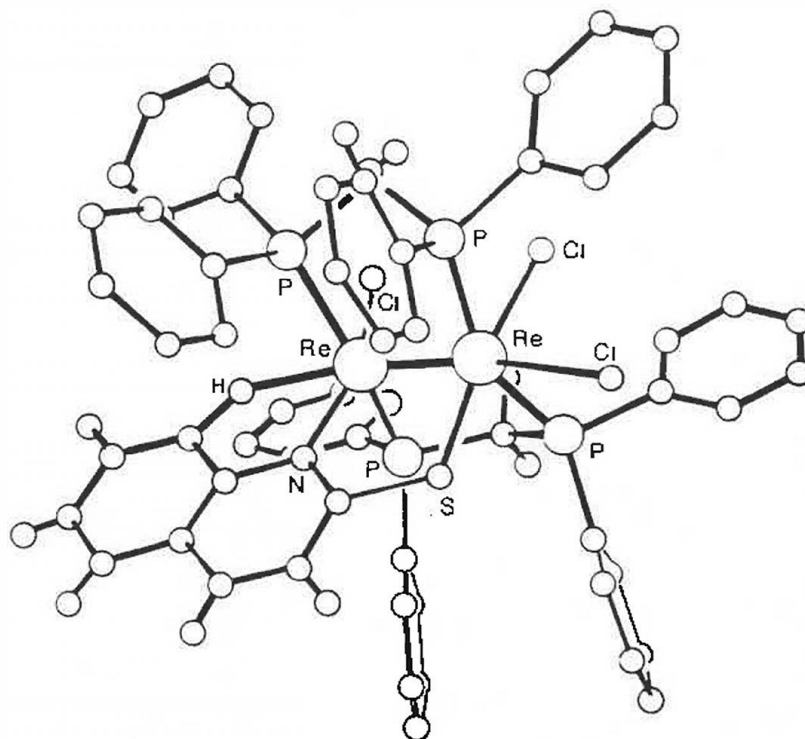
Figure 1.15:   X-Ray Structure of [Re$_2$Cl$_3$(dppm)$_2$(Squin)]$^+$ [66]

Van Doorn and Van Leeuwen[68] have reacted 8-quinolinol with [Ru$_3$(CO)$_{12}$] to afford the cluster [Ru$_3$(C$_9$H$_6$NO)$_2$(CO)$_8$] as the major product.   In this

Figure 1.16
The 8-Quinolinol Ligand
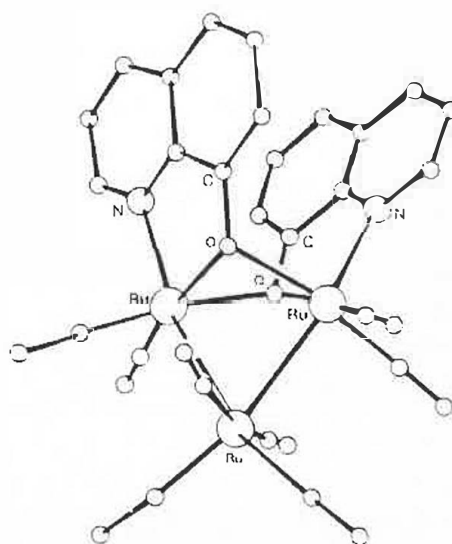
Figure 1.17
X-ray Structure of
[Ru$_3$(C$_9$H$_6$NO)$_2$(CO)$_8$][68]

cluster each oxygen atom acts as a three-electron donor, giving a total of 50 valence electrons. The two ligands bridge the edge of the ruthenium triangle where no Ru-Ru bond is found.

While the ligands 8-diphenylphosphinoquinoline and 8-diphenylarsino-quinoline are similar to the 2-diphenylphosphinoquinoline ligand and may well have provided insight into the chemistry of the latter, no reactions of the former two ligands with [Ru$_3$(CO)$_{12}$] have as yet been carried out. Reactions of these 8-substituted quinolines with [Pt(cod)-(CH$_3$)$_2$][69] (cod = 1,5-cyclooctadiene) afford the complexes [Pt(8-di-phenylphosphinoquinoline)(CH$_3$)$_2$] and [Pt(8-diphenylarsinoquinoline)-(CH$_3$)$_2$], the ligand co-ordinating to the platinum in a chelating fashion.

1.7 THE 2-DIPHENYLPHOSPHINOQUINOLINE LIGAND

As noted in the introduction the aim of the research presented in this thesis is to investigate the reactions of the Ph$_2$Pquin ligand with [Ru$_3$(CO)$_{12}$], to determine the nature of the products formed and to study their chemistry. Triruthenium dodecacarbonyl was chosen as the precursor for the development of the co-ordination chemistry of the Ph$_2$Pquin ligand largely because, as discussed in Sections 1.3, 1.4 and 1.5, the chemistry of its reactions with bidentate ligands which are very similar to the Ph$_2$Pquin ligand had already been investigated. The Ph$_2$Pquin ligand is most closely related to the 2-diphenylphosphino-pyridine ligand (Ph$_2$Ppy) discussed in Section 1.3; but there are differences. The quinoline ring system is bulkier than the pyridine ring system and thus the steric requirement of the two ligands will not be the same. The dispositions of the two donor atoms P and N in Ph$_2$Pquin and Ph$_2$Ppy are the same but there could be differences in the

electron donating properties of the N-donor atoms in particular, since this atom is part of a larger Π-delocalized system in Ph$_2$Pquin (the quinoline moiety) than in Ph$_2$Ppy (the pyridine ring). Because the Π^*-orbitals of quinoline are lower in energy than those of pyridine we assume that Ph$_2$Pquin will be a weaker N-donor ligand than Ph$_2$Ppy but the difference will be small; to the best of our knowledge studies of the relative donor strengths of pyridine and quinoline have not been reported.

Our expectation was that the initial co-ordination of Ph$_2$Pquin to [Ru$_3$(CO)$_{12}$] would be via the P-donor atom of the diphenylphosphino moiety; certainly this was found in the reaction of Ph$_2$Ppy with [Ru$_3$(CO)$_{12}$]. The key question is however; "Will the Ph$_2$Pquin ligand dephenylate following initial co-ordination to form a triply-bridging μ_3-η^2-P(C$_6$H$_5$)(C$_9$H$_6$N) ligand moiety in a manner analogous to its pyridine analogue?" Indeed, all of the bidentate ligands discussed here *viz.* Ph$_2$Ppy, Hapy and HSpy undergo a similar reaction to form a triply-bridging ligand moiety which caps the triruthenium triangle; refer to Sections 1.3, 1.4 and 1.5. Such capping ligands allow a variety of interesting organic transformations to take place at the cluster surface without disintegration of the cluster framework and our hope was that this could be achieved with the Ph$_2$Pquin ligand as well.

CHAPTER TWO

SYNTHESIS AND CHARACTERIZATION OF THE
2-DIPHENYLPHOSPHINOQUINOLINE LIGAND

2.1 INTRODUCTION

The synthesis of the 2-diphenylphosphinoquinoline ligand is based on the procedure used for the synthesis of the closely related 2-diphenylphos-phinopyridine ligand. The latter was first synthesized by Mann and Watson[70] in 1948 by the reaction of 2-pyridylmagnesiumbromide[71,72a] with chlorodiphenylphosphine (yield 20.4%). This basic procedure was sub-sequently used by many researchers to synthesize various pyridylphos-phines.[72] A variation of this method,[73] which became generally used in the 1970's,[74] involves the use of 2-pyridyllithium rather than the magnesiumbromide derivative. However, both of the above reactions have two inherent problems; the yields achieved are relatively low and unwanted side products are formed.

In 1955, Burger et al.[75] reported that neither 2-chloro- nor 2-bromo-pyridine react when subjected to either Arbuzov or Michaelis-Becker reaction conditions. This prompted the statement by Redmore[76] (1976) that pyridyl halides do not react with phosphorus nucleophiles. Although it was known that 2-halopyridines, in general, are relatively unreactive toward nucleophilic substitution[77] this seemed an over-statement of the results seeing that it was based on such limited data.[75]

It was only two years later that Newkome and Hager[74] published their paper reporting the synthesis of pyridyldiphenylphosphines via direct

nucleophilic substitution of pyridyl halides by lithium diphenylphos-
phide. They prepared the lithium diphenylphosphide from chlorodiphenyl-
phosphine and lithium metal in an ethereal solvent[74,78] but also listed
various other methods for the preparation of this reagent.[79-82]
Reaction of the lithium diphenylphosphide with 2-bromopyridine afforded
2-diphenylphosphinopyridine in 55% yield, a considerable improvement
over earlier methods. Interestingly, Newkome and Hager[74] noted that
Isslieb and Brüsenhaber[83] (1965) had mentioned the addition of metal-
diphenylphosphine across the C=N bond of pyridine and quinoline.
However, no specific examples were cited and no experimental details
were given.

The most recent method for the preparation of 2-diphenylphosphino-
pyridine was reported by Maisonnet et al.[84] in 1982. In this procedure
n-butyllithium was reacted with diphenylphosphine, followed by addition
of 2-chloropyridine. This afforded the desired product in 94% yield
(based on PPh$_2$H).

2.2 SYNTHESIS AND CHARACTERIZATION OF 2-DIPHENYLPHOSPHINOQUINOLINE

The procedure for the synthesis of 2-diphenylphosphinoquinoline is based
on the procedure used by Newkome and Hager[74] for the synthesis of 2-
diphenylphosphinopyridine. Lithium diphenylphosphide was generated from
chlorodiphenylphosphine and lithium metal in dry THF. In the litera-
ture,[74,85] it is maintained that this reaction should be carried out
under a dry nitrogen atmosphere. This seems anomalous since lithium is
known to react with nitrogen, sometimes violently.[86] This synthesis was
therefore carried out under a dry argon atmosphere. The yield of
lithium diphenylphosphide was taken to be 80%. This assumption is based
on results obtained in this laboratory during the synthesis of other

diphenylphosphino-substituted heterocycles.

The lithium diphenylphosphide was then reacted with an equimolar amount of 2-chloroquinoline. A $^{31}P\{^1H\}$ NMR spectrum of the resulting solution showed two major peaks; one which was subsequently identified as corresponding to the Ph$_2$Pquin ligand and one which corresponded to the oxidized form of the ligand (Table 2.1). The reaction mixture was then acidified with concentrated hydrochloric acid so as to protonate the phosphorus atom of the Ph$_2$Pquin ligand. This prevents oxidation of the ligand during subsequent purification. Dilute hydrochloric acid was added to decompose any unreacted lithium diphenylphosphide while still maintaining a highly acidic medium. Impurities were then extracted from the reaction solution and the solution basified to afford the neutral ligand. The ligand was then extracted into diethyl ether, the volume reduced and methanol added. On cooling at -30°C, the Ph$_2$Pquin ligand precipitated out of solution.

The ligand was characterized by $^{31}P\{^1H\}$ NMR spectroscopy, microanalysis and a mass spectrum. The melting point was also determined. The results of the characterization are summarized in Table 2.1 and Figure 2.1 below.

$^{31}P\{^1H\}$ NMR δ(ppm) (measured in CDCl$_3$ relative to 85% H$_3$PO$_4$)	PPh$_2$-quin -2.82 OPPh$_2$-quin (Oxidized form) 22.36
Mass spectrum M$^+$	313
Microanalysis C, H, N	C$_2$H$_{16}$NP(313.32) requires 80.50, 5.15, 4.47% Found: 80.56, 5.11, 4.33%
Melting point	74.8°C

Table 2.1: Characterization data for the Ph$_2$Pquin ligand
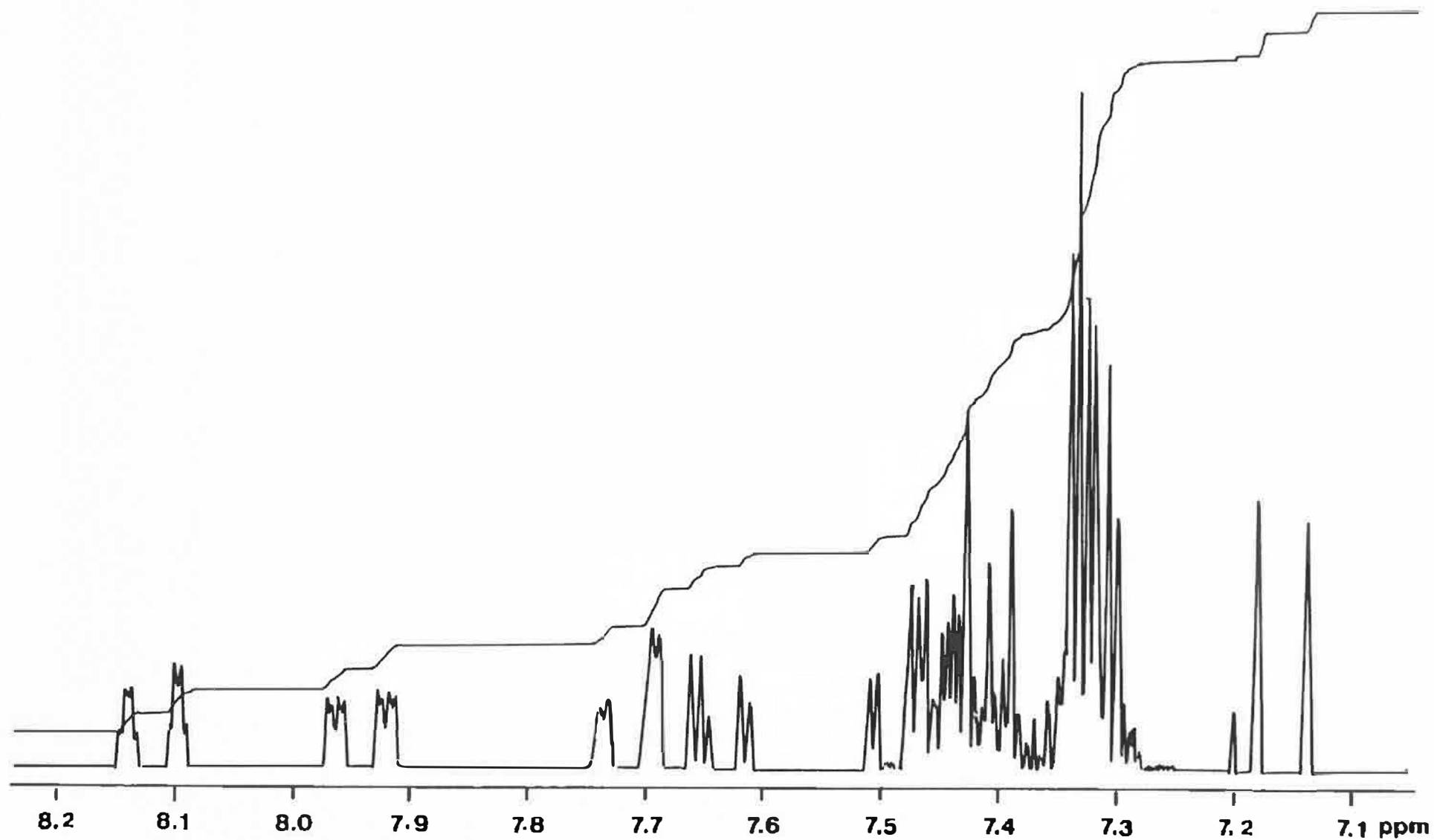
Figure 2.1: ¹H NMR spectrum of the Ph₂Pquin ligand

Since the Ph$_2$Pquin ligand is very similar to the Ph$_2$Ppy ligand (Section 1.7), one would expect the ^{31}P{^{1}H} NMR signals to be almost the same. This is indeed the case, the shift for the Ph$_2$Pquin ligand being only slightly more downfield than the shift of δ -3.36 ppm for the Ph$_2$Ppy ligand.[87]

The molecular ion peak in the mass spectrum is consistent with the calculated molecular mass for Ph$_2$Pquin of 313.32 mass units. Certain characteristic mass losses are also observed. The loss of 77 mass units corresponds to the loss of a phenyl ring. A loss of a further 52 mass units corresponds to the breakup of the ring system while a loss of 31 mass units corresponds to the loss of a phosphorus atom.

The microanalysis results are consistent with expectations and the melting point falls in a similar temperature range to that of Ph$_2$Ppy (83-84°C).[75] The ^{1}H NMR spectrum is shown in Figure 2.1.

2.3 EXPERIMENTAL

The ligand synthesis was carried out under a dry argon atmosphere using standard Schlenk techniques. The THF used was first distilled from sodium and benzophenone and then redistilled from calcium hydride under an argon atmosphere to ensure absolute dryness. The 2-chloroquinoline (Aldrich) was dried under reduced pressure prior to use. The chlorodi-phenylphosphine (Strem), lithium and all other chemicals were used with-out further purification.

2.3.1 *Synthesis of lithium diphenylphosphide*

A solution of chlorophenylphosphine (8.43 g, 38.20 mmol) in dry THF

(25 ml) was added dropwise to excess lithium (400 mg) in dry THF (50 ml) with vigorous stirring. The resulting exothermic reaction was allowed to proceed for ca. 30 minutes. The deep red solution was refluxed for an additional hour and filtered hot through a frit prior to use. Yield: assumed to be 80% (Section 2.2)

2.3.2 Synthesis of 2-diphenylphosphinoquinoline

The solution of lithium diphenylphosphide described in 2.3.1 was cooled in a methanol/liquid nitrogen bath (-78°C). Dry 2-chloroquinoline (5 g, 30.56 mmol) was added with stirring and the solution left overnight to warm slowly to room temperature. The resulting green solution was acidified with concentrated HCl (10 ml) and 3N HCl (30 ml) and then extracted with diethyl ether. The aqueous fraction was cooled in an ice bath (0°C) and basified with concentrated ammonia solution till a pH of between 9 and 10 was achieved. The product was then extracted into diethyl ether. The volume of the ether was reduced to a minimum under reduced pressure and methanol was added. The solution was refrigerated at -30°C to precipitate the 2-diphenylphosphinoquinoline (1) as a pale cream coloured solid. Yield: 50% based on 2-chloroquinoline.

CHAPTER THREE

SYNTHESIS AND CHARACTERIZATION OF RUTHENIUM DERIVATIVES OF THE 2-DIPHENYLPHOSPHINOQUINOLINE LIGAND

3.1 REACTIONS OF THE LIGAND 2-DIPHENYLPHOSPHINOQUINOLINE (Ph$_2$Pquin) WITH TRIRUTHENIUM DODECACARBONYL [Ru$_3$(CO)$_{12}$]

3.1.1 Synthesis of [Ru$_3$(η^1-Ph$_2$Pquin)(CO)$_{11}$] (2)

Addition of one mole equivalent of Ph$_2$Pquin to [Ru$_3$(CO)$_{12}$] in THF affords the monosubstituted product [Ru$_3$(η^1-Ph$_2$Pquin)(CO)$_{11}$] (2) provided sodium benzophenoneketyl is used as a catalyst.
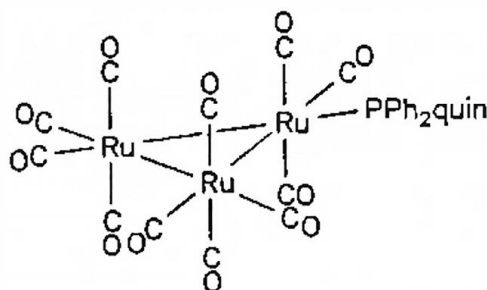
Figure 3.1: [Ru$_3$(η^1-Ph$_2$Pquin)(CO)$_{11}$] (2)

The quantity of catalyst required to bring the reaction to completion depends largely on the dryness of the THF used as solvent since the catalyst is highly moisture sensitive. It was subsequently found, however, that it is desirable to use a minimum amount of the catalyst because the decomposition products of the catalyst interfere with further reactions of [Ru$_3$(η^1-Ph$_2$Pquin)(CO)$_{11}$] (2). This compound could

not be isolated pure but was characterized spectroscopically as follows.

The ν(CO) stretching peaks in the infrared spectrum of (2) (Table 3.17) showed a pattern typical of compounds of the type $[Ru_3(L)(CO)_{11}]$[3,7] (L = phosphine ligand). A $^{31}P\{^1H\}$ NMR spectrum of the reaction mixture revealed two peaks. The major peak, a singlet at 38.58 ppm, is indicative of a terminally bonded phosphorus ligand[88] and compares favourably with a value of 37.42 ppm found for the analogous Ph_2Ppy complex $[Ru_3(\eta^1-Ph_2Ppy)(CO)_{11}]$[23] in which only the phosphorus atom is co-ordinated. The other peak in the $^{31}P\{^1H\}$ NMR spectrum, a low intensity singlet at 48.05 ppm, was identified as corresponding to $[Ru_3\{\mu-\eta^2-C(O)(C_6H_5)\}\{\mu_3-\eta^2-P(C_6H_5)(C_9H_6N)\}(CO)_9]$ (3) (see below). It is because of the ready conversion of complex (2) into complex (3) that isolation of the former as a pure product was not possible.

Cluster (2) was also obtained by the reaction of Ph_2Pquin with $[Ru_3(Me-CN)(CO)_{11}]$ (See Section 3.1.3). This method was, however, not pursued since it involves two synthetic steps.

3.1.2 <u>Synthesis of $[Ru_3\{\mu-\eta^2-C(O)(C_6H_5)\}\{\mu_3-\eta^2-P(C_6H_5)(C_9H_6N)\}-$ $(CO)_9]$ (3)</u>

In Section 1.7, the question was posed as to whether the co-ordinated Ph_2Pquin ligand in complex (2) would dephenylate as has been found for the Ph_2Ppy ligand.[23] That this does indeed happen is evidenced by the spontaneous formation of $[Ru_3\{\mu-\eta^2-C(O)(C_6H_5)\}\{\mu_3-\eta^2-P(C_6H_5)(C_9H_6N)\}-$ $(CO)_9]$ (3) in the reaction of Ph_2Pquin with $[Ru_3(CO)_{12}]$ in THF at room temperature described in Section 3.1.1. Although the dephenylation reaction is spontaneous it was found to be very slow, the reaction being incomplete even after several days at a slightly elevated temperature

(40°C). This contrasts with the results for the dephenylation of the analogous cluster $[Ru_3(\eta^1-Ph_2Ppy)(CO)_{11}]^{23}$ where the dephenylation is complete within 48 hours at room temperature or two hours at 40°C. However, refluxing the THF solution of cluster (2) brings the reaction to completion within *ca.* 1 hour. It is proposed that the mechanism for the above reaction follows the same sequence as the mechanism proposed by Bruce *et al.*[3,8] for the dephenylation of the Ph$_2$Ppy ligand in the analogous cluster $[Ru_3(\eta^1-Ph_2Ppy)(CO)_{11}]$ (see Section 1.2). Two factors greatly influence the yield of the product of the dephenylation of cluster (2). The first, already mentioned above, is the quantity of catalyst added. The second factor is the purity of the triruthenium dodecacarbonyl used. Traces of a black solid, assumed to be a ruthenium oxide, found in the commercially acquired $[Ru_3(CO)_{12}]$ appear to catalyze the decomposition of the acyl cluster (3), yields being reduced by up to 80 percent when larger amounts of this material were present. Purification of the $[Ru_3(CO)_{12}]$ was achieved by extracting the triruthenium dodecacarbonyl into dichloromethane and filtering the extract through neutral aluminum oxide, followed by crystallization from the dichloromethane at ~30°C.

The $^{31}P\{^1H\}$ NMR spectrum of complex (3), measured in THF, shows a resonance at 48.05 ppm which can be assigned to the phosphorus atom of the bridging phosphido unit; the value is consistent with the $P(C_6H_5)$-(C_9H_6N) moiety bridging an open edge of the ruthenium triangle[23,88] of this 50-electron cluster. Comparing this value to that obtained for the analogous $P(C_6H_5)(C_5H_4N)$-capped cluster $[Ru_3\{\mu-\eta^2-C(O)(C_6H_5)\}\{\mu_3-\eta^2-P(C_6H_5)(C_5H_4N)\}(CO)_9]$ (48.93 ppm) suggests that the $P(C_6H_5)(C_9H_6N)$ moiety is also co-ordinated in a $\mu_3-\eta^2-$ mode. Evidence for the presence of the acyl group was obtained by ^{13}C NMR spectroscopy which showed a characteristic resonance[23] at 303.69 ppm (measured in CDCl$_3$) for the

carbon atom of the acyl group.   The signal is a doublet indicating coupling of the acyl carbon atom with the bridging phosphorus atom. This feature was also reported for the $P(C_6H_5)(C_5H_4N)$-capped cluster mentioned above, the signal for this cluster being a doublet centred at 302.37 ppm.[23]   In order to confirm the overall structure of cluster (3), a single crystal X-ray diffraction study was carried out.   Figure 3.2 gives a perspective view of cluster (3).   Tables 3.2 and 3.3 list the interatomic distances and interatomic angles respectively.
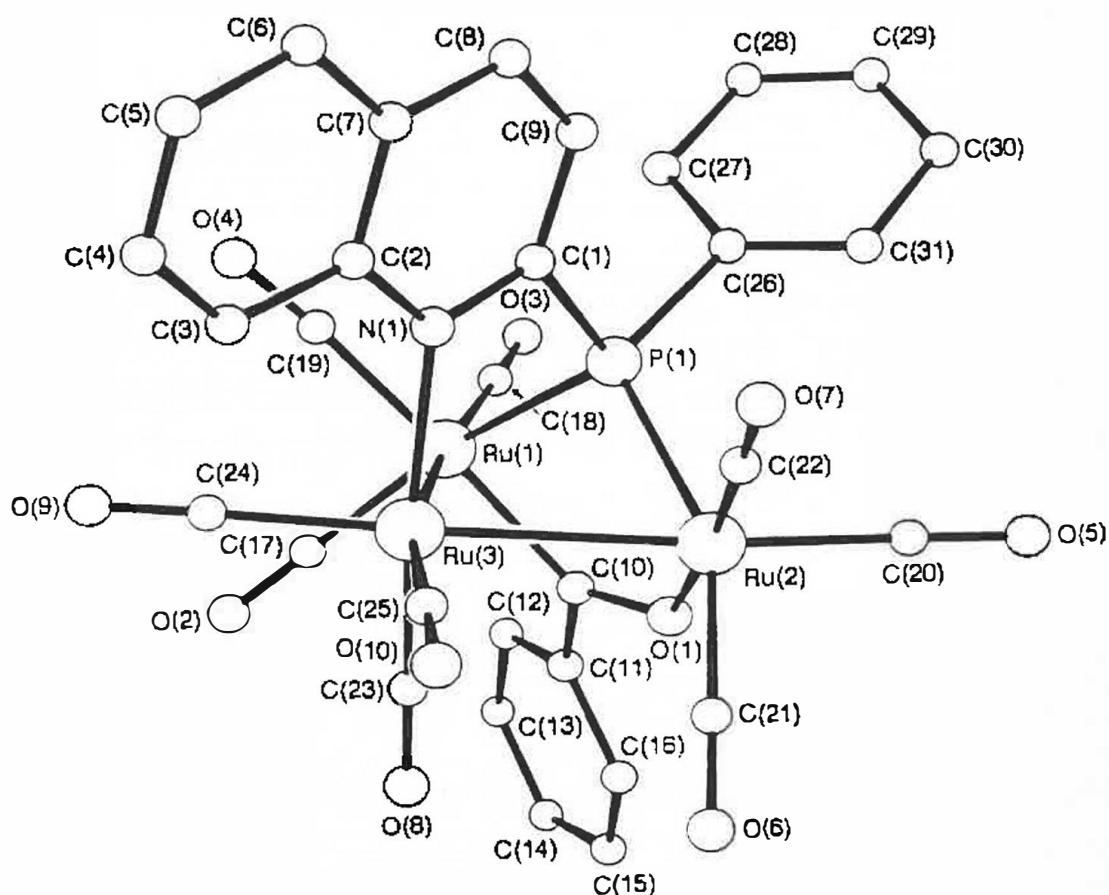
Figure 3.2: Perspective view of $[Ru_3\{\mu-\eta^2-C(O)(C_6H_5)\}\{\mu_3-\eta^2-P(C_6H_5)-(C_9H_6N)\}(CO)_9]$ (3) showing the atom labelling scheme

The 50-electron cluster $[Ru_3\{\mu-\eta^2-C(O)(C_6H_5)\}\{\mu_3-\eta^2-P(C_6H_5)(C_9H_6N)\}-(CO)_9]$ (3) contains a triangle of ruthenium atoms, two of its edges corresponding to Ru-Ru single bonds $\{Ru(1)-Ru(3) = 2.865(1)\text{Å}, Ru(2)-Ru(3) = 2.844(1)\text{Å}\}$ with the third being an open edge with no bond between the Ru atoms $\{Ru(1)-Ru(2) = 3.640(1)\text{Å}\}$. The acyl group, which bridges the open edge via the carbon and oxygen atoms C(10) and O(i) respectively, lies on one side of the triruthenium plane. The capping $P(C_6H_5)(C_9H_6N)$ group lies on the other side of the triruthenium plane with the phosphorus atom bridging the open edge (see Figure 3.2). The bond angle subtended at the P atom is 100.6°, a value which is substantially larger than the typical value of *ca.* 75° for phosphido groups which bridge closed edges of Ru clusters.[23,88] There is a small difference in the Ru-P bond lengths (0.036Å) but the P atom is essentially symmetrically bridging. The triruthenium core is further stabilized by co-ordination of the nitrogen atom of the $P(C_6H_5)(C_9H_6N)$ ligand moiety to the unique ruthenium atom Ru(3) $\{Ru(3)-N(1) = 2.207(5)\text{Å}\}$. This bond is 0.042Å larger than the corresponding Ru-N bond in the analogous cluster $[Ru_3\{\mu-\eta^2-C(O)(C_6H_5)\}\{\mu_3-\eta^2-P(C_6H_5)(C_5H_4N)\}-(CO)_9]$. This fact supports the assumption made in Section 1.7, that the $Ph_2Ppquin$ ligand, will be a slightly weaker nitrogen-donor ligand than the Ph_2Ppy ligand but steric factors may well play a role in causing the lengthening of the Ru-N bond. The two equatorial carbonyl ligands C(18)-O(13) and C(20)-O(5), adjacent to the bridging acyl group, are essentially colinear with the metal-metal bonds Ru(3)-Ru(1) and Ru(3)-Ru(2) respectively. The other four carbonyl ligands adjacent to the bridging acyl group, two at each Ru atom, are at approximately 90° to the same two metal-metal bonds and lie above and below the triruthenium plane. One carbonyl ligand of each pair is *trans* to the Ru-acyl linkage $\{Ru(1)-C(10)$ or $Ru(2)-O(1)\}$ while the other is *cis* to it.

As was discussed in Section 1.3, the presence of a face-capping ligand on a metal cluster is a desirable feature as it helps to curtail fragmentation of the cluster on further reaction. The presence of an acyl group {-O=C-(C$_6$H$_6$)} bridging an open edge of a metal cluster has been found to have a stereospecific labilizing effect[23,33,34] assigned to the oxygen atom. Incoming ligands are found to co-ordinate to the metal atom to which the oxygen is bonded and in a position *cis* relative to that oxygen atom. For this reason [Ru$_3$(μ-η^2-C(O)(C$_6$H$_5$)}{μ_3-η^2-P(C$_6$H$_5$)-(C$_9$H$_6$N)}(CO)$_9$] (3) was expected to readily undergo substitution of a carbonyl ligand in the aforementioned position {C(21)-O(6) or C(20)-O(5), see Figure 3.2}. This was indeed found to be the case (Sections 3.2 and 3.3).

3.1.3 Synthesis of [Ru$_3$(η^1-Ph$_2$Pquin)$_2$(CO)$_{10}$] (4)

Attempts to substitute two carbonyl ligands on [Ru$_3$(CO)$_{12}$] by reaction of the latter with two mole equivalents of Ph$_2$Pquin using the sodium benzophenoneketyl catalyst were unsuccessful, the reaction in THF producing a mixture of mono-, di-, and trisubstituted products, which were difficult to separate. It was therefore decided to use [Ru$_3$(MeCN)$_2$-(CO)$_{10}$] as the starting material, the acetonitrile ligands being very labile.[21,22] This cluster was prepared by using an adaptation of the method first used by Lewis *et al.*[21] in which trimethylamine-N-oxide was employed to oxidize the carbonyl ligands on [Ru$_3$(CO)$_{12}$] in the presence of acetonitrile to afford the desired cluster. It had been reported that this reaction afforded the bis(acetonitrile) species in 85% yield, the other 15% being the mono-acetonitrile species.[21] We found the reaction to be essentially quantitative based on trimethylamine-N-oxide.

The precursor $[Ru_3(MeCN)_2(CO)_{10}]$ reacts readily with two mole equivalents of Ph_2Pquin at ambient temperature in an acetonitrile/dichloromethane mixture (1:3) to afford the cluster $[Ru_3(\eta^1-Ph_2Pquin)_2(CO)_{10}]$ (**4**) as the major product (see Figure 3.3). The latter complex is, however, quite unstable in the reaction mixture and must be isolated rapidly to prevent its decomposition into an unidentified and insoluble red material. Cluster (**4**) was isolated as a dark red crystalline material by thin layer chromatography (petroleum ether/dichloromethane as eluent) followed by recrystallization from a dichloromethane/hexane mixture.
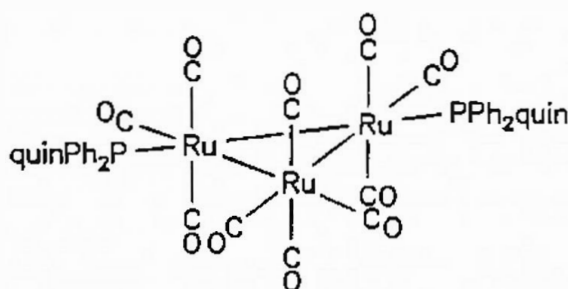
Figure 3.3: Proposed structure of $[Ru_3(\eta^1-Ph_2Pquin)_2(CO)_{10}]$ (**4**)

The $\nu(CO)$ stretching peaks in the infrared spectrum of (**4**) (Table 3.17) are consistent with the structure proposed in Figure 3.3 showing a pattern similar to that obtained for $[Ru_3(\eta^1-PMe_3)_2(CO)_{10}]$[7] and $[Ru_3(\eta^1-PPh_3)_2(CO)_{10}]$.[3] The $^{31}P\{^1H\}$ NMR spectrum of cluster (**4**) shows only one signal, a singlet at 35.94 ppm. This indicates that both Ph_2Pquin ligands occupy equivalent positions on the cluster and are terminally co-ordinated through the phosphorus atom[88] in a manner equivalent to that found in $[Ru_3(\eta^1-Ph_2Pquin)(CO)_{11}]$ (**2**) (σ = 38.58 ppm).

The reaction of one mole equivalent of Ph_2Pquin with $[Ru_3(MeCN)_2(CO)_{10}]$ was also attempted, the aim being to produce a cluster with a single bridging Ph_2Pquin ligand $i.e.$ $[Ru_3(\mu-Ph_2Pquin)(CO)_{10}]$. The major product of this reaction was cluster (4) with small amounts of a cluster with a $^{31}P\{^1H\}$ NMR resonance of 19.4 ppm also being detected. This product was, however, highly unstable and could not be isolated for further analysis. Reaction of one mole equivalent of Ph_2Pquin with the mono(acetonitrile) species $[Ru_3(MeCN)(CO)_{11}]$ (synthesized in a manner analogous to $[Ru_3(MeCN)_2(CO)_{10}]^{21})$ afforded the cluster $[Ru_3(\eta^1-Ph_2-Pquin)(CO)_{11}]$ (2) (see Section 3.1.1).

3.1.4 Synthesis of $[Ru_3(\mu-\eta^2-Ph_2Pquin)_2(CO)_8]$ (5)

Three methods were employed in an attempt to induce the pendant Ph_2Pquin ligands in $[Ru_3(\eta^1-Ph_2Pquin)_2(CO)_{10}]$ (4) to adopt a bridging co-ordination mode. Refluxing a THF solution of complex (4) did not produce the desired cluster, but rather caused one Ph_2Pquin ligand to dephenylate and assume a triply bridging co-ordination mode as was found when a THF solution of $[Ru_3(\eta^1-Ph_2Pquin)(CO)_{11}]$ (2) was refluxed (see Section 3.1.1). The other Ph_2Pquin ligand retained its pendant position. The synthesis and characterization of the resultant cluster $[Ru_3\{\mu-\eta^2-C(O)(C_6H_5)\}\{\mu_3-\eta^2-P(C_6H_5)(C_9H_6N)\}(\eta^1-Ph_2Pquin)(CO)_8]$ (6) are discussed in Section 3.2.1 below. The second procedure involved the addition of two mole equivalents of trimethylamine-N-oxide to a THF solution of complex (4) with the aim of activating a further two carbonyl ligands on the cluster to replacement by the nitrogen atoms of the pendant Ph_2Pquin ligands $i.e.$ to induce bridging by both of the Ph_2-Pquin ligands. The reaction did produce a small amount of the desired cluster (5); however, yields were very low with most of the starting material decomposing Treatment of $[Ru_3(CO)_{12}]$ with two mole equi-

valents of Ph$_2$Pquin and four mole equivalents of trimethylamine-N-oxide in acetone solution led to a colour change from orange to dark red. A ^{31}P{^{1}H} NMR spectrum of the reaction mixture showed the presence of both cluster (4) and the desired cluster (5). These were separated by thin layer chromatography and complex (5) was isolated as an orange powder by crystallization from a THF/methanol solution.
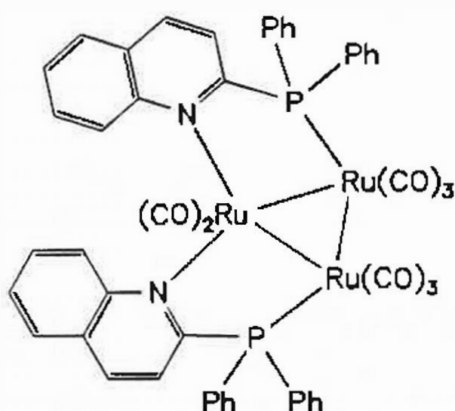
Figure 3.4: Proposed structure of [Ru$_3$(μ-η^2-Ph$_2$Pquin)$_2$(CO)$_8$] (5)

The ν(CO) stretching peaks in the infrared spectrum of cluster (5) (Table 3.17) show the same pattern as was found for [Ru$_3$(μ-dppe)$_2$(CO)$_8$] (dppe = Ph$_2$PCH$_2$CH$_2$PPh$_2$)[3] indicating that the Ph$_2$Pquin ligands have indeed adopted a bridging co-ordination mode. The ^{31}P{^{1}H} NMR spectrum showed a single resonance at 9.06 ppm. The presence of this resonance as a singlet again indicates that both ligands occupy identical positions on the cluster, i.e. is consistent with the structure proposed in Figure 3.4 above.

3.2 REACTIONS OF $[Ru_3\{\mu-\eta^2-C(O)(C_6H_5)\}\{\mu_3-\eta^2-P(C_6H_5)(C_9H_6N)\}(CO)_9]$ (3) WITH Ph$_2$Pquin AND HYDROGEN

3.2.1 Synthesis of $[Ru_3\{\mu-\eta^2-C(O)(C_6H_5)\}\{\mu_3-\eta^2-P(C_6H_5)(C_9H_6N)\}(\eta^1-$ Ph$_2$Pquin)(CO)$_8$] (6)

Treatment of the acyl cluster (3) with one mole equivalent of Ph$_2$Pquin in THF at ambient temperature, and without the use of a catalyst, leads to a colour change from orange to red and affords the new cluster $[Ru_3\{\mu-\eta^2-C(O)(C_6H_5)\}\{\mu_3-\eta^2-P(C_6H_5)(C_9H_6N)\}(\eta^1-Ph_2Pquin)(CO)_8]$ (6). Cluster (6) was isolated as a light red solid by thin layer chromato-graphy followed by crystallization from THF/methanol. The ν(CO) stretching peaks in the infrared spectrum of this cluster (Table 3.17) show the same band pattern as that found for the isostructural cluster $[Ru_3\{\mu-\eta^2-C(O)(C_6H_5)\}\{\mu_3-\eta^2-P(C_6H_5)(C_5H_4N)\}(PPh_3)(CO)_8]$[23] in which the PPh$_3$ ligand is co-ordinated to the ruthenium atom to which the oxygen of the acyl group is bonded, and in a position *cis* to that oxygen, as confirmed by X-ray crystallography.[23] The ^{31}P{^{1}H} NMR spectrum of cluster (6) contains two doublets. The first, centred at 48.89 ppm, may be assigned to the phosphorus atom of the triply bridging P(C$_6$H$_5$)(C$_9$H$_6$N) ligand moiety, while the second, centred at 27.24 ppm, is assigned to the phosphorus atom of the terminally co-ordinated Ph$_2$Pquin ligand. These assignments are made on the basis of comparison to the ^{31}P{^{1}H} NMR spectrum of the P(C$_6$H$_5$)(C$_5$H$_4$N)-capped cluster $[Ru_3\{\mu-\eta^2-C(O)(C_6H_5)\}\{\mu_3-\eta^2-P(C_6H_5)(C_5H_4N)\}(PPh_3)(CO)_8]$ which shows two doublets at similar chemical shifts.[23] The small coupling constant J(P-P) = 15.7 Hz indicates that the terminally bound Ph$_2$Pquin ligand is co-ordinated in a position *cis* to the phosphorus atom of the triply bridging P(C$_6$H$_5$)-(C$_9$H$_6$N) ligand fragment.[23,88] Furthermore, this ^{31}P{^{1}H} NMR spectral pattern correlates directly with the ^{31}P{^{1}H} NMR spectral pattern found

for the cluster $[Ru_3\{\mu-\eta^2-C(O)\{C_6H_5\}\}\{\mu_3-\eta^2-P(C_6H_5)(C_5H_4N)\}(PPh_3)-(CO)_8]$,[23] mentioned above. On the basis of these data, the following structure is proposed for cluster (6).
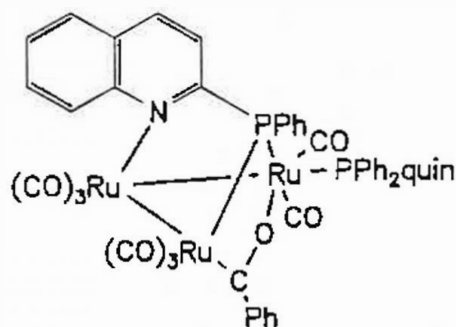
Figure 3.5: Proposed structure of $[Ru_3\{\mu-\eta^2-C(O)(C_6H_5)\}\{\mu_3-\eta^2-P(C_6H_5)-(C_9H_6N)\}(\eta^1-Ph_2Pquin)(CO)_8]$ **(6).**

The ^{13}C NMR spectrum of complex (6) shows a resonance at 302.56 ppm which is characteristic for the carbon atom of the bridging acyl group.[23] The signal consists of a doublet of doublets with overlapping inner peaks $(J_{(C-P)} = 3.9$ Hz) $i.e.$ the signal appears as a triplet. This indicates that the carbon atom of the acyl group couples to both the bridgehead phosphorus atom as well as to the phosphorus atom of the terminally co-ordinated Ph_2Pquin ligand. Since the ^{13}C NMR spectrum of $[Ru_3\{\mu-\eta^2-C(O)(C_6H_5)\}\{\mu_3-\eta^2-P(C_6H_5)(C_5H_4N)\}(PPh_3)(CO)_8]$ shows only a singlet for the carbon atom of the acyl group (at 302.6 ppm)[23] the possibility exists that the Ph_2Pquin ligand in cluster (6) may in fact be co-ordinated to the ruthenium atom to which the carbon atom of the acyl group is bound. However, if one considers the fact that cluster (6) may also be synthesized from $[Ru_3(\eta^1-Ph_2Pquin)_2(CO)_{10}]$ (4) (see Section 3.1.4) and if one examines closely the mechanism of this transformation (Scheme 3.1), it becomes clear that the pendant Ph_2Pquin ligand is indeed co-ordinated as shown in Figure 3.5.
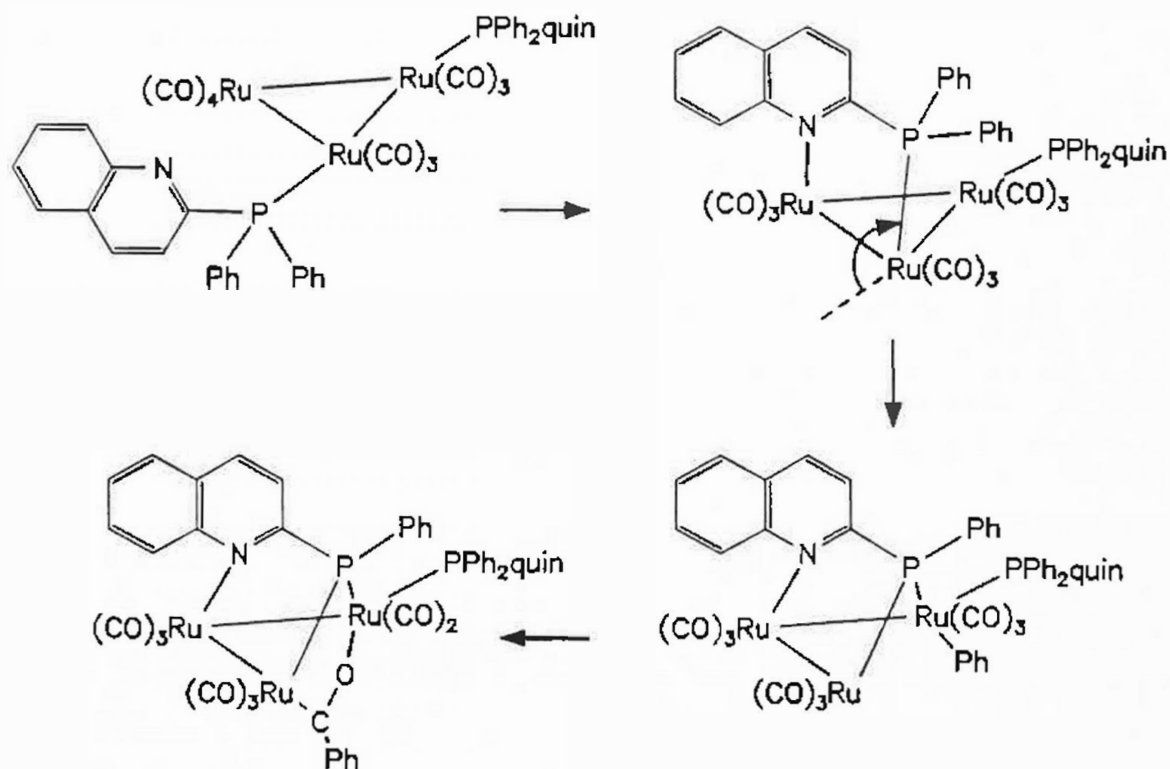
Scheme 3.1

Proposed mechanism for the formation of $[Ru_3\{\mu-\eta^2-C(O)(C_6H_5)\}\{\mu_3-\eta^2-P-(C_6H_5)(C_9H_6N)\}\{\eta^1-Ph_2Pquin\}(CO)_8]$ (6) from $[Ru_3(\eta^1-Ph_2Pquin)_2(CO)_{10}]$ (4)

3.2.2 Synthesis of $[Ru_3(\mu-H)\{\mu_3-\eta^2-P(C_6H_5)(C_9H_6N)\}(CO)_9]$ (7)

and $[PPN][Ru_3\{\mu_3-\eta^2-P(C_6H_5)(C_9H_6N)\}(CO)_9]$ (8)

Two methods were used in attempts to remove the acyl group from the

cluster $[Ru_3\{\mu-\eta^2-C(O)(C_6H_5)\}\{\mu_3-\eta^2-P(C_6H_5)(C_9H_6N)\}(CO)_9]$ (3). In the

first method cluster (3) was reacted with molecular hydrogen to afford

the hydride cluster $[Ru_3(\mu-H)\{\mu_3-\eta^2-P(C_6H_5)(C_9H_6N)\}(CO)_9]$ (7) and

benzene. The reaction was carried out in refluxing cyclohexane, the

higher temperature being necessary to effectively labilize the acyl

group. Cluster (7) was isolated as an orange powder by removal of the solvent followed by crystallization of the residue from a dichloro-methane/methanol solution. Finally, traces of a brown decomposition product were removed by washing with methanol. The band pattern of the $\nu(CO)$ stretching peaks in the infrared spectrum of cluster (7) (Table 3.17) is the same as that found for the analogous cluster $[Ru_3(\mu-H)\{\mu_3-\eta^2-P(C_6H_5)(C_5H_4N)\}(CO)_9]$.[35] The $^{31}P\{^1H\}$ NMR spectrum shows a singlet at 114.57 ppm in contrast to the starting material which exhibits a single resonance at 48.05 ppm. It has been suggested[88] that the chemical shift of the phosphorus atom of bridging phosphido ligands in metal clusters depends largely on the metal-phosphorus-metal bond angle, with a decreased bond angle generally resulting in a downfield shift. The change from a bridging acyl group (3-electron donor) in cluster (3) to a bridging hydride (1-electron donor) in cluster (7) means that the number of cluster valence electrons decreases from fifty to forty-eight. This decrease in cluster electrons is balanced by the formation of a metal-metal bond between the ruthenium atoms across which the phosphorus atom of the $P(C_6H_5)(C_9H_6N)$ ligand moiety bridges. Clearly, the shortening of the ruthenium-ruthenium distance from a non-bonding to a bonding value must cause a significant decrease in the Ru-P-Ru bond angle (see discussion of the crystal structure of (7) below). It is this decrease in bond angle which causes the large downfield shift for the bridging phosphorus atom when going from cluster (3) to cluster (7). The ^1H NMR spectrum shows a resonance at -15.31 ppm, typical of a bridging hydride. The signal is a doublet ($J_{P-H} = 24.6$ Hz) indicating coupling of the hydrogen to the bridgehead phosphorus atom. A single crystal X-ray diffraction study was carried out to confirm the structure of the cluster. Figure 3.6 gives a perspective view of the molecule showing the atom labelling scheme. Interatomic distances and interatomic angles are given in Tables 3.7 and 3.8 respectively.
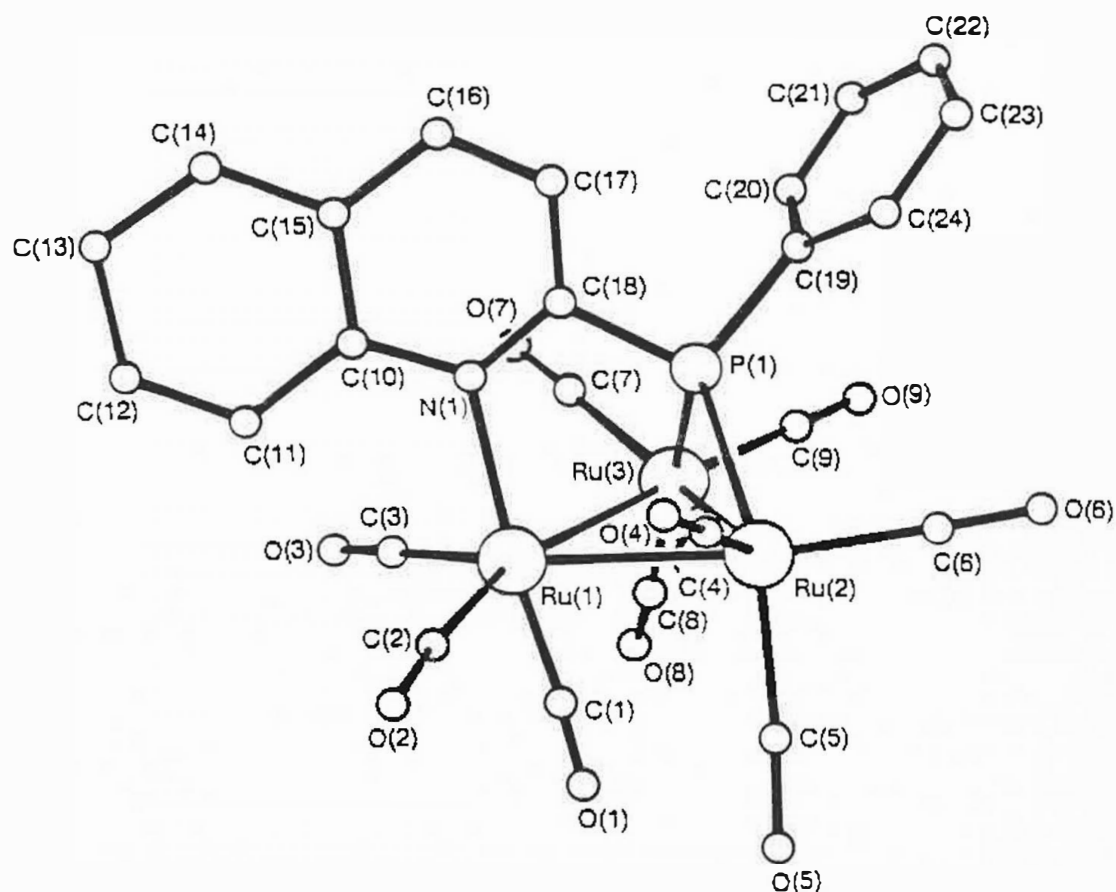
Figure 3.6: Perspective view of $[Ru_3(\mu-H)\{\mu_3-\eta^2-P(C_6H_5)(C_9H_6N)\}(CO)_9]$
(7) showing the atom labelling scheme

Cluster (7) is a 48-electron cluster containing a closed triangle of ruthenium atoms with one edge {Ru(2)-Ru(3) = 2.933(1)Å} slightly longer than the other two {Ru(1)-Ru(2) = 2.815(1)Å, Ru(1)-Ru(3) = 2.807(1)Å}. This edge is symmetrically bridged by the phosphorus atom of the $P(C_6H_5)C_9H_6N$ ligand moiety {P(1)-Ru(2) = 2.315(3)Å, P(1)-Ru(3) =

2.304(3)Å}. The Ru(2)-P(1)-Ru(3) bond angle of 78.8(1)° is much smaller
than the value of 100.6(1)° found for the angle subtended at the
phosphorus atom in cluster (3). As was discussed above, it is the large
decrease in this bond angle which accounts for the large downfield shift
of the resonance associated with the bridging phosphorus atom in cluster
(7) as compared to that for the bridging phosphorus atom in cluster
(3).[88] Examination of the residual electron density in the difference
Fourier map showed evidence for a hydrogen atom in a bridging position
between Ru(2) and Ru(3) *i.e.* between the two ruthenium atoms which are
also bridged by the phosphido group. However, its position could not be
located with certainty and, therefore, it was assumed that the hydrogen
atom bridges this edge of the Ru_3 triangle. Certainly, by adopting this
position, approximate C_s symmetry is maintained for the cluster, the
mirror plane passing through the hydrogen atom, the phosphorus atom, the
quinoline unit, the unique ruthenium atom Ru(1), as well as C(1), O(1) ,
C(22) and C(19) and bisecting the Ru(2)-Ru(3) bond (see Figure 3.6).
Table 3.9 shows the results of the meanplane calculations[89] for cluster
(7). The distances of the carbonyl ligands and ruthenium atoms from the
meanplane clearly indicate that the $P(C_6H_5)(C_9H_6N)$ ligand moiety caps
the cluster face symmetrically, with the carbonyl ligands also position-
ing themselves such that overall C_s symmetry is attained by the cluster.
Indeed, Hardcastle and co-workers[65] calculated the position of the
hydrogen atom in the closely related cluster $[Ru_3(\mu-H)(\mu_3-Spy)(CO)_9]$ and
found that it lies on the molecular symmetry plane passing through the
Spy ligand moiety.

Removal of the acyl group of cluster (3) was also achieved by treatment
of this cluster with one mole equivalent of bis(triphenylphosphine)-
imminium borohydride [PPN][BH_4] in a refluxing THF solution, the
solution colour changing from bright orange to dark brown. The

resultant anionic cluster $[PPN][Ru_3\{\mu_3\text{-}\eta^2\text{-}P(C_6H_5)(C_9H_6N)\}(CO)_9]$ (8) (Scheme 3.2) was isolated as a brown solid by removal of the solvent and
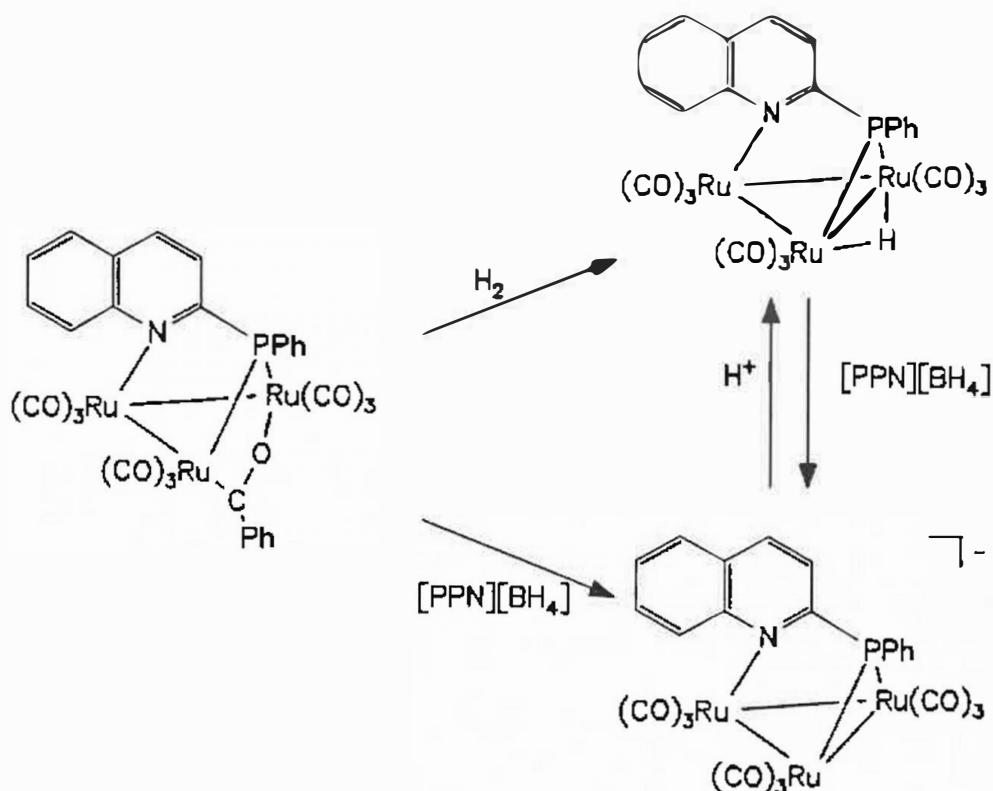
Scheme 3.2: Transformations on the surface of $[Ru_3\{\mu\text{-}\eta^2\text{-}C(O)(C_6H_5)\}\text{-}$
$\{\mu_3\text{-}\eta^2\text{-}P(C_6H_5)(C_9H_6N)\}(CO)_9]$ (3)

crystallization of the residue from a dichloromethane/hexane solution. This procedure removes the benzaldehyde which is a side product of the above reaction. The pattern of the $\nu(CO)$ stretching bands in the infrared spectrum of complex (8) (Table 3.17) shows an overall shift of ca. 50 cm^{-1} to lower wavenumbers when compared to the parent cluster (3), a feature typical for anionic clusters. The band pattern is also very similar to that for the analogous complex $[PPN][Ru_3\{\mu_3\text{-}\eta^2\text{-}P(C_6H_5)\text{-}$ $(C_5H_4N)\}(CO)_9]$.[35] The $^{31}P\{^1H\}$ NMR spectrum of complex (8) reveals two

singlets. The first at 20.04 ppm, is typical of the [PPN] cation while the second, at 136.64 ppm, is assigned to the phosphorus atom of the face-capping ligand moiety. The fact that the two signals are not coupled also points to the cluster being ionic with separated cations and anions in solution. Subsequent titration of the anionic cluster (8) with trifluoroacetic acid in THF solution affords the neutral hydrido cluster (7) described above. The reverse reaction, *i.e.* the deprotonation of the hydrido complex (7) by [PPN][BH$_4$] (carried out in a manner analogous to the de-acylation of cluster (3)) afforded the anionic cluster (8). It has been proposed[35] that the [PPN] cation provides improved stabilization of large cluster anions. This does indeed appear to be true since attempts to achieve the deprotonation of cluster (7) with sodium borohydride led only to cluster degradation. Scheme 3.2 summarizes the reactions discussed in Section 3.2.2.

3.2.3 Synthesis of [Ru$_3$(μ-H){μ_3-η^2-P(C$_6$H$_5$)(C$_9$H$_6$N)} (η^1-Ph$_2$Pquin)(CO)$_8$] (9)

The cluster [Ru$_3$(μ-H){μ_3-η^2-P(C$_6$H$_5$)(C$_9$H$_6$N)}(η^1-Ph$_2$Pquin)(CO)$_8$] (9) was synthesized both by the de-acylation of [Ru$_3${μ-η^2-C(O)(C$_6$H$_5$)}{μ_3-η^2-P(C$_6$H$_5$)(C$_9$H$_6$N)}(η^1-Ph$_2$Pquin)(CO)$_8$] (6) using molecular hydrogen and by substitution of one carbonyl ligand of the hydrido cluster [Ru$_3$(μ-H){μ_3-η^2-P(C$_6$H$_5$)(C$_9$H$_6$N)}(CO)$_9$] (7) by Ph$_2$Pquin. The former reaction, carried out in refluxing cyclohexane to effectively labilize the acyl group, (*cf.* Section 3.2.2) only affords cluster (9) in low yield due to the instability of this cluster at higher temperatures. The latter synthesis involves treatment of [Ru$_3$(μ-H){μ_3-η^2-P(C$_6$H$_5$)(C$_9$H$_6$N)}(CO)$_9$] (7) with one mole equivalent of Ph$_2$Pquin in THF at room temperature without the use of a catalyst (*cf.* Section 3.2.1). The solution gradually changes colour from orange to red. The cluster, an orange

powder, was isolated in high yield by thin layer chromatography followed by crystallization from a THF/methanol solution.

The pattern of the ν(CO) stretching peaks in the infrared spectrum of cluster (9) (Table 3.17) is very similar to that found for one of the starting materials *viz.* [Ru$_3${μ-η^2-C(O)(C$_6$H$_5$)}{μ_3-η^2-P(C$_6$H$_5$)(C$_9$H$_6$N)}(η^1-Ph$_2$Pquin)(CO)$_8$] (6) (Table 3.17) indicating that the two clusters have the same distribution of carbonyl ligands. The ^{31}P{^{1}H} NMR spectrum of cluster (9) exhibits two doublets, one at 129.47 ppm and the other at 36.43 ppm. The downfield doublet may be assigned to the bridgehead phosphorus atom on the basis of a comparison with the ^{31}P{^{1}H} NMR spectrum of the parent hydrido cluster (7) which also exhibits a low-field resonance (at 114.57 ppm) due to the bridgehead phosphorus atom. The higher field doublet is assigned to the phosphorus atom of the pendant Ph$_2$Pquin ligand and is found in the expected range.[88] The small coupling constant ($J_{(P-P)}$ = 13.4 Hz) for these doublets indicates that the pendant Ph$_2$Pquin ligand is in a position *cis* to that of the bridge-head phosphorus atom.[35,88] The ^{1}H NMR spectrum of cluster (9) shows a resonance centred at -14.50 ppm, such a highfield position being typical of a bridging hydride ligand. This set occurs as a doublet of doublets indicating coupling of the hydride with the phosphorus atoms of both the bridging ligand moiety P(C$_6$H$_5$)(C$_9$H$_6$N) and the pendant Ph$_2$Pquin ligand ($J_{(P-H)}$ = 21.1 Hz and 15.0 Hz). On the basis of these data the following structure is proposed for cluster (9).
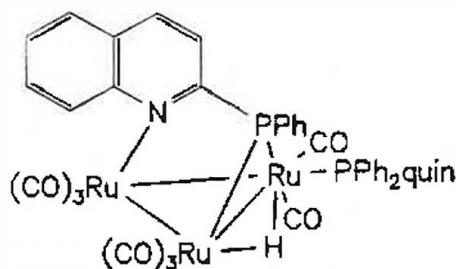
Figure 3.7: Proposed structure of $[Ru_3(\mu-H)\{\mu_3-\eta^2-P(C_6H_5)(C_9H_6N)\}-(\eta^1-Ph_2Pquin)(CO)_8]$ (9)

3.3 REACTIONS OF $[Ru_3\{\mu-\eta^2-C(O)(C_6H_5)\}\{\mu_3-\eta^2-P(C_6H_5)(C_9H_6N)\}(CO)_9]$ (3) WITH DIPHENYLPHOSPHINE AND SUBSEQUENT REACTIONS

3.3.1 Synthesis of $[Ru_3\{\mu-\eta^2-C(O)(C_6H_5)\}\{\mu_3-\eta^2-P(C_6H_5)(C_9H_6N)\}-(PPh_2H)(CO)_8]$ (10)

As found for the reaction of Ph$_2$Pquin with cluster (3) (Section 3.2.1), diphenylphosphine (PPh$_2$H) reacts with this cluster at ambient temperature and without the aid of a catalyst to afford $[Ru_3\{\mu-\eta^2-C(O)(C_6H_5)\}-\{\mu_3-\eta^2-P(C_6H_5)(C_9H_6N)\}(PPh_2H)(CO)_8]$ (10). The reaction was carried out in THF with the colour of the solution gradually changing from orange to red. Cluster (10) was isolated as a red powder by means of thin layer chromatography followed by crystallization from a THF/methanol solution. The ν(CO) stretching peaks in the infrared spectrum of cluster (10) (Table 3.17) occur with the same band pattern as that found for the analogous P(C_6H_5)(C_5H_4N) complex $[Ru_3\{\mu-\eta^2-C(O)(C_6H_5)\}\{\mu_3-\eta^2-P(C_6H_5)-(C_5H_4N)\}(PPh_2H)(CO)_8]$[35], indicating that the same carbonyl ligand distribution is present in the two complexes. The $^{31}P\{^1H\}$ NMR spectrum of cluster (10) (Figure 3.8) indicates the presence of two isomers of

this cluster in solution.
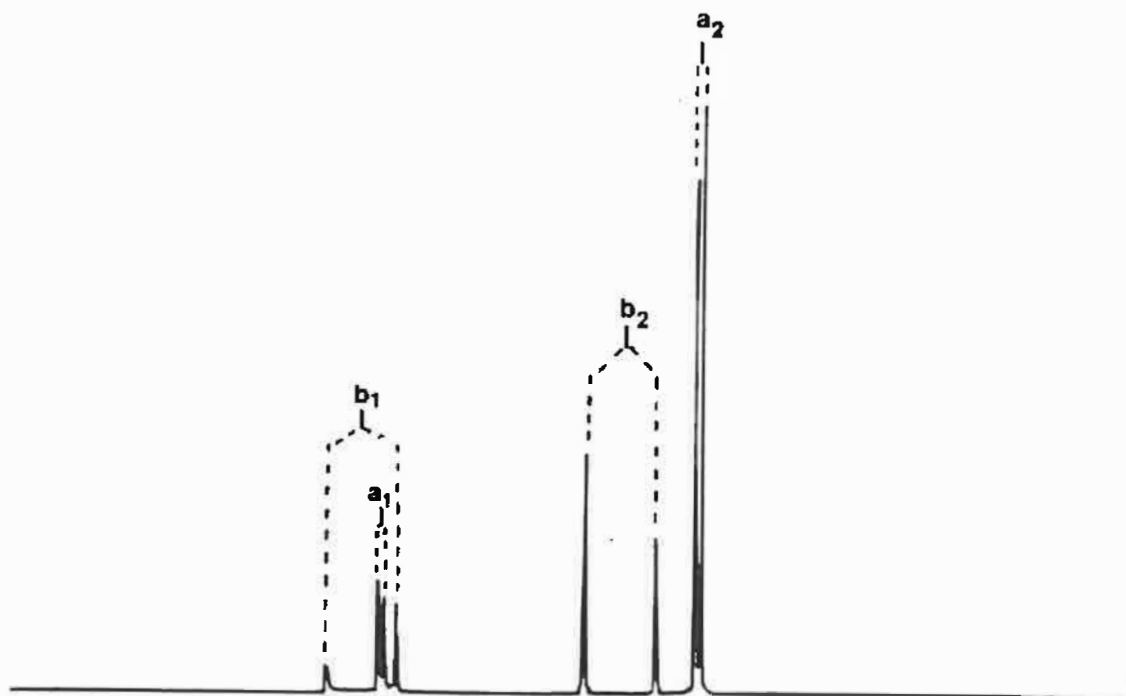
Figure 3.8: $^{31}P\{^1H\}$ NMR spectrum of $[Ru_3\{\mu-\eta^2-C(O)(C_6H_5)\}\{\mu_3-\eta^2-P(C_6H_5)(C_9H_6N)\}(PPh_2H)(CO)_8]$ (10) measured in CH_2Cl_2

Assignments of the sets of resonances in this spectrum to the various phosphorus atoms present have been made by comparison with the $^{31}P\{^1H\}$ NMR spectrum of the analogous cluster $[Ru_3\{\mu-\eta^2-C(O)(C_6H_5)\}\{\mu_3-\eta^2-P(C_6H_5)(C_5H_4N)\}(PPh_2H)(CO)_8]^{[35]}$ and cluster (6). The doublets labelled a_1 and a_2, centred at 48.24 ppm and 16.88 ppm, are assigned to the phosphorus atoms of the bridging ligand moiety $P(C_6H_5)(C_9H_6N)$ and of the terminal PPh_2H ligand of isomer "a" respectively. The small coupling constant ($J_{(P-P)}$ = 17.0 Hz) is typical of *cis* disposed phosphorus atoms[23,88], indicating that the pendant PPh_2H ligand is in a position *cis* to the bridgehead phosphorus atom. The other pair of doublets b_1 and b_2, centred at 50.48 ppm and 24.10 ppm are assigned to the phosphorus atoms of the bridging ligand moiety $P(C_6H_5)(C_9H_6N)$ and of the terminal PPh_2H ligand of isomer "b" respectively. Here the coupling constant is large ($J_{(P-P)}$ = 233.6 Hz). This is typical of *trans* disposed phosphorus atoms[23,88] indicating that, in this isomer, the

pendant PPh$_2$H ligand is in a position *trans* to the bridgehead phosphorus atom. The relative intensities of the peaks in the ^{31}P{^{1}H} NMR spectrum also indicate that a larger amount of isomer "a" than isomer "b" is present in solution. This was also found for the analogous P(C$_6$H$_5$)-(C$_5$H$_4$N)-capped cluster mentioned above where the *cis/trans* ratio is 10:1. The ^{13}C NMR spectrum of cluster (10) also indicates the presence of two isomers in solution. Two sets of resonances were identified. These are a doublet of doublets centred at 302.13 ppm which appears as a triplet because the phosphorus-carbon coupling constants are virtually identical ($J_{(C-P)}$ = 5.5 Hz and 5.6 Hz) and a doublet of doublets centred at 301.60 ppm ($J_{(C-P)}$ = 3.0 Hz and 6.0 Hz). Since the ^{13}C NMR spectrum of the analogous P(C$_6$H$_5$)(C$_5$H$_4$N)-capped cluster, mentioned above, only showed a single resonance at 276.6 ppm,[23] tentative assignments were made by comparing the relative intensities of the two sets of resonances in the ^{13}C NMR spectrum of cluster (10) and noting that in the ^{31}P{^{1}H} NMR spectrum of this cluster the more intense peaks are assigned to the *cis* isomer "a" and the smaller peaks to the *trans* isomer "b". Thus, the triplet at 302.13 ppm, which has the smaller integral, is assigned to the carbon atom of the acyl group in the *trans* isomer "b" while the doublet of doublets, centred at 301.60 ppm, which has the larger integral, is assigned to the carbon atom of the acyl group in the *cis* isomer "a". In both cases the phosphorus-carbon coupling constants are small indicating that the pendant PPh$_2$H ligand is in a position *cis* to the acyl group. Based on the above infrared and NMR data the following structures are proposed for the two isomers of cluster (10). Note that the pendant PPh$_2$H ligand is drawn attached to the ruthenium atom to which the acyl oxygen is bonded, in line with the conclusions drawn in Section 3.2.1 with regard to the site of co-ordination of the Ph$_2$Pquin ligand in [Ru$_3$\{μ-η^2-C(O)(C$_6$H$_5$)\}\{μ_3-η^2-P(C$_6$H$_5$)(C$_9$H$_6$N)\}(η^1-Ph$_2$Pquin)(CO)$_8$] (6).
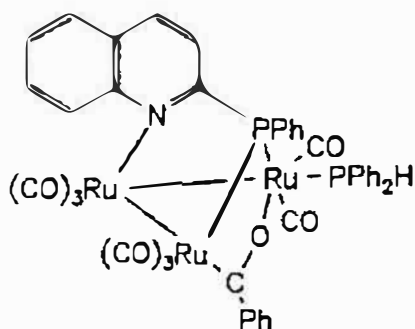
Figure 3.9
Proposed Structure of isomer "a"
of [Ru$_3$\{μ-η^2-C(O)(C$_6$H$_5$)\}\{μ_3-η^2-
P(C$_6$H$_5$)(C$_9$H$_6$N)\}(PPh$_2$H)(CO)$_8$] (10)
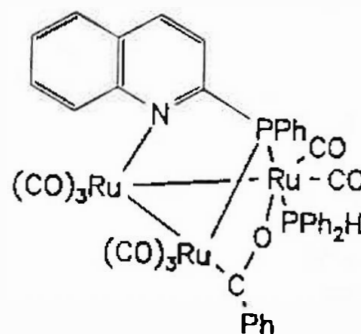
Figure 3.10
Proposed Structure of isomer "b"
of [Ru$_3$\{μ-η^2-C(O)(C$_6$H$_5$)\}\{μ_3-η^2-
P(C$_6$H$_5$)(C$_9$H$_6$N)\}(PPh$_2$H)(CO)$_8$] (10)

3.3.2 Synthesis of [Ru$_3$\{μ_3-η^2-P(C$_6$H$_5$)(C$_9$H$_6$N)\}(μ-PPh$_2$)(μ-CO)$_2$(CO)$_6$] (11)

The most important difference between the substituted acyl clusters [Ru$_3$\{μ-η^2-C(O)(C$_6$H$_5$)\}\{μ_3-η^2-P(C$_6$H$_5$)(C$_9$H$_6$N)\}(η^1-Ph$_2$Pquin)(CO)$_8$] (6) and [Ru$_3$\{μ-η^2-C(O)(C$_6$H$_5$)\}\{μ_3-η^2-P(C$_6$H$_5$)(C$_9$H$_6$N)\}(PPh$_2$H)(CO)$_8$] (10) lies in the availability, on the pendant ligand of the latter cluster, of a hydrogen atom which can be involved in further reaction. Mild thermolysis (80°C) of complex (10) in cyclohexane leads to a colour change from red to burgundy. The new cluster [Ru$_3$\{μ_3-η^2-P(C$_6$H$_5$)-(C$_9$H$_6$N)\}(μ-PPh$_2$)(μ-CO)$_2$(CO)$_6$] (11) was isolated as a burgundy-coloured crystalline solid by thin layer chromatography followed by crystallization from dichloromethane/methanol solution. The reaction involves addition of the phosphorus-hydrogen bond to the metal followed by reductive carbon-hydrogen coupling[35] to afford this cluster along with benzaldehyde as the organic product. No attempt was made to trace the organic product.

The presence of the bridging carbonyl groups was confirmed by means of infrared spectroscopy, the $\nu(CO)$ region showing a peak at 1830 cm^{-1}, characteristic of bridging carbonyl ligands. The $^{31}P\{^{1}H\}$ NMR spectrum of cluster (11) contains a resonance at the surprisingly low field of 369.00 ppm, a region where the phosphorus atom of phosphinidine, rather than of phosphido, groups usually resonate,[88,96] as well as a resonance at 41.03 ppm. The latter occurs in the range normally reported for bridging phosphido groups.[88] The question thus arises as to whether this downfield resonance should be assigned to the phosphorus atom of the PPh$_2$ or to that of the P(C$_6$H$_5$)(C$_9$H$_6$N) ligand moiety. Bonnet and co-workers[35] also observed a very lowfield resonance in the $^{31}P\{^{1}H\}$ NMR spectrum of the analogous cluster [Ru$_3$\{μ_3-η^2-P(C$_6$H$_5$)(C$_5$H$_4$N)\}(μ-PPh$_2$)-(μ-CO)$_2$(CO)$_6$] which they assigned to the phosphorus atom of the bridging diphenylphosphido group. On the basis of their assignment[35] we also assign the downfield resonance to the phosphorus atom of the bridging PPh$_2$ ligand moiety in cluster (11). The low coupling constant ($J_{(P-P)}$ = 15.1 Hz) indicates that the two phosphorus atoms are *cis* to one another, which implies that the μ-PPh$_2$ group must occupy an equatorial position between the two ruthenium atoms which it bridges (Figure 3.11). The structure was confirmed by a single crystal X-ray diffraction study. Figure 3.11 gives a perspective view of cluster (11). Tables 3.13 and 3.14 list the interatomic distances and interatomic angles respectively.

Cluster (11) is a 48-electron cluster containing a closed triangle of ruthenium atoms {Ru(1)-Ru(2) = 2.760(1)Å, Ru(1)-Ru(3) = 2.844(1)Å, Ru(2)-Ru(3) = 2.827(1)Å}. The shortest edge, Ru(1)-Ru(2), is bridged by both a carbonyl ligand, which occupies an equatorial position, and by the phosphorus atom of the capping P(C$_6$H$_5$)(C$_9$H$_6$N) ligand fragment which occupies an axial position. The Ru(2)-Ru(3) edge is bridged by a carbonyl ligand which occupies an equatorial position between these two
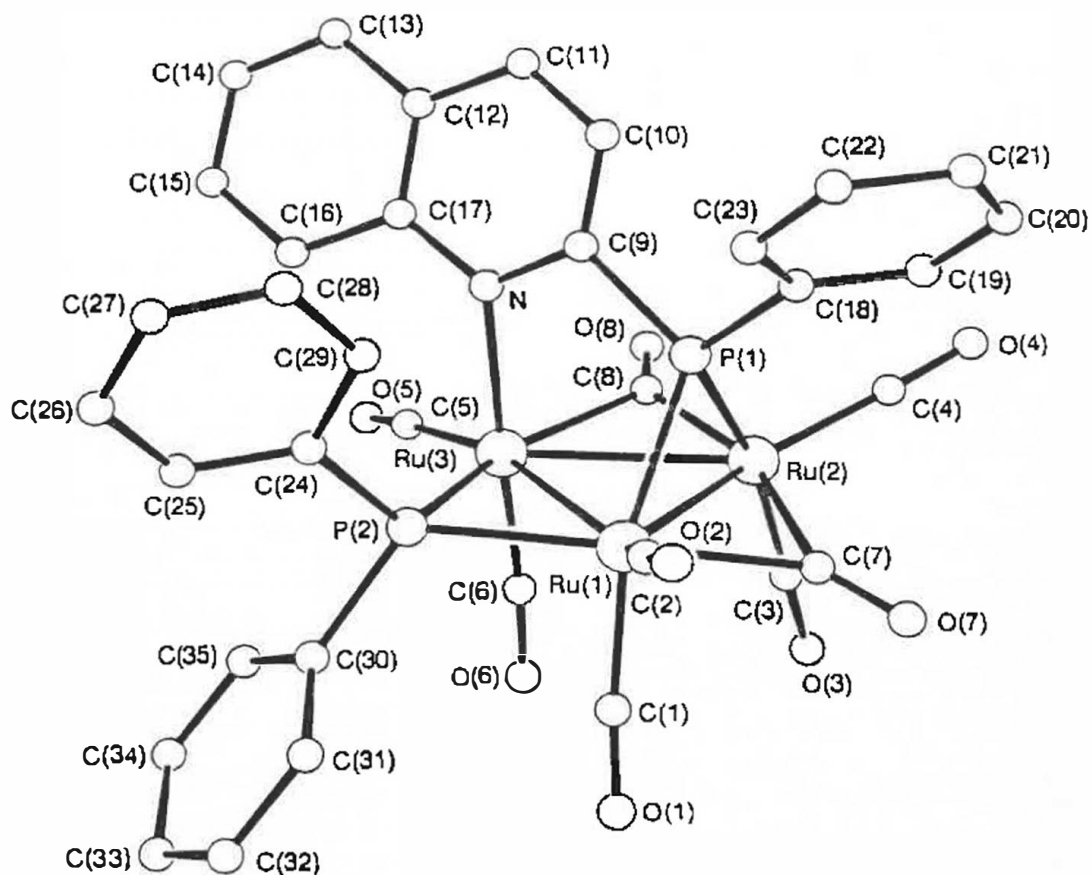
Figure 3.11: A perspective view of cluster $[Ru_3\{\mu_3-\eta^2-P(C_6H_5)(C_9H_6N)\}-(\mu-PPh_2)(\mu-CO)_2(CO)_6]$ (11) showing the atom labelling scheme

ruthenium atoms. The third edge, Ru(1)-Ru(3), is bridged by a PPh$_2$ ligand fragment with the phosphorus atom of this group occupying an equatorial position between Ru(1) and Ru(3). The angles subtended at the two phosphorus atoms by the ruthenium atoms to which they are bonded may be compared. These are 71.8(1)° and 74.5(1)° at P(1) and P(2)

respectively. As was discussed in Section 3.2.2 it has been proposed[88] that the chemical shift of the phosphorus atom of bridging phosphido ligands depends largely on the metal-phosphorus-metal bond angle with a decreased bond angle generally resulting in a downfield shift. Cluster (11) does not follow this trend. Firstly, the bond angle at P(1) is smaller by 7 degrees than the equivalent bond angle in $[Ru_3(\mu-H)\{\mu_3-\eta^2-P(C_6H_5)(C_9H_6N)\}(CO)_9]$ (7) while the chemical shift of the phosphorus atom of the capping $P(C_6H_5)(C_9H_6N)$ ligand moiety is 73.54 ppm further upfield in the former cluster than in the latter. Even more surprising is that the chemical shift of the phosphorus atom of the bridging PPh_2 group in cluster (11) occurs at 369.00 ppm, which is 327.97 ppm further downfield than the chemical shift of the bridgehead phosphorus atom, despite the fact that the bond angle at the former phosphorus atom is larger than that at the latter. It has been speculated[88] that a change from an equatorial to an axial position may influence the chemical shift of the phosphorus atom of a bridging phosphido group. However, too few clusters, with the same bridging phosphido ligand in both axial and equatorial positions, have been synthesized to allow for a systematic study of the dependence of the bridging phosphorus atom's chemical shift on its co-ordination site.[88] As was found for clusters (3) and (7), the nitrogen atom of the capping $P(C_6H_5)(C_9H_6N)$ ligand moiety is co-ordinated to the ruthenium atom not bridged by the phosphorus atom of the same ligand fragment {Ru(3)-N(1) = 2.229(5)Å} providing increased stability to the trimetal core. It is also noteworthy that all three ruthenium atoms in cluster (11) are heptaco-ordinated, that is if the metal-metal bonds are included. As was discussed in Section 1.3, such a strained structure can only be partially stabilized by bridging carbonyl ligands and such a cluster probably would by very reactive. In fact, cluster (11) is likely to be even more reactive than the analogous $P(C_6H_5)(C_5H_4N)$-capped complex $[Ru_3\{\mu_3-\eta^2-P(C_6H_5)(C_5H_4N)\}(\mu-PPh_2)(\mu-CO)_2-$

$(CO)_6$] because of the increased steric demands of the capping $P(C_6H_5)$-(C_9H_5N) ligand moiety in cluster (11) as opposed to the $P(C_6H_5)(C_5H_4N)$ ligand moiety in the $P(C_6H_5)(C_5H_4N)$-capped complex mentioned above. That this is indeed the case has been clearly demonstrated by the high degree of reactivity of cluster (11) towards both phosphorus ligands and carbon monoxide (discussed below), the analogous $P(C_6H_5)(C_5H_4N)$-capped cluster being less reactive to the same molecules.[35]

3.3.3 Synthesis of [Ru$_3${μ_3-η^2-P(C$_6$H$_5$)(C$_9$H$_6$N)}{μ-PPh$_2$)(CO)$_9$] (12)

Reaction of [Ru$_3${μ_3-η^2-P(C$_6$H$_5$)(C$_9$H$_6$N)}(μ-PPh$_2$)(μ-CO)$_2$(CO)$_6$] (11) with carbon monoxide in dichloromethane solution at room temperature, affords the nonacarbonyl cluster [Ru$_3${μ_3-η^2-P(C$_6$H$_5$)(C$_9$H$_6$N)}(μ-PPh$_2$)(CO)$_9$] (12) extremely rapidly, the conversion being complete in about 20 seconds. It appears that all that is required is for the solution to become saturated with carbon monoxide, the reaction itself being almost instantaneous. Comparing this to the ca. 30 minutes required for the conversion of the analogous $P(C_6H_5)(C_5H_4N)$-capped complex [Ru$_3${μ_3-η^2-P(C$_6$H$_5$)(C$_5$H$_4$N)}(μ-PPh$_2$)(μ-CO)$_2$(CO)$_6$] to the nonacarbonyl[35] cluster, confirms that the increased steric strain in cluster (11) does indeed result in an increase in its reactivity. Reduction of the solvent volume by continuous bubbling of CO gas through the solution followed by addition of hexane and refrigeration at $-30°C$ led to the precipitation of cluster (12) as an orange solid. However, cluster (12) was found to decarbonylate very readily even in the solid state, and a suitably pure sample for microanalysis could not be obtained. The cluster was spectroscopically analyzed in CH$_2$Cl$_2$ solution under a carbon monoxide atmosphere (see below). Decarbonylation of cluster (12) in a dichloro-methane solution is also readily effected by bubbling argon through the solution, the reaction being complete within ca. 45 seconds.

The interconversion between cluster (11), a 48-electron cluster, and cluster (12), a 50-electron cluster, involves the reversible opening and closing of one of the edges of the triruthenium framework. Only a limited number of such reactions on addition or removal of carbon dioxide are known. Examples include the reversible addition of CO to $[Ru_3\{\mu_3-\eta^2-P(C_6H_5)(C_5H_4N)\}(\mu-PPh_2)(\mu-CO)_2(CO)_6]$ to afford $[Ru_3\{\mu_3-\eta^2-P(C_6H_5)(C_5H_4N)\}(\mu-PPh_2)(CO)_9]$,[35] the reversible addition of CO to $[Ru_3(\mu_3-PPh)(\mu_2-PPh_2)_2(CO)_7]$ to afford $[Ru_3(\mu_3-PPh)(\mu_2-PPh_2)_2(CO)_{7+n}]$[91] (n = 1-3), the reversible addition of CO to $[Fe_2Mn(\mu_3-PPh)(\eta^5-C_5H_5)(CO)_8]$ to afford $[Fe_2Mn(\mu_3-PPh)(\eta^5-C_5H_5)(CO)_{8+n}]$ (n = 1 or 2)[92] and the reversible addition of CO to $[Ru_4(\mu_4-PPh)_2(\mu-CO)_2(CO)_{10}]$ to afford $[Ru_4(\mu_4-PPh)_2(CO)_{13}]$.[93]

All the carbonyl ligands present in $[Ru_3\{\mu_3-\eta^2-P(C_6H_5)(C_9H_6N)\}(\mu-PPh_2)-(CO)_9]$ (12) occupy terminal positions as indicated by the $\nu(CO)$ bands in the infrared spectrum of this cluster (Table 3.17). The $\nu(CO)$ pattern of cluster (12) is the same as was found for the analogous $P(C_6H_5)-(C_5H_4N)$-capped cluster $[Ru_3\{\mu_3-\eta^2-P(C_6H_5)(C_5H_4N)\}(\mu-PPh_2)(CO)_9]$.[35] The $^{31}P\{^1H\}$ NMR spectrum of cluster (12) shows two doublets, one centred at 122.43 ppm and the other centred at an unusually highfield position of -14.99 ppm. At first it was not clear to which phosphorus atom in cluster (12) the highfield resonance should be assigned, since no such assignments had been made for the analogous cluster $[Ru_3\{\mu_3-\eta^2-P(C_6H_5)-(C_5H_4N)\}(\mu-PPh_2)(CO)_9]$[35], which shows two doublets centred at 116.4 ppm and 7.2 ppm.[35] It is, however, possible to assign these resonances to specific phosphorus atoms in the $P(C_6H_5)(C_5H_4N)$-capped cluster if one looks at the X-ray structure of this cluster[35] (Figure 3.12).
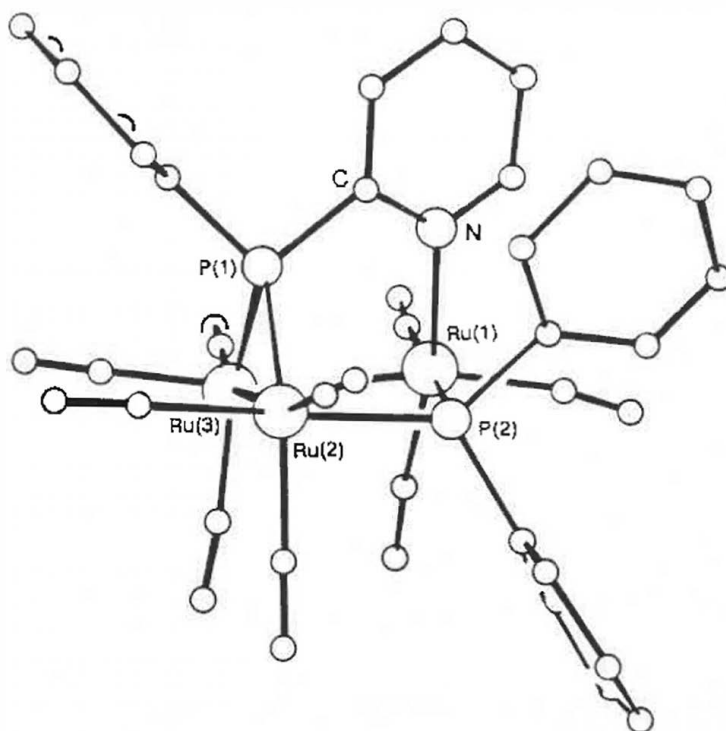
Figure 3.12: Crystal structure of
$[Ru_3\{\mu_3-\eta^2-P(C_6H_5)(C_5H_4N)\}(\mu-PPh_2)(CO)_9]$ [35]

The open Ru-Ru edge in this cluster is the edge which is bridged by the

PPh_2 group. As a result, the Ru(1)-P(2)-Ru(2) bond angle is large

(106.4°). The Ru(2)-P(1)-Ru(3) bond angle, which involves the capping

$P(C_6H_5)(C_5H_4N)$, group is more than 30 degrees smaller (76.04°). Now if

one considers that in general the smaller metal-phosphorus-metal bond

angle for a bridging phosphido ligand means that the chemical shift of

the phosphorus atom of that bridging ligand will be further downfield,[88]

then one must clearly assign the downfield resonance (116.4 ppm) in the

$^{31}P\{^1H\}$ NMR spectrum of the $P(C_6H_5)(C_5H_4N)$-capped cluster to the phos-

phorus atom of the capping $P(C_6H_5)(C_5H_4N)$ ligand moiety. The upfield

resonance (7.2 ppm) can then be assigned to the phosphorus atom of the

bridging PPh_2 group. On the basis of these assignments one can then

assign the downfield resonance (122.43 ppm) in the $^{31}P\{^1H\}$ NMR spectrum

of cluster (12) to the phosphorus atom of the capping $P(C_6H_5)(C_9H_6N)$

ligand moiety, while the high field resonance at -14.99 ppm can be

assigned to the phosphorus atom of the bridging PPh_2 group. Thus, the opening of a Ru-Ru bond on the addition of a carbonyl ligand to cluster (11) to form cluster (12) and the consequent increase in the Ru-P-Ru bond angle involving the bridging PPh_2 group, causes a remarkable change in the chemical shift of the phosphorus atom of the bridging PPh_2 group, a change from 369.00 ppm in cluster (11) to -14.99 ppm in cluster (12).
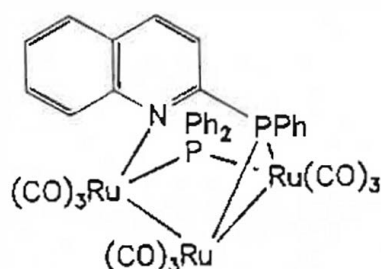
Figure 3.13: Proposed structure of
$[Ru_3\{\mu_3-\eta^2-P(C_6H_5)(C_9H_6N)\}(\mu-PPh_2)(CO)_9]$ (12)

3.3.4 Synthesis of $[Ru_3\{\mu_3-\eta^2-P(C_6H_5)(C_9H_6N)\}(\mu-PPh_2)_2(\mu-H)(CO)_6]$ (13)

Attempts to substitute one carbonyl ligand in $[Ru_3\{\mu_3-\eta^2-P(C_6H_5)(C_9H_6-N)\}(\mu-PPh_2)(\mu-CO)_2(CO)_6]$ (11) by triphenylphosphine were unsuccessful, the products of the reaction being highly unstable and decomposing almost instantaneously; the decomposition products were not identified. However, the reaction of complex (11) with a mole equivalent of diphenylphosphine in THF at room temperature proceeds very rapidly with a colour change from burgundy to brown, to afford the new cluster $[Ru_3\{\mu_3-\eta^2-P(C_6H_5)(C_9H_6N)\}(\mu-PPh_2)_2(\mu-H)(CO)_6]$ (13). The reaction is complete within ca. 20 seconds. The equivalent reaction for the analogous $P(C_6H_5)(C_5H_4N)$-capped cluster takes 12 hours to reach completion. This again illustrates the enhanced reactivity of the

$P(C_6H_5)(C_9H_6N)$-capped cluster (11) as opposed to the analogous $P(C_6H_5)$-(C_5H_4N)-capped cluster. Two isomers of cluster (13), namely (13a) and (13b), were isolated as orange and red crystalline products respectively by thin layer chromatography followed by crystallization from a dichloromethane/methanol solution. The difference between the reaction of cluster (11) with triphenylphosphine and its reaction with diphenyl-phosphine lies in the availability of a proton on the latter ligand which may undergo further reaction. The initial substituted product, assumed to be $[Ru_3\{\mu_3-\eta^2-P(C_6H_5)(C_9H_6N)\}(\mu-PPh_2)\{\mu-CO)_2(CO)_5(PPh_2H)]$, is highly unstable and is not isolated but rapidly converts to cluster (13). The equivalent triphenylphosphine substituted product is also highly unstable but can clearly not undergo the same rearrangement and therefore decomposes.

The $\nu(CO)$ pattern in the infrared spectrum of isomer (13a) (Table 3.17) is similar to that found for the symmetrical isomer of the analogous $P(C_6H_5)(C_5H_4N)$-capped cluster $[Ru_3\{\mu_3-\eta^2-P(C_6H_5)(C_5H_4N)\}(\mu-PPh_2)_2(\mu-H)-(CO)_6]$[35], indicating that the distribution of carbonyl ligands in both clusters is the same. The $^{31}P\{^1H\}$ NMR spectrum of isomer (13a) shows two sets of resonances. The first is a doublet, centred at a lowfield position of 247.72 ppm, while the second is a triplet, centred at 68.83 ppm. Bonnet and co-workers[35] observed two similar sets of resonances in the $^{31}P\{^1H\}$ NMR spectrum of the symmetrical isomer of the analogous $P(C_6H_5)(C_5H_4N)$-capped cluster mentioned above. They assigned the low-field resonance to the two phosphorus atoms of the two bridging PPh_2 groups and the higher field resonance to the phosphorus atom of the capping $P(C_6H_5)(C_5H_4N)$ ligand moiety. On the basis of their assignments, we also assign the lowfield resonance in the $^{31}P\{^1H\}$ NMR spectrum of isomer (13a) (247.72 ppm) to the bridging PPh_2 groups. The triplet at 68.83 ppm is assigned to the phosphorus atom of the capping $P(C_6H_5)$-

(C_9H_6N) ligand moiety. This triplet in fact consists of a doublet of doublets with the two inner peaks overlapping. This occurs because the coupling of the phosphorus atom of the capping $P(C_6H_5)(C_9H_6N)$ moiety to each of the other phosphorus atoms in the bridging PPh_2 groups has the same magnitude ($J_{(P-P)}$ = 13.9 Hz). This in turn implies that the two PPh_2 groups occupy chemically equivalent positions on the cluster relative to the bridgehead phosphorus atom. The small magnitude of the coupling further suggests that the phosphorus atoms of the bridging PPh_2 groups occupy positions *cis* to the phosphorus atom of the capping $P(C_6H_5)(C_9H_6N)$ ligand moiety. The ^1H NMR spectrum of isomer (13a) shows a set of resonances centred at ~11.24 ppm, which is characteristic of a bridging hydride. The resonance is a doublet of triplets which implies that the hydride is coupled to two phosphorus atoms in equivalent positions (see above, $J_{(P-H)}$ = 19.4 Hz) and to another phosphorus atom in a different position ($J_{(P-H)}$ = 37.5 Hz). On the basis of the above infrared and NMR data, the following structure is proposed for isomer (13a).
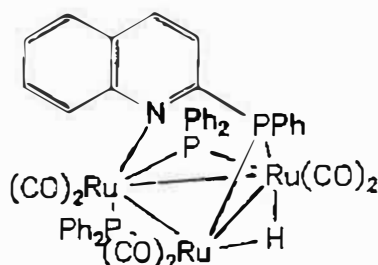
Figure 3.14: Proposed structure of isomer (13a) of
$[Ru_3\{\mu_3-\eta^2-P(C_6H_5)(C_9H_6N)\}(\mu-PPh_2)_2(\mu-H)(CO)_6]$ (13)

The $\nu(CO)$ pattern in the infrared spectrum of isomer (13b) (Table 3.17) is similar to that found for the asymmetrical isomer of the analogous

P(C_6H_5)(C_5H_4N)-capped cluster [$Ru_3\{\mu_3-\eta^2-P(C_6H_5)(C_5H_4N)\}(\mu-PPh_2)_2(\mu-H)-$($CO)_6$][35], indicating that the distribution of carbonyl ligands is the same in both clusters. The $^{31}P\{^1H\}$ NMR spectrum of isomer (13b) shows three sets of resonances. These are all doublets of doublets centred at 263.75 ppm, 200.28 ppm and 47.62 ppm respectively. Assignments to the various phosphorus atoms in isomer (13b) are made on the basis of comparison to the $^{31}P\{^1H\}$ NMR spectrum of the asymmetrical isomer of the P(C_6H_5)(C_5H_4N)-capped cluster which also contains three sets of doublets of doublets having similar chemical shifts[35] to those found for isomer (13b). Bonnet and co-workers[35] assigned the two lowfield sets of resonances to the two phosphorus atoms of the bridging PPh_2 groups and the higher field set of resonances to the phosphorus atom of the capping P(C_6H_5)(C_5H_4N) moiety. On the basis of these assignments, we assign the two doublets of doublets at 263.75 ppm and 200.28 ppm respectively to the phosphorus atoms of the bridging PPh_2 groups and the doublet of doublets at 47.62 ppm to the phosphorus atom of the capping P(C_6H_5)-(C_5H_4N) moiety. The fact that the sets of resonances for all three phosphorus atoms are doublets of doublets indicates that the phosphorus atoms all occupy chemically inequivalent positions in isomer (13b). The coupling between the phosphorus atoms of the two bridging PPh_2 groups is large (131.4 Hz) implying that these two groups must occupy positions *trans* to one another[88] in isomer (13b). The coupling between each of the phosphorus atoms of the bridging PPh_2 groups and the bridgehead phosphorus atom is much smaller (13.0 Hz and 73.2 Hz respectively) and one may therefore conclude that these phosphorus atoms occupy positions *cis* to one another[88] in isomer (13b). The ^1H NMR spectrum of isomer (13b) shows a set of resonances centred at -10.33 ppm which is characteristic of a bridging hydride. In this case the resonance is a doublet of doublets of doublets with coupling constants ($J_{(P-H)}$ = 9.1 Hz, 18.1 Hz and 32.9 Hz). This indicates that the hydride is coupled to

three phosphorus atoms which all occupy chemically inequivalent
positions in isomer (13b). On the basis of the above infrared and NMR
data, the following structure is proposed for isomer (13b).
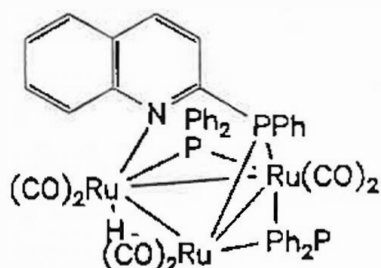
Figure 3.15: Proposed structure of isomer (13b) of
$[Ru_3\{\mu_3-\eta^2-P(C_6H_5)(C_9H_6N)\}(\mu-PPh_2)_2(\mu-H)(CO)_6]$ (13)

3.5 CONCLUSION

The reactions described in this chapter are summarized in Scheme 3.3

The reactions of the Ph_2Pquin ligand with $[Ru_3(CO)_{12}]$ are essentially
the same as those of the Ph_2Ppy ligand. Once co-ordinated to
$[Ru_3(CO)_{12}]$ the Ph_2Pquin ligand dephenylates spontaneously to afford a
capped cluster in a manner analogous to its pyridine analogue. The
presence of the capping $P(C_6H_5)(C_9H_6N)$ ligand moiety allows this cluster
to undergo a variety of further reactions without disintegration.
Although the products of these reactions are analogous to those obtained
from the equivalent reactions with the $P(C_6H_5)(C_5H_4N)$-capped cluster,
there are significant differences in the reactivity and stability of the
products. The most notable is the greatly enhanced reactivity of
$[Ru_3\{\mu_3-\eta^2-P(C_6H_5)(C_9H_6N)\}(\mu-PPh_2)(\mu-CO)_2(CO)_6]$ (11), as opposed to the
analogous $P(C_6H_5)(C_5H_4N)$-capped cluster $[Ru_3\{\mu_3-\eta^2-P(C_6H_5)(C_5H_4N)\}-$

$(\mu\text{-PPh}_2)(\mu\text{-CO})_2(\text{CO})_6]$, to both phosphorus ligands and carbon monoxide. Also the instability of the nonacarbonyl cluster $[\text{Ru}_3\{\mu_3\text{-}\eta^2\text{-P}(\text{C}_6\text{H}_5)\text{-}(\text{C}_9\text{H}_6\text{N})\}(\mu\text{-PPh}_2)(\text{CO})_9]$ (12), which prevented its isolation as a pure solid, may be contrasted with the stability of the analogous $\text{P}(\text{C}_6\text{H}_5)\text{-}(\text{C}_5\text{H}_4\text{N})$-capped cluster in the solid state. These differences may be partly due to differences in nitrogen-donor strengths of the quinoline and pyridine fragments, but are most likely due to increased steric demands of the quinoline fragment as opposed to the pyridine fragment in the capping ligands.

[Ru_3(CO)_{12}]

2Me_3NO
2MeCN

Ph_2Pquin/catalyst

[Ru_3(MeCN)_2(CO)_{10}]

4Me_3NO/2Ph_2Pquin

2Ph_2Pquin

[Ru_5(η^1–Ph_2Pquin)(CO)_n](2)

[Ru_3(η^1–Ph_2Pquin)_2(CO)_{10}](4)

Δ/low yield

[Ru_3(μ–η^2–Ph_2Pquin)_2(CO)_8](5)

Δ

Δ

[Ru_3{μ–η^2–C(O)(C_6H_5)}{μ_3–η^2–P(C_6H_5)(C_9H_6N)}(CO)_9](3)

Ph_2Pquin

[Ru_3{μ–η^2–C(O)(C_6H_5)}{μ_3–η^2–P(C_6H_5)(C_9H_6N)}(η^1–Ph_2Pquin)(CO)_9](6)

[PPN][BH_4]

H_2/Δ

H_2/Δ/low yield

PPh_2H

Ph_2Pquin

[PPN][Ru_3{μ_3–η^2–P(C_6H_5)(C_9H_6N)}(CO)_9](8)

CF_3COOH

[Ru_3(μ–H){μ_3–η^2–P(C_6H_5)(C_9H_6N)}(CO)_9](7)

[Ru_3(μ–H){μ_3–η^2–P(C_6H_5)(C_9H_6N)}(η^1–Ph_2Pquin)(CO)_8](9)

[PPN][BH_4]

Δ

+CO

−CO

[Ru_3{μ–η^2–C(O)(C_6H_5)}{μ_3–η^2–P(C_6H_5)(C_9H_6N)}(PPh_2H)(CO)_9](10)

[Ru_3{μ_3–η^2–P(C_6H_5)(C_9H_6N)}(μPPh_2)(μ–CO)_2(CO)_6](11)

[Ru_3{μ_3–η^2–P(C_6H_5)(C_9H_6N)}(μPPh_2)(CO)_9](12)

PPh_2H

[Ru_3{μ_3–η^2–P(C_6H_5)(C_9H_6N)}(μPPh_2)_2(μ–H)(CO)_8](13)

Scheme 3.3: Summary of the reactions discussed in Chapter 3

3.4 EXPERIMENTAL

3.4.1 *Synthesis of $[Ru_3(\eta^1-Ph_2Pquin)(CO)_{11}]$* (2)

Ph_2Pquin (122 mg, 0.39 mmol) was added to a solution of $[Ru_3(CO)_{12}]$ (250 mg, 0.39 mmol) in dry THF (100 ml) and allowed to dissolve. Three drops of sodium benzophenoneketyl catalyst were added. The solution immediately turned dark red. Monitoring by infrared spectroscopy showed the formation of the cluster $[Ru_3(\eta^1-Ph_2Pquin)(CO)_{11}]$ (2) to be complete within 2 minutes. The solvent was removed under reduced pressure. The $^{31}P\{^1H\}$ NMR spectrum of the residue, dissolved in CH_2Cl_2, showed the presence of traces of (3) at this stage and it was thus not possible to isolate (2) pure.

3.4.2 *Synthesis of $[Ru_3\{\mu-\eta^2-C(O)(C_6H_5)\}\{\mu_3-\eta^2-P(C_6H_5)(C_9H_6N)\}(CO)_9]$* (3)

The THF solution of complex (2), described above in 3.4.1, was refluxed for *ca.* 1 hour, the colour gradually changing to an orange/brown. The solvent was removed under reduced pressure and the residue was chromatographed on TLC plates using 5:1 petroleum ether (40-60)/dichloromethane as eluent. A fast moving yellow band (traces of unreacted $[Ru_3(CO)_{12}]$) was followed by a slower moving orange band (complex (3)). The silica gel containing complex (3) was scraped from the TLC plates and the complex was eluted from the silica gel using THF. The solvent was reduced to a minimum under reduced pressure, methanol was added and the solution refrigerated at -30°C to precipitate $[Ru_3\{\mu-\eta^2-C(O)(C_6H_5)\}\{\mu_3-\eta^2-P(C_6H_5)(C_9H_6N)\}(CO)_9]$ (3) as a bright orange crystalline solid. Yield: 75%.

3.4.3 Synthesis of $[Ru_3(\eta^1\text{-}Ph_2Pquin)_2(CO)_{10}]$ (4)

(a) Synthesis of $[Ru_3(MeCN)_2(CO)_{10}]$

$[Ru_3(CO)_{12}]$ (250 mg, 0.39 mmol) was dissolved in THF (100 ml), aceto-nitrile (10 ml) was added and the solution cooled in an ice bath (0°C). A solution of trimethylamine-N-oxide ($Me_3NO\cdot H_2O$; 87 mg, 0.78 mmol) in acetonitrile (25 ml) was added dropwise. The colour of the reaction solution changed from orange to dark orange and then to yellow. The ice bath was removed and the solvent removed under reduced pressure. The yellow residue was washed with diethyl ether to remove trace quantities of a brown impurity and so afford pure $[Ru_3(MeCN)_2(CO)_{10}]$. Yield: > 90%.

(b) Reaction of $[Ru_3(MeCN)_2(CO)_{10}]$ with Ph_2Pquin

A solution of $[Ru_3(MeCN)_2(CO)_{10}]$ (250 mg, 0.38 mmol) in acetonitrile (10 ml) and dichloromethane (20 ml) was added to a dichloromethane solution (10 ml) of Ph_2Pquin (238 mg, 0.76 mmol). The reaction solution rapidly turned dark red. After stirring for ca. 10 minutes the solvent was removed under reduced pressure and the residue chromatographed on TLC plates using 3:1 petroleum ether (40-60)/dichloromethane as eluent. A pale yellow band (unreacted $[Ru_3(MeCN)_2(CO)_{10}]$) was followed by a slower moving orange band (traces of an unidentified product) and finally a dark red band (complex (4)). The silica gel containing com-plex (4) was scraped from the TLC plate and cluster (4) was eluted from the silica gel using dichloromethane. The solvent was reduced to a minimum under reduced pressure, methanol was added and the solution refrigerated at -30°C to precipitate $[Ru_3(\eta^1\text{-}Ph_2Pquin)(CO)_{10}]$ (4) as a sticky red powder. Crystallization from a 1:1 dichloromethane/hexane

solution afforded cluster (4) as a dark red crystalline material. Yield: 40%.

3.4.4 Synthesis of $[Ru_3(\mu-\eta^2-Ph_2Pquin)_2(CO)_8]$ (5)

$[Ru_3(CO)_{12}]$ (250 mg, 0.39 mmol) was dissolved in acetone (100 ml) and the solution cooled (-78°C; methanol/liquid air). Ph_2Pquin (244 mg, 0.78 mmol) and trimethylamine-N-oxide ($Me_3NO \cdot H_2O$; 174 mg, 1.56 mmol) were added. The cooling bath was removed and the mixture allowed to warm to room temperature, the solution colour changing from orange to red. After stirring for *ca*. 3 hours the solvent was removed under reduced pressure and the residue chromatographed on TLC plates using 3:1 petroleum ether (40-60)/dichloromethane as eluent. An orange band (complex (5)) was followed by a slower moving red band (complex (4)). The silica gel containing complex (5) was scraped from the TLC plate and cluster (5) was eluted from the silica gel using THF. The solvent was reduced to a minimum under reduced pressure and methanol was added. The solution was refrigerated at -30°C to precipitate $[Ru_3\{\mu-\eta^2-Ph_2Pquin)_2(CO)_8]$ (5) as an orange powder. Yield: 40%.

3.4.5 Synthesis of $[Ru_3\{\mu-\eta^2-C(O)(C_6H_5)\}\{\mu_3-\eta^2-P(C_6H_5)(C_9H_6N)\}(\eta^1-Ph_2Pquin)(CO)_8]$ (6)

Ph_2Pquin (88 mg, 0.28 mmol) was added to a THF solution (25 ml) of cluster (3) (250 mg, 0.28 mmol) and the solution left to stir for *ca*. 24 hours. The solution colour gradually changed from orange to red. The solvent was removed under reduced pressure and the residue chromatographed on TLC plates using 3:1 petroleum ether (40-60)/dichloromethane as eluent. An orange band (traces of unreacted cluster (3)) was followed by a slower moving red band (complex (6)). The silica gel

containing cluster (6) was scraped from the TLC plate and cluster (6) was eluted from the silica gel using THF. The solvent was reduced to a minimum under reduced pressure and methanol was added. The solution was refrigerated at -30°C to precipitate $[Ru_3\{\mu-\eta^2-C(O)(C_6H_5)\}\{\mu_3-\eta^2-P(C_6H_5)(C_9H_6N)\}(\eta^1-Ph_2Pquin)(CO)_8]$ (6) as a light red solid. Yield: 75%.

3.4.6. *Synthesis of* $[Ru_3(\mu-H)\{\mu_3-\eta^2-P(C_6H_5)(C_9H_6N)\}(CO)_9]$ (7)

Cluster (3) (250 mg, 0.28 mmol) was suspended in cyclohexane (50 ml). On heating the complex rapidly dissolved. Hydrogen was bubbled through the solution while it was refluxed for *ca.* 3 hours. The solvent was removed under reduced pressure and the residue dissolved in a minimum of dichloromethane. Methanol was added and the solution was refrigerated at -30°C to precipitate $[Ru_3(\mu-H)\{\mu_3-\eta^2-P(C_6H_5)(C_9H_6N)\}(CO)_9]$ (7) as an orange powder. The precipitate was washed with cold methanol (3 x 10 ml) to remove traces of a brown impurity. Yield: 85%

3.4.7 *Synthesis of* $[PPN][Ru_3\{\mu_3-\eta^2-P(C_6H_5)(C_9H_6N)\}(CO)_9]$ (8)

(a) *From* $[Ru_3\{\mu-\eta^2-C(O)(C_6H_5)\}\{\mu_3-\eta^2-P(C_6H_5)(C_9H_6N)\}(CO)_9]$ (3)

Cluster (3) (250 mg, 0.28 mmol) was dissolved in THF (20 ml). [PPN]-[BH$_4$] (155 mg, 0.28 mmol) was added and the solution refluxed for *ca.* 30 minutes, the colour changing rapidly from orange to brown. The solvent was reduced to a minimum under reduced pressure and methanol was added. Refrigeration at -30°C induced precipitation of small quantities of unreacted cluster (3). The supernatant solution was removed by pasteur pipette and the solvent was removed under reduced pressure to afford a brown oil. The oil was redissolved in a minimum dichloromethane and

hexane was added. $[PPN][Ru_3\{\mu_3-\eta^2-P(C_6H_5)(C_9H_6N)\}(CO)_9]$ (8) pre-cipitated as a brown semi-solid. Drying under reduced pressure afforded cluster (8) as a brown solid. Yield: 50%.

(b) From $[Ru_3(\mu-H)\{\mu_3-\eta^2-P(C_6H_5)(C_9H_6N)\}(CO)_9]$ (7)

Reaction of equimolar quantities of cluster (7) and $[PPN][BH_4]$ affords complex (9) in a manner analogous to that described in (a) above. Yield: 50%.

3.4.8 Synthesis of $[Ru_3(\mu-H)\{\mu_3-\eta^2-P(C_6H_5)(C_9H_6N)\}(\eta^1-Ph_2Pquin)(CO)_8]$ (9)

Ph_2Pquin (100 mg, 0.32 mmol) was added to a THF solution (25 ml) of com-plex (7) (250 mg, 0.32 mmol) and the solution left to stir for ca. 48 hours. The solution colour gradually changed from orange to red. The solvent was removed under reduced pressure and the residue chromato-graphed on TLC plates using 3:1 petroleum ether (40-60)/dichloromethane as eluent. An orange band (unreacted complex (7)) was followed by a slower moving red band (complex (9)). The silica gel containing cluster (9) was scraped from the TLC plate and cluster (9) was eluted from the silica gel using THF. The solvent was reduced to a minimum under reduced pressure and methanol was added. The solution was refrigerated at -30°C to precipitate $[Ru_3(\mu-H)\{\mu_3-\eta^2-P(C_6H_5)(C_9H_6N)\}(\eta^1-Ph_2Pquin)-(CO)_8]$ (9) as an orange solid. Yield: 70%.

3.4.9 Synthesis of $[Ru_3\{\mu-\eta^2-C(O)(C_6H_5)\}\{\mu_3-\eta^2-P(C_6H_5)-(C_9H_6N)\}(PPh_2H)(CO)_8]$ (10)

Diphenylphosphine (52 mg, 43.7 μl; 0.28 mmol) was added to a THF solu-

tion (20 ml) of cluster (3) (250 mg, 0.28 mmol). The solution was stirred for ca. 24 hours, the colour gradually changing from orange to red. The solvent was removed under reduced pressure and the residue was chromatographed on TLC plates using 3:1 petroleum ether (40-60)/dichloromethane as eluent. An orange band (unreacted complex (3)) was followed by a slower moving red band (complex (10)). The silica gel containing cluster (10) was scraped from the TLC plates and cluster (10) was eluted from the silica gel using THF, the solvent was reduced to a minimum under reduced pressure and methanol was added. Upon refrigeration at $-30°C$ $[Ru_3\{\mu-\eta^2-C(O)(C_6H_5)\}\{\mu_3-\eta^2-P(C_6H_5)(C_9H_6N)\}(PPh_2H)(CO)_8]$ (10) precipitated from the solution as a red powder. Yield: 70%.

3.4.10 *Synthesis of $[Ru_3\{\mu_3-\eta^2-P(C_6H_5)(C_9H_6N)\}(\mu-PPh_2)(\mu-CO)_2(CO)_6]$ (11)*

Cluster (10) (250 mg, 0.26 mmol) was dissolved in hot cyclohexane (80°C, 20 ml) and the solution refluxed for ca. 30 minutes. The solvent was removed under reduced pressure and the residue was chromatographed on TLC plates using 2:1 petroleum ether (40-60)/dichloromethane as eluent. One major band (burgundy coloured, complex (11)) was eluted along with several minor bands (various decomposition products). The silica gel containing cluster (11) was scraped from the TLC plates and cluster (11) was eluted from the silica gel using dichloromethane. The solvent was reduced to a minimum under reduced pressure and methanol was added. Refrigeration of the solution at $-30°C$ led to the precipitation of $[Ru_3\{\mu_3-\eta^2-P(C_6H_5)(C_9H_6N)\}(\mu-PPh_2)(\mu-CO)_2(CO)_6]$ (11) as a burgundy coloured crystalline solid. Yield: $\leq$ 40%.

3.4.11 *Synthesis of* $[Ru_3\{\mu_3-\eta^2-P(C_6H_5)(C_9H_6N)\}(\mu-PPh_2)(CO)_9]$ *(12)*

Cluster (11) (250 mg, 0.26 mmol) was dissolved in dichloromethane (5 ml) and carbon dioxide was bubbled through the solution. The solution colour rapidly changed from burgundy to orange, the reaction being complete in *ca.* 20 seconds. Hexane (15 ml) was added, the solution being kept under a carbon monoxide atmosphere. Upon refrigeration at $-30°C$ $[Ru_3\{\mu_3-\eta^2-P(C_6H_5)(C_9H_6N)\}(\mu-PPh_2)(CO)_9]$ (12) precipitated from the solution as an orange solid. However, cluster (12) decarbonylates very readily even in the solid state and could therefore not be isolated pure.

3.4.12 *Synthesis of* $[Ru_3\{\mu_3-\eta^2-P(C_6H_5)(C_9H_6N)\}(\mu-PPh_2)_2(\mu-H)(CO)_6]$ *(13)*

A solution of diphenylphosphine (48 mg, 40.4 μl; 0.26 mmol) in THF (5 ml) was added to a THF solution (20 ml) of cluster (11) (250 mg, 0.26 mmol). The colour of the solution rapidly changed from burgundy to brown, the reaction being complete in *ca.* 20 seconds. The solvent was removed under reduced pressure and the residue was chromatographed on TLC plates using 2:1 hexane/dichloromethane as eluent. An orange band (isomer "a" of cluster (13) *i.e.* (13a)) was very closely followed by a red band (isomer "b" of cluster (13) *i.e.* (13b)). Several minor bands corresponding to various unidentified decomposition products were also eluted. The silica gel containing isomers (13a) and (13b) respectively was scraped from the TLC plates. Clusters (13a) and (13b) were eluted from the silica gel using dichloromethane. In both cases the solvent was reduced to a minimum under reduced pressure and methanol was added. Refrigeration of the solutions at $-30°C$ led to the precipitation of the two isomers (13a) and (13b) of $[Ru_3\{\mu_3-\eta^2-P(C_6H_5)(C_9H_6N)\}(\mu-PPh_2)_2(\mu-H)-(CO)_6]$ (13). Yield: ≤ 40% for (13) *i.e.* (13a) + (13b). The ratio of

(13a) to (13b) depends on how fast the diphenylphosphine solution is added to the solution of cluster (11).

3.4.13 Single Crystal X-ray Diffraction Study of $[Ru_3\{\mu-\eta^2-C(O)(C_6H_5)\}\{\mu_3-\eta^2-P(C_6H_5)(C_9H_6N)\}(CO)_9]$ (3)

Orange-red crystals of cluster (3) were obtained by the slow evaporation of a $CDCl_3$ solution of this cluster. The general approach used for the intensity data collection is described in Appendix II(a) and the general approach to structure solution in Appendix II(b). The crystallographic data are given in Table 3.1, the interatomic distances in Table 3.2, the interatomic angles in Table 3.3, the fractional co-ordinates and iso-tropic thermal parameters in Table 3.4 and the anisotropic thermal parameters in Table 3.5. The observed and calculated structure factors may be found on microfiche in an envelope fixed to the inside back cover.

3.4.14 Single Crystal X-ray Diffraction Study of $[Ru_3(\mu-H)\{\mu_3-\eta^2-P(C_6H_5)(C_9H_6N)\}(CO)_9]$ (7)

Orange-red crystals of cluster (7) were obtained by the slow evaporation of a $CDCl_3$ solution of this cluster. The general approach used for the intensity data collection is described in Appendix II(a) and the general approach to structure solution in Appendix II(b). The crystallographic data are given in Table 3.6, the interatomic distances in Table 3.7, the interatomic angles in Table 3.8, the fractional co-ordinates and isotropic thermal parameters in Table 3.10 and the anisotropic thermal parameters in Table 3.11. The observed and calculated structure factors may be found on microfiche in an envelope fixed to the inside back cover.

3.4.15 *Single Crystal X-ray Diffraction Study of $[Ru_3\{\mu_3-\eta^2-$*
$P(C_6H_5)(C_9H_6N)\}(\mu-PPh_2)(\mu-CO)_2(CO)_6]$ (**11**)

Burgundy coloured crystals of cluster (11) were obtained by the slow evaporation of a CH_2Cl_2 solution of this cluster. The general approach used for the intensity data collection is described in Appendix II(a) and the general approach to structure solution in Appendix II(b). The crystallographic data are given in Table 3.12, the interatomic distances in Table 3.13, the interatomic angles in Table 3.14, the fractional co-ordinates in Table 3.15 and the anisotropic thermal parameters in Table 3.16. The observed and calculated structure factors may be found on microfiche in an envelope fixed to the inside back cover.

TABLE 3.1

CRYSTAL DATA AND DETAILS OF THE CRYSTALLOGRAPHIC ANALYSIS FOR
$[Ru_3\{\mu-\eta^2-C(O)(C_6H_5)\}\{\mu_3-\eta^2-P(C_6H_5)(C_9H_6N)\}(CO)_9]$ (3)

Formula	$Ru_3C_{31}H_{16}NO_{10}P$
Molecular mass	896.66
Crystal system	Monoclinic
Space group	$P2_1/n$
a(Å)	11.864(1)
b(Å)	15.509(1)
c(Å)	17.393(2)
$\beta(°)$	100.68(9)
$V(Å^3)$	3144.8(6)
Z	4
D_c (g cm^{-3})	1.894
F(000)	1744
λ(Mo-$K\alpha$) (Å)	0.71069
Scan mode	$\omega-2\theta$
ω scan angle	$0.80 + 0.34 \tan \theta$
Horizontal aperture width/mm	$2.70 + 0.4 \tan \theta$
Scattering range/°	$3 < \theta < 23$
μ/cm^{-1}	231.608
Absorption corrections	Empirical[95]
Measured intensities	4704
Unique intensities	4234
Unique intensities with $[I > 3\sigma(I)]$	3841
Structure solution	Direct and Fourier methods
Weighting scheme	$1.0/[\sigma^2(F) + 0.0046F^2]$
$R = \Sigma(F_o-F_c)/\Sigma F_o$	0.0421
$R_w = \Sigma_w^{\frac{1}{2}}(F_o-F_c)/\Sigma_w^{\frac{1}{2}}F_o$	0.0601
$(\Delta/\sigma)_{max}$	0.089
$\Delta\rho_{max}$/e $Å^{-3}$	1.22
Number of parameters	260

Table 3.2
INTERATOMIC DISTANCES (Å) FOR
$[Ru_3\{\mu-\eta^2-C(O)(C_6H_5)\}\{\mu_3-\eta^2-P(C_6H_5)(C_9H_6N)\}(CO)_9]$ (3)

Ru(1)-Ru(3)	2.865(1)	Ru(1)-P(1)	2.383(2)
Ru(1)-C(10)	2.093(7)	Ru(1)-C(17)	1.924(8)
Ru(1)-C(18)	1.909(8)	Ru(1)-C(19)	1.970(8)
Ru(2)-Ru(3)	2.844(1)	Ru(2)-P(1)	2.347(2)
Ru(2)-O(1)	2.109(5)	Ru(2)-C(20)	1.940(9)
Ru(2)-C(21)	1.943(9)	Ru(2)-C(22)	1.855(8)
Ru(3)-P(1)	2.943(2)	Ru(3)-N(1)	2.207(5)
Ru(3)-C(23)	1.867(7)	Ru(3)-C(24)	1.920(8)
Ru(3)-C(25)	1.904(8)	P(1)-C(1)	1.847(7)
P(1)-C(26)	1.831(8)	O(1)-C(10)	1.265(8)
O(2)-C(17)	1.125(8)	O(3)-C(18)	1.131(10)
O(4)-C(19)	1.122(9)	O(5)-C(20)	1.129(9)
O(6)-C(21)	1.138(10)	O(7)-C(22)	1.130(9)
O(8)-C(23)	1.136(8)	O(9)-C(24)	1.145(9)
O(10)-C(25)	1.133(9)	N(1)-C(1)	1.311(9)
N(1)-C(2)	1.387(8)	C(1)-C(9)	1.412(10)
C(2)-C(3)	1.423(9)	C(2)-C(7)	1.404(9)
C(3)-C(4)	1.375(10)	C(4)-C(5)	1.412(12)
C(5)-C(6)	1.346(11)	C(6)-C(7)	1.419(10)
C(7)-C(8)	1.379(11)	C(8)-C(9)	1.389(11)
C(10)-C(11)	1.514(10)	C(11)-C(12)	1.399(11)
C(11)-C(16)	1.393(10)	C(12)-C(13)	1.447(13)
C(13)-C(14)	1.377(14)	C(14)-C(15)	1.356(13)
C(15)-C(16)	1.381(12)	C(26)-C(27)	1.403(12)
C(26)-C(31)	1.372(12)	C(27)-C(28)	1.410(14)
C(28)-C(29)	1.33(2)	C(29)-C(30)	1.37(2)
C(30)-C(31)	1.436(14)		

Table 3.3

INTERATOMIC ANGLES (°) FOR

$[Ru_3\{\mu-\eta^2-C(O)(C_6H_5)\}\{\mu_3-\eta^2-P(C_6H_5)(C_9H_6N)\}(CO)_9]$ (3)

Ru(3)-Ru(1)-P(1)	67.5(0)	Ru(3)-Ru(1)-C(10)	88.8(2)
P(1)-Ru(1)-C(10)	86.6(2)	Ru(3)-Ru(1)-C(17)	92.1(2)
P(1)-Ru(1)-C(17)	158.7(2)	C(10)-Ru(1)-C(17)	87.2(3)
Ru(3)-Ru(1)-C(18)	166.3(2)	P(1)-Ru(1)-C(18)	99.0(2)
C(10)-Ru(1)-C(18)	92.5(3)	C(17)-Ru(1)-C(18)	101.6(3)
Ru(3)-Ru(1)-C(19)	83.2(2)	P(1)-Ru(1)-C(19)	91.4(2)
C(10)-Ru(1)-C(19)	171.9(3)	C(17)-Ru(1)-C(19)	91.9(3)
C(18)-Ru(1)-C(19)	95.6(3)	Ru(3)-Ru(2)-P(1)	68.3(0)
Ru(3)-Ru(2)-O(1)	89.8(1)	P(1)-Ru(2)-O(1)	84.7(1)
Ru(3)-Ru(2)-C(20)	175.1(2)	P(1)-Ru(2)-C(20)	106.8(2)
O(1)-Ru(2)-C(20)	89.9(3)	Ru(3)-Ru(2)-C(21)	88.4(2)
P(1)-Ru(2)-C(21)	156.0(2)	O(1)-Ru(2)-C(21)	89.6(3)
C(20)-Ru(2)-C(21)	96.4(3)	Ru(3)-Ru(2)-C(22)	86.6(2)
P(1)-Ru(2)-C(22)	92.1(2)	O(1)-Ru(2)-C(22)	175.8(3)
C(20)-Ru(2)-C(22)	93.5(3)	C(21)-Ru(2)-C(22)	92.3(3)
Ru(1)-Ru(3)-Ru(2)	79.2(0)	Ru(1)-Ru(3)-P(1)	48.4(0)
Ru(2)-Ru(3)-P(1)	47.8(0)	Ru(1)-Ru(3)-N(1)	89.8(1)
Ru(2)-Ru(3)-N(1)	89.7(1)	P(1)-Ru(3)-N(1)	59.8(1)
Ru(1)-Ru(3)-C(23)	84.3(2)	Ru(2)-Ru(3)-C(23)	84.8(2)
P(1)-Ru(3)-C(23)	112.9(2)	N(1)-Ru(3)-C(23)	172.6(2)
Ru(1)-Ru(3)-C(24)	89.1(2)	Ru(2)-Ru(3)-C(24)	168.3(2)
P(1)-Ru(3)-C(24)	124.0(2)	N(1)-Ru(3)-C(24)	91.7(3)
C(23)-Ru(3)-C(24)	92.7(3)	Ru(1)-Ru(3)-C(25)	168.0(2)
Ru(2)-Ru(3)-C(25)	89.4(2)	P(1)-Ru(3)-C(25)	125.0(2)
N(1)-Ru(3)-C(25)	94.1(3)	C(23)-Ru(3)-C(25)	90.8(3)
C(24)-Ru(3)-C(25)	102.1(3)	Ru(1)-P(1)-Ru(2)	100.6(1)
Ru(1)-P(1)-Ru(3)	64.1(0)	Ru(2)-P(1)-Ru(3)	63.9(0)
Ru(1)-P(1)-C(1)	109.8(2)	Ru(2)-P(1)-C(1)	107.4(2)
Ru(3)-P(1)-C(1)	73.3(2)	Ru(1)-P(1)-C(26)	117.4(3)
Ru(2)-P(1)-C(26)	120.6(3)	Ru(3)-P(1)-C(26)	173.8(3)
C(1)-P(1)-C(26)	100.7(3)	Ru(2)-O(1)-C(10)	125.6(4)
Ru(3)-N(1)-C(1)	114.1(4)	Ru(3)-N(1)-C(2)	127.2(4)
C(1)-N(1)-C(2)	118.5(5)	P(1)-C(1)-N(1)	112.7(5)
P(1)-C(1)-C(9)	123.6(5)	N(1)-C(1)-C(9)	123.8(7)
N(1)-C(2)-C(3)	119.8(6)	N(1)-C(2)-C(7)	121.5(6)

Table 3.3 (continued)

C(3)-C(2)-C(7)	118.7(6)	C(2)-C(3)-C(4)	119.8(7)
C(3)-C(4)-C(5)	120.7(7)	C(4)-C(5)-C(6)	120.4(8)
C(5)-C(6)-C(7)	120.4(7)	C(2)-C(7)-C(6)	120.0(7)
C(2)-C(7)-C(8)	117.8(7)	C(6)-C(7)-C(8)	122.1(7)
C(7)-C(8)-C(9)	121.4(7)	C(1)-C(9)-C(8)	116.9(7)
Ru(1)-C(10)-O(1)	122.9(5)	Ru(1)-C(10)-C(11)	126.6(5)
O(1)-C(10)-C(11)	110.5(6)	C(10)-C(11)-C(12)	121.6(7)
C(10)-C(11)-C(16)	118.9(6)	C(12)-C(11)-C(16)	119.2(7)
C(11)-C(12)-C(13)	119.4(8)	C(12)-C(13)-C(14)	117.7(9)
C(13)-C(14)-C(15)	122.8(10)	C(14)-C(15)-C(16)	119.8(9)
C(11)-C(16)-C(15)	120.9(8)	Ru(1)-C(17)-O(2)	179.1(7)
Ru(1)-C(18)-O(3)	178.0(8)	Ru(1)-C(19)-O(4)	177.1(7)
Ru(2)-C(20)-O(5)	171.1(8)	Ru(2)-C(21)-O(6)	179.1(8)
Ru(2)-C(22)-O(7)	174.5(7)	Ru(3)-C(23)-O(8)	179.3(6)
Ru(3)-C(24)-O(9)	176.3(6)	Ru(3)-C(25)-O(10)	176.3(7)
P(1)-C(26)-C(27)	118.2(6)	P(1)-C(26)-C(31)	121.4(7)
C(27)-C(26)-C(31)	120.2(8)	C(26)-C(27)-C(28)	120.1(9)
C(27)-C(28)-C(29)	118.5(11)	C(28)-C(29)-C(30)	124.0(12)
C(29)-C(30)-C(31)	118.2(11)	C(26)-C(31)-C(30)	118.9(9)

Table 3.4

FRACTIONAL CO-ORDINATES (X10^4) AND ISOTROPIC THERMAL FACTORS (Å, X10^3)

FOR [Ru$_3$(μ-η^2-C(O)(C$_6$H$_5$))$\{\mu_3$-η^2-P(C$_6$H$_5$)(C$_9$H$_6$N))$\}$(CO)$_9$] (3)

	x/a	y/b	z/c	U_{eq}
Ru(1)	475(1)	648(1)	3600(1)	45(1)
Ru(2)	631(1)	1686(1)	1746(1)	47(1)
Ru(3)	-965(1)	445(1)	2096(1)	41(1)
P(1)	1541(2)	593(1)	2567(1)	48(1)
O(1)	546(4)	2336(3)	2798(3)	54(1)
O(2)	-1593(5)	854(4)	4396(3)	74(1)
O(3)	2478(6)	781(5)	4965(4)	102(2)
O(4)	265(5)	-1338(3)	3625(4)	79(2)
O(5)	2500(6)	2882(5)	1358(5)	115(2)
O(6)	-1411(6)	2769(5)	912(5)	109(2)
O(7)	804(6)	637(4)	336(3)	84(2)
O(8)	-2230(4)	1972(3)	2575(3)	69(1)
O(9)	-2456(5)	-798(4)	2842(4)	79(2)
O(10)	-2299(5)	634(4)	437(4)	80(2)
N(1)	162(4)	-598(3)	1819(3)	45(1)
C(1)	1260(6)	-437(4)	2033(4)	52(2)*
C(2)	-169(5)	-1349(4)	1405(3)	44(1)*
C(3)	-1354(7)	-1549(5)	1177(4)	58(2)*
C(4)	-1682(7)	-2287(5)	756(4)	62(2)*
C(5)	-853(7)	-2847(6)	542(5)	73(2)*
C(6)	273(7)	-2673(5)	758(5)	64(2)*
C(7)	642(6)	-1921(4)	1198(4)	52(2)*
C(8)	1787(7)	-1726(5)	1438(5)	67(2)*
C(9)	2134(6)	-984(5)	1863(4)	63(2)*
C(10)	407(5)	1984(4)	3430(4)	47(1)*
C(11)	176(6)	2658(4)	4011(4)	53(2)*
C(12)	334(7)	2482(6)	4813(5)	72(2)*
C(13)	4(9)	3120(7)	5336(6)	88(3)*
C(14)	-449(8)	3884(7)	5015(6)	86(3)*
C(15)	-590(8)	4058(6)	4239(5)	81(2)*
C(16)	-309(7)	3442(5)	3732(4)	63(2)*
C(17)	-826(6)	773(5)	4107(4)	55(2)*
C(18)	1720(7)	737(5)	4466(5)	62(2)*
C(19)	372(6)	-619(5)	3624(4)	57(2)*

Table 3.4 (continued)

C(20)	1822(7)	2473(6)	1558(5)	67(2)*
C(21)	-657(7)	2365(5)	1214(5)	63(2)*
C(22)	683(6)	1041(5)	855(4)	55(2)*
C(23)	-1745(6)	1397(4)	2395(4)	50(2)*
C(24)	-1888(6)	-357(5)	2549(4)	55(2)*
C(25)	-1789(6)	537(4)	1050(4)	53(2)*
C(26)	3108(7)	559(5)	2841(5)	61(2)*
C(27)	3596(8)	26(6)	3466(5)	77(2)*
C(28)	4799(10)	-52(8)	3673(7)	101(3)*
C(29)	5447(10)	379(8)	3255(8)	104(3)*
C(30)	5018(10)	913(8)	2640(7)	110(3)*
C(31)	3795(8)	993(7)	2417(6)	86(3)*

* isotropic temperature factor.

$$U_{eq} = \tfrac{1}{3} \Sigma_i \Sigma_j U_{ij} a_i^* a_j^* (a_i . a_j)$$

Table 3.5

ANISOTROPIC THERMAL FACTORS ($Å^2$, $X10^3$) FOR

$[Ru_3\{\mu-\eta^2-C(O)(C_6H_5)\}\{\mu_3-\eta^2-P(C_6H_5)(C_9H_6N)\}(CO)_9]$ (3)

	U(11)	U(22)	U(33)	U(23)	U(13)	U(12)
Ru(1)	43(1)	40(1)	51(1)	2(1)	7(1)	0(1)
Ru(2)	43(1)	43(1)	55(1)	3(1)	13(1)	-4(1)
Ru(3)	31(1)	39(1)	53(1)	0(1)	8(1)	1(1)
P(1)	35(1)	49(1)	59(1)	-3(1)	6(1)	3(1)
O(1)	60(3)	42(3)	63(3)	-2(2)	17(2)	-3(2)
O(2)	64(3)	79(4)	86(4)	3(3)	30(3)	-2(3)
O(3)	99(5)	96(5)	89(4)	-1(4)	-41(4)	-14(4)
O(4)	84(4)	38(3)	118(5)	14(3)	21(3)	6(3)
O(5)	108(5)	95(5)	150(7)	0(5)	48(5)	-66(4)
O(6)	101(5)	102(5)	123(6)	50(5)	22(4)	33(4)
O(7)	107(5)	78(4)	70(4)	-12(3)	23(4)	-9(3)
O(8)	53(3)	60(3)	99(4)	-13(3)	23(3)	12(2)
O(9)	80(4)	68(4)	101(4)	-1(3)	44(3)	-14(3)
O(10)	73(4)	87(4)	72(4)	6(3)	-5(3)	-5(3)
N(1)	35(3)	43(3)	58(3)	1(2)	9(2)	0(2)

TABLE 3.6

CRYSTAL DATA AND DETAILS OF THE CRYSTALLOGRAPHIC ANALYSIS FOR

$[Ru_3(\mu-H)\{\mu_3-\eta^2-P(C_6H_5)(C_9H_6N)\}(CO)_9]$ (7)
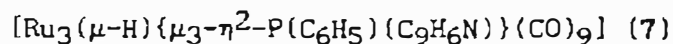
Formula	$Ru_3C_{24}H_{12}NO_9P$
Molecular mass	792.54
Crystal system	Orthorhombic
Space group	*Pbca*
$a(Å)$	9.984(1)
$b(Å)$	15.197(2)
$c(Å)$	34.929(3)
$\beta(°)$	90
$V(Å^3)$	5299.6(9)
Z	8
D_c (g cm^{-3})	1.987
F(000)	3056
λ(Mo-$K\alpha$) (Å)	0.71069
Scan mode	$\omega-2\theta$
ω scan angle	$0.80 + 0.34 \tan \theta$
Horizontal aperture width/mm	$2.70 + 0.4 \tan \theta$
Scattering range/°	$3 < \theta < 23$
μ/cm^{-1}	274.500
Absorption corrections	Empirical[95]
Measured intensities	4165
Unique intensities	3261
Unique intensities with $[I > 3\sigma(I)]$	2396
Structure solution	Direct and Fourier methods
Weighting scheme	$1.0/[\sigma^2(F) + 0.010F^2]$
$R = \Sigma(F_o-F_c)/\Sigma F_o$	0.0530
$R_w = \Sigma_w^{\frac{1}{2}}(F_o-F_c)/\Sigma_w^{\frac{1}{2}}F_o$	0.0577
$(\Delta/\sigma)_{max}$	0.003
$\Delta\rho_{max}/e$ Å^{-3}	0.49
Number of parameters	223

INTERATOMIC DISTANCES (Å) FOR $[Ru_3(\mu-H)\{\mu_3-\eta^2-P(C_6H_5)(C_9H_6N)\}(CO)_9]$ (7)

Ru(1)-Ru(2)	2.815(1)	Ru(1)-Ru(3)	2.807(1)
Ru(1)-N	2.226(10)	Ru(1)-C(1)	1.860(14)
Ru(1)-C(2)	1.933(15)	Ru(1)-C(3)	1.927(15)
Ru(2)-Ru(3)	2.933(1)	Ru(2)-P	2.315(3)
Ru(2)-C(4)	1.916(15)	Ru(2)-C(5)	1.932(15)
Ru(2)-C(6)	1.929(15)	Ru(3)-P	2.304(3)
Ru(3)-C(7)	1.85(2)	Ru(3)-C(8)	1.91(2)
Ru(3)-C(9)	1.91(2)	P-C(18)	1.843(12)
P-C(19)	1.820(12)	O(1)-C(1)	1.16(2)
O(2)-C(2)	1.12(2)	O(3)-C(3)	1.12(2)
O(4)-C(4)	1.12(2)	O(5)-C(5)	1.13(2)
O(6)-C(6)	1.13(2)	O(7)-C(7)	1.17(2)
O(8)-C(8)	1.15(2)	O(9)-C(9)	1.14(2)
N-C(10)	1.39(2)	N-C(18)	1.314(15)
C(10)-C(11)	1.44(2)	C(10)-C(15)	1.45(2)
C(11)-C(12)	1.37(2)	C(12)-C(13)	1.48(2)
C(13)-C(14)	1.35(2)	C(14)-C(15)	1.42(2)
C(15)-C(16)	1.43(2)	C(16)-C(17)	1.36(2)
C(17)-C(18)	1.39(2)	C(19)-C(20)	1.41(2)
C(19)-C(24)	1.41(2)	C(20)-C(21)	1.37(2)
C(21)-C(22)	1.43(2)	C(22)-C(23)	1.37(2)
C(23)-C(24)	1.37(2)		

Table 3.8

INTERATOMIC ANGLES (°) FOR $[Ru_3(\mu-H)\{\mu_3-\eta^2-P(C_6H_5)(C_9H_6N)\}(CO)_9]$ (7)

Ru(2)-Ru(1)-Ru(3)	62.9(0)	Ru(2)-Ru(1)-N	92.2(2)
Ru(3)-Ru(1)-N	92.7(3)	Ru(2)-Ru(1)-C(1)	82.5(4)
Ru(3)-Ru(1)-C(1)	82.2(5)	N-Ru(1)-C(1)	173.9(5)
Ru(2)-Ru(1)-C(2)	95.8(4)	Ru(3)-Ru(1)-C(2)	158.5(4)
N-Ru(1)-C(2)	90.2(5)	C(1)-Ru(1)-C(2)	93.3(6)
Ru(2)-Ru(1)-C(3)	158.1(4)	Ru(3)-Ru(1)-C(3)	95.5(4)
N-Ru(1)-C(3)	92.2(5)	C(1)-Ru(1)-C(3)	91.6(6)
C(2)-Ru(1)-C(3)	105.7(6)	Ru(1)-Ru(2)-Ru(3)	58.4(0)
Ru(1)-Ru(2)-P	72.3(1)	Ru(3)-Ru(2)-P	50.4(1)
Ru(1)-Ru(2)-C(4)	88.5(4)	Ru(3)-Ru(2)-C(4)	136.9(4)
P-Ru(2)-C(4)	96.1(4)	Ru(1)-Ru(2)-C(5)	93.0(4)
Ru(3)-Ru(2)-C(5)	113.0(4)	P-Ru(2)-C(5)	161.9(4)
C(4)-Ru(2)-C(5)	94.0(6)	Ru(1)-Ru(2)-C(6)	167.5(4)
Ru(3)-Ru(2)-C(6)	110.1(4)	P-Ru(2)-C(6)	96.6(4)
C(4)-Ru(2)-C(6)	98.7(6)	C(5)-Ru(2)-C(6)	96.7(6)
Ru(1)-Ru(3)-Ru(2)	58.7(0)	Ru(1)-Ru(3)-P	72.7(1)
Ru(2)-Ru(3)-P	50.8(1)	Ru(1)-Ru(3)-C(7)	89.5(5)
Ru(2)-Ru(3)-C(7)	136.4(5)	P-Ru(3)-C(7)	94.1(5)
Ru(1)-Ru(3)-C(8)	93.9(5)	Ru(2)-Ru(3)-C(8)	114.4(4)
P-Ru(3)-C(8)	163.7(5)	C(7)-Ru(3)-C(8)	95.1(7)
Ru(1)-Ru(3)-C(9)	164.6(5)	Ru(2)-Ru(3)-C(9)	106.7(5)
P-Ru(3)-C(9)	94.4(6)	C(7)-Ru(3)-C(9)	99.9(7)
C(8)-Ru(3)-C(9)	97.3(7)	Ru(2)-P-Ru(3)	78.8(1)
Ru(2)-P-C(18)	114.6(4)	Ru(3)-P-C(18)	117.4(4)
Ru(2)-P-C(19)	123.7(4)	Ru(3)-P-C(19)	120.8(4)
C(18)-P-C(19)	101.7(6)	Ru(1)-N-C(10)	123.6(8)
Ru(1)-N-C(18)	118.0(8)	C(10)-N-C(18)	118.2(10)
Ru(1)-C(1)-O(1)	175.7(14)	Ru(1)-C(2)-O(2)	174.8(13)
Ru(1)-C(3)-O(3)	176.4(14)	Ru(2)-C(4)-O(4)	176.0(14)
Ru(2)-C(5)-O(5)	176.1(14)	Ru(2)-C(6)-O(6)	174.4(14)
Ru(3)-C(7)-O(7)	179(2)	Ru(3)-C(8)-O(8)	176.1(13)
Ru(3)-C(9)-O(9)	178(2)	N-C(10)-C(11)	122.3(11)
N-C(10)-C(15)	119.4(11)	C(11)-C(10)-C(15)	118.2(11)
C(10)-C(11)-C(12)	121.0(13)	C(11)-C(12)-C(13)	120.5(13)
C(12)-C(13)-C(14)	118.1(14)	C(13)-C(14)-C(15)	123.6(13)

Table 3.8 (continued)

C(10)-C(15)-C(14)	118.4(11)	C(10)-C(15)-C(16)	118.4(12)
C(14)-C(15)-C(16)	123.2(12)	C(15)-C(16)-C(17)	119.4(12)
C(16)-C(17)-C(18)	118.4(12)	P-C(18)-N	111.7(9)
P-C(18)-C(17)	122.3(9)	N-C(18)-C(17)	126.0(11)
P-C(19)-C(20)	119.8(9)	P-C(19)-C(24)	122.1(10)
C(20)-C(19)-C(24)	118.1(12)	C(19)-C(20)-C(21)	121.2(13)
C(20)-C(21)-C(22)	120(2)	C(21)-C(22)-C(23)	118.2(14)
C(22)-C(23)-C(24)	122.1(13)	C(19)-C(24)-C(23)	120.3(13)

TABLE 3.9

RESULTS OF THE MEANPLANE CALCULATIONS FOR $[Ru_3(\mu-H)\{\mu_3-\eta^2-P(C_6H_5)-(C_9H_6N)\}(CO)_9]$ USING THE PROGRAM PLANE[89]

Atom defining plane	Ru(1), N(1), C(10), C(11), C(12), C(13), C(14), C(15), C(16), C(17), C(18), P(1), C(19), C(22), C(1), O(1)
Equation of plane	$-0.7901x -0.2648y - 0.5520z = 3.7773$
Displacement of atoms from meanplane (Å)	Ru(1) -0.008(2), N(1) -0.028(9), C(10) 0.000(12), C(11) -0.108(14), C(12) -0.134(14), C(13) -0.050(15), C(14) 0 081(13), C(15) 0.076(13), C(16) 0.136(13), C(17) 0.064(13), C(18) 0.028(11), P(1) 0.026(2), C(19) -0.024(9), C(22) -0.129(14), C(1) 0.022(14), O(1) 0.049(10)

Atoms on one side of plane	Displacement from the plane (Å)	Corresponding atoms on other side of plane	Displacement from the plane (Å)
C(3)	-1.575(15)	C(2)	1.498(14)
O(3)	-2.506(12)	O(2)	2.422(11)
C(7)	-2.784(15)	C(4)	2.887(14)
O(7)	-3.643(13)	O(4)	3.630(12)
C(8)	-2.175(15)	C(5)	2.304(13)
O(8)	-2.697(13)	O(5)	2.797(11)
C(9)	-1.910(19)	C(16)	2.236(15)
O(9)	-2.233(19)	O(6)	2.745(13)
C(2)	-1.260(13)	C(24)	1.148(14)
C(21)	-1.329(16)	C(23)	1.072(13)
Ru(3)	-1.405(2)	Ru(2)	1.529(2)

Table 3.10

FRACTIONAL CO-ORDINATES ($\times 10^4$) AND ISOTROPIC THERMAL FACTORS ($\mathring{A}$, $\times 10^3$)

FOR $[Ru_3(\mu-H)\{\mu_3-\eta^2-P(C_6H_5)(C_9H_6N)\}(CO)_9]$ (7)

	x/a	y/b	z/c	U_{eq}
Ru(1)	1329(1)	2363(1)	926(1)	36(1)
Ru(2)	-1191(1)	1969(1)	1243(1)	33(1)
Ru(3)	1103(1)	2444(1)	1726(1)	39(1)
P	-544(3)	3333(2)	1473(1)	33(1)
O(1)	1884(10)	442(6)	1070(3)	65(3)
O(2)	453(11)	1966(8)	107(3)	75(3)
O(3)	4325(10)	2726(9)	919(4)	85(4)
O(4)	-2406(13)	2661(8)	506(3)	84(3)
O(5)	-1111(11)	73(7)	948(3)	68(3)
O(6)	-3781(12)	1804(9)	1707(4)	85(4)
O(7)	3177(13)	3890(9)	1736(4)	104(4)
O(8)	3160(12)	979(9)	1860(4)	85(3)
O(9)	83(16)	2566(11)	2548(4)	114(5)
N	804(9)	3778(6)	856(3)	34(2)
C(1)	1645(14)	1180(10)	1028(4)	50(4)*
C(2)	817(14)	2140(9)	401(4)	45(3)*
C(3)	3221(15)	2612(10)	912(4)	49(3)*
C(4)	-2002(14)	2394(10)	782(4)	50(4)*
C(5)	-1136(13)	762(10)	1070(4)	44(3)*
C(6)	-2785(15)	1858(10)	1552(4)	54(4)*
C(7)	2380(16)	3328(11)	1734(4)	60(4)*
C(8)	2351(15)	1508(10)	1810(4)	56(4)*
C(9)	448(18)	2527(12)	2239(6)	74(5)*
C(10)	1246(11)	4294(8)	553(4)	35(3)*
C(11)	2210(14)	3983(9)	279(4)	54(4)*
C(12)	2671(14)	4519(9)	-8(4)	54(4)*
C(13)	2184(14)	5432(10)	-43(5)	58(4)*
C(14)	1255(12)	5714(9)	211(4)	46(3)*
C(15)	773(12)	5196(9)	519(4)	39(3)*
C(16)	-148(13)	5516(9)	798(4)	49(3)*
C(17)	-512(12)	4987(8)	1095(4)	40(3)*
C(18)	-43(11)	4126(8)	1101(3)	32(3)*
C(19)	-1584(11)	4012(8)	1783(4)	35(3)*
C(20)	-988(13)	4511(9)	2076(4)	46(3)*

Table 3.10 (continued)

C(21)	-1738(16)	5046(11)	2307(5)	63(4)*
C(22)	-3153(14)	5109(10)	2251(4)	53(4)*
C(23)	-3723(13)	4617(9)	1964(4)	50(3)*
C(24)	-2982(14)	4067(9)	1736(4)	49(3)*

* isotropic temperature factor.

$$U_{eq} = \tfrac{1}{3} \Sigma_i \Sigma_j U_{ij} a_i^* a_j^* (a_i \cdot a_j)$$

Table 3.11

ANISOTROPIC THERMAL FACTORS ($Å^2$, $×10^3$) FOR

$[Ru_3\{\mu-H\}\{\mu_3-\eta^2-P(C_6H_5)(C_9H_6N)\}(CO)_9]$ (7)

	U(11)	U(22)	U(33)	U(23)	U(13)	U(12)
Ru(1)	36(1)	30(1)	41(1)	4(1)	8(1)	3(1)
Ru(2)	35(1)	30(1)	34(1)	1(1)	3(1)	-4(1)
Ru(3)	39(1)	41(1)	38(1)	6(1)	-5(1)	1(1)
P	33(2)	33(2)	34(2)	0(1)	-2(1)	-1(1)
O(1)	66(6)	31(5)	97(9)	21(5)	34(6)	14(5)
O(2)	75(7)	94(9)	54(7)	-13(6)	1(6)	-16(6)
O(3)	37(6)	95(10)	125(11)	20(8)	7(6)	-4(6)
O(4)	105(9)	76(8)	70(8)	24(7)	-36(8)	-5(7)
O(5)	78(7)	47(6)	79(9)	-17(5)	16(6)	-9(6)
O(6)	79(8)	90(9)	87(10)	-19(7)	35(7)	-20(7)
O(7)	77(8)	87(9)	147(14)	22(9)	-38(9)	-33(7)
O(8)	75(7)	91(9)	88(9)	33(7)	0(7)	28(7)
O(9)	147(13)	143(12)	52(8)	5(8)	6(9)	26(12)
N	30(5)	23(5)	50(7)	-8(5)	3(5)	-12(4)

TABLE 3.12

CRYSTAL DATA AND DETAILS OF THE CRYSTALLOGRAPHIC ANALYSIS FOR
$[Ru_3\{\mu_3-\eta^2-P(C_6H_5)(C_9H_6N)\}(\mu-PPh_2)(\mu-CO)_2(CO)_6]$ (**11**)
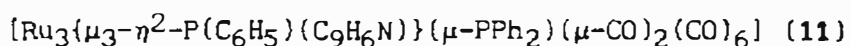
Formula	$Ru_3C_{35}H_{21}NO_8P_2$
Molecular mass	948.73
Crystal system	Monoclinic
Space group	$P2_1/c$
a(Å)	17.790(2)
b(Å)	13.244(2)
c(Å)	15.240(2)
$\beta(°)$	108.13(1)
V(Å^3)	3412.4(6)
Z	4
D_c (g cm^{-3})	1.847
F(000)	1856
λ(Mo-$K\alpha$) (Å)	0.71069
Scan mode	$\omega-2\theta$
ω scan angle	$0.76 + 0.34 \tan\theta$
Horizontal aperture width/mm	$2.70 + 0.4 \tan\theta$
Scattering range/°	$3 < \theta < 23$
μ/cm^{-1}	215.813
Absorption corrections	Empirical[95]
Measured intensities	5199
Unique intensities	4572
Unique intensities with $[I > 3\sigma(I)]$	4240
Structure solution	Direct and Fourier methods
Weighting scheme	$1.0/[\sigma^2(F) + 0.005F^2]$
$R = \Sigma(F_o-F_c)/\Sigma F_o$	0.0296
$R_w = \Sigma_w^{\frac{1}{2}}(F_o-F_c)/\Sigma_w^{\frac{1}{2}}F_o$	0.0389
$(\Delta/\sigma)_{max}$	0.509
$\Delta\rho_{max}$/e Å^{-3}	0.76
Number of parameters	442

Table 3.13

INTERATOMIC DISTANCES (Å) FOR

$[Ru_3\{\mu_3-\eta^2-P(C_6H_5)(C_9H_6N)\}(\mu-PPh_2)(\mu-CO)_2(CO)_6]$ (11)
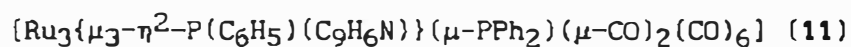
Ru(1)-Ru(2)	2.761(0)	Ru(1)-Ru(3)	2.846(0)
Ru(1)-P(1)	2.370(1)	Ru(1)-P(2)	2.357(1)
Ru(1)-C(1)	1.916(5)	Ru(1)-C(2)	1.904(5)
Ru(1)-C(7)	2.140(5)	Ru(2)-Ru(3)	2.828(0)
Ru(2)-P(1)	2.343(1)	Ru(2)-C(3)	1.898(5)
Ru(2)-C(4)	1.885(5)	Ru(2)-C(7)	2.172(5)
Ru(2)-C(8)	2.045(4)	Ru(3)-P(2)	2.338(1)
Ru(3)-N	2.233(3)	Ru(3)-C(5)	1.894(5)
Ru(3)-C(6)	1.851(5)	Ru(3)-C(8)	2.249(4)
P(1)-C(9)	1.820(4)	P(1)-C(18)	1.821(5)
P(2)-C(24)	1.821(5)	P(2)-C(30)	1.831(5)
O(1)-C(1)	1.144(7)	O(2)-C(2)	1.135(7)
O(3)-C(3)	1.155(6)	O(4)-C(4)	1.142(6)
O(5)-C(5)	1.138(6)	O(6)-C(6)	1.144(6)
O(7)-C(7)	1.137(6)	O(8)-C(8)	1.166(5)
N-C(9)	1.329(6)	N-C(17)	1.390(5)
C(9)-C(10)	1.408(6)	C(10)-C(11)	1.344(7)
C(11)-C(12)	1.429(6)	C(12)-C(13)	1.447(7)
C(12)-C(17)	1.397(6)	C(13)-C(14)	1.372(7)
C(14)-C(15)	1.388(8)	C(15)-C(16)	1.380(7)
C(16)-C(17)	1.416(6)	C(18)-C(19)	1.402(7)
C(18)-C(23)	1.372(7)	C(19)-C(20)	1.390(8)
C(20)-C(21)	1.370(8)	C(21)-C(22)	1.403(8)
C(22)-C(23)	1.418(8)	C(24)-C(25)	1.392(7)
C(24)-C(29)	1.401(7)	C(25)-C(26)	1.410(8)
C(26)-C(27)	1.349(10)	C(27)-C(28)	1.370(9)
C(28)-C(29)	1.419(8)	C(30)-C(31)	1.382(7)
C(30)-C(35)	1.406(7)	C(31)-C(32)	1.395(8)
C(32)-C(33)	1.372(9)	C(33)-C(34)	1.369(9)
C(34)-C(35)	1.404(7)		

<u>Table 3.14</u>

INTERATOMIC ANGLES (°) FOR

$[Ru_3\{\mu_3-\eta^2-P(C_6H_5)(C_9H_6N)\}(\mu-PPh_2)(\mu-CO)_2(CO)_6]$ (11)
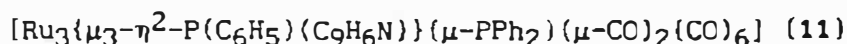
Ru(2)-Ru(1)-Ru(3)	60.6(0)	Ru(2)-Ru(1)-P(1)	53.7(0)
Ru(3)-Ru(1)-P(1)	71.9(0)	Ru(2)-Ru(1)-P(2)	112.9(0)
Ru(3)-Ru(1)-P(2)	52.4(0)	P(1)-Ru(1)-P(2)	101.1(0)
Ru(2)-Ru(1)-C(1)	105.7(2)	Ru(3)-Ru(1)-C(1)	102.6(2)
P(1)-Ru(1)-C(1)	159.1(2)	P(2)-Ru(1)-C(1)	90.3(2)
Ru(2)-Ru(1)-C(2)	136.1(2)	Ru(3)-Ru(1)-C(2)	148.6(2)
P(1)-Ru(1)-C(2)	97.2(2)	P(2)-Ru(1)-C(2)	103.8(2)
C(1)-Ru(1)-C(2)	97.1(2)	Ru(2)-Ru(1)-C(7)	50.7(1)
Ru(3)-Ru(1)-C(7)	109.9(1)	P(1)-Ru(1)-C(7)	78.5(1)
P(2)-Ru(1)-C(7)	160.1(1)	C(1)-Ru(1)-C(7)	84.8(2)
C(2)-Ru(1)-C(7)	96.0(2)	Ru(1)-Ru(2)-Ru(3)	61.2(0)
Ru(1)-Ru(2)-P(1)	54.6(0)	Ru(3)-Ru(2)-P(1)	72.7(0)
Ru(1)-Ru(2)-C(3)	107.6(2)	Ru(3)-Ru(2)-C(3)	101.9(2)
P(1)-Ru(2)-C(3)	162.0(2)	Ru(1)-Ru(2)-C(4)	141.5(1)
Ru(3)-Ru(2)-C(4)	146.0(2)	P(1)-Ru(2)-C(4)	100.4(2)
C(3)-Ru(2)-C(4)	93.4(2)	Ru(1)-Ru(2)-C(7)	49.7(1)
Ru(3)-Ru(2)-C(7)	109.5(1)	P(1)-Ru(2)-C(7)	78.4(1)
C(3)-Ru(2)-C(7)	87.7(2)	C(4)-Ru(2)-C(7)	101.2(2)
Ru(1)-Ru(2)-C(8)	112.9(1)	Ru(3)-Ru(2)-C(8)	52.0(1)
P(1)-Ru(2)-C(8)	97.2(1)	C(3)-Ru(2)-C(8)	92.2(2)
C(4)-Ru(2)-C(8)	97.7(2)	C(7)-Ru(2)-C(8)	161.1(2)
Ru(1)-Ru(3)-Ru(2)	58.2(0)	Ru(1)-Ru(3)-P(2)	53.0(0)
Ru(2)-Ru(3)-P(2)	111.2(0)	Ru(1)-Ru(3)-N	94.0(1)
Ru(2)-Ru(3)-N	94.8(1)	P(2)-Ru(3)-N	88.6(1)
Ru(1)-Ru(3)-C(5)	167.3(1)	Ru(2)-Ru(3)-C(5)	130.7(1)
P(2)-Ru(3)-C(5)	117.4(1)	N-Ru(3)-C(5)	94.1(2)
Ru(1)-Ru(3)-C(6)	84.2(2)	Ru(2)-Ru(3)-C(6)	83.8(2)
P(2)-Ru(3)-C(6)	90.7(1)	N-Ru(3)-C(6)	178.1(2)
C(5)-Ru(3)-C(6)	87.8(2)	Ru(1)-Ru(3)-C(8)	103.7(1)
Ru(2)-Ru(3)-C(8)	45.8(1)	P(2)-Ru(3)-C(8)	155.9(1)
N-Ru(3)-C(8)	87.1(1)	C(5)-Ru(3)-C(8)	86.5(2)
C(6)-Ru(3)-C(8)	92.9(2)	Ru(1)-P(1)-Ru(2)	71.7(0)
Ru(1)-P(1)-C(9)	121.4(1)	Ru(2)-P(1)-C(9)	114.3(1)
Ru(1)-P(1)-C(18)	119.3(1)	Ru(2)-P(1)-C(18)	124.9(1)
C(9)-P(1)-C(18)	103.9(2)	Ru(1)-P(2)-Ru(3)	74.6(0)

Table 3.14 (continued)

Ru(1)-P(2)-C(24)	120.2(2)	Ru(3)-P(2)-C(24)	126.0(1)
Ru(1)-P(2)-C(30)	119.4(1)	Ru(3)-P(2)-C(30)	115.8(2)
C(24)-P(2)-C(30)	101.0(2)	Ru(3)-N-C(9)	116.2(3)
Ru(3)-N-C(17)	125.0(3)	C(9)-N-C(17)	117.6(4)
Ru(1)-C(1)-O(1)	174.9(5)	Ru(1)-C(2)-O(2)	175.1(6)
Ru(2)-C(3)-O(3)	175.9(5)	Ru(2)-C(4)-O(4)	178.1(5)
Ru(3)-C(5)-O(5)	168.6(4)	Ru(3)-C(6)-O(6)	177.0(4)
Ru(1)-C(7)-Ru(2)	79.6(2)	Ru(1)-C(7)-O(7)	141.8(4)
Ru(2)-C(7)-O(7)	138.3(4)	Ru(2)-C(8)-Ru(3)	82.2(2)
Ru(2)-C(8)-O(8)	144.6(4)	Ru(3)-C(8)-O(8)	133.1(4)
P(1)-C(9)-N	113.1(3)	P(1)-C(9)-C(10)	122.8(3)
N-C(9)-C(10)	124.1(4)	C(9)-C(10)-C(11)	118.4(4)
C(10)-C(11)-C(12)	119.8(4)	C(11)-C(12)-C(13)	121.4(4)
C(11)-C(12)-C(17)	118.6(4)	C(13)-C(12)-C(17)	119.9(4)
C(12)-C(13)-C(14)	119.0(5)	C(13)-C(14)-C(15)	120.0(5)
C(14)-C(15)-C(16)	122.5(5)	C(15)-C(16)-C(17)	118.8(4)
N-C(17)-C(12)	120.6(4)	N-C(17)-C(16)	120.0(4)
C(12)-C(17)-C(16)	119.3(4)	P(1)-C(18)-C(19)	122.0(4)
P(1)-C(18)-C(23)	119.9(4)	C(19)-C(18)-C(23)	118.1(5)
C(18)-C(19)-C(20)	120.5(5)	C(19)-C(20)-C(21)	121.6(5)
C(20)-C(21)-C(22)	119.2(5)	C(21)-C(22)-C(23)	118.7(5)
C(18)-C(23)-C(22)	121.9(5)	P(2)-C(24)-C(25)	122.0(4)
P(2)-C(24)-C(29)	118.9(4)	C(25)-C(24)-C(29)	119.1(5)
C(24)-C(25)-C(26)	119.6(5)	C(25)-C(26)-C(27)	121.1(6)
C(26)-C(27)-C(28)	120.5(5)	C(27)-C(28)-C(29)	120.2(6)
C(24)-C(29)-C(28)	119.4(5)	P(2)-C(30)-C(31)	121.5(4)
P(2)-C(30)-C(35)	119.0(3)	C(31)-C(30)-C(35)	119.5(4)
C(30)-C(31)-C(32)	120.0(5)	C(31)-C(32)-C(33)	120.8(5)
C(32)-C(33)-C(34)	119.8(5)	C(33)-C(34)-C(35)	120.9(5)
C(30)-C(35)-C(34)	119.0(5)		

Table 3.15

FRACTIONAL CO-ORDINATES ($\times 10^4$)

$[Ru_3\{\mu_3-\eta^2-P(C_6H_5)(C_9H_6N)\}(\mu-PPh_2)(\mu-CO)_2(CO)_6]$ (11)
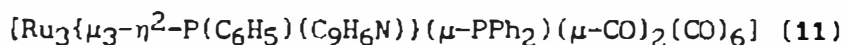
	x/a	y/b	z/c	U_{eq}
Ru(1)	-8145(1)	-275(1)	-6069(1)	28(1)
Ru(2)	-6715(1)	-212(1)	-6422(1)	28(1)
Ru(3)	-6978(1)	1149(1)	-5117(1)	24(1)
P(1)	-6984(1)	-1177(1)	-5265(1)	27(1)
P(2)	-8222(1)	897(1)	-4936(1)	29(1)
O(1)	-9264(3)	973(4)	-7618(3)	82(1)
O(2)	-9295(3)	-1949(4)	-6008(4)	103(2)
O(3)	-6961(3)	1120(3)	-8122(3)	78(1)
O(4)	-5517(3)	-1562(3)	-6882(3)	70(1)
O(5)	-6043(2)	3021(3)	-4335(3)	58(1)
O(6)	-7689(2)	2482(3)	-6752(3)	61(1)
O(7)	-8082(2)	-1356(3)	-7860(3)	62(1)
O(8)	-5281(2)	1074(3)	-5371(3)	43(1)
N	-6464(2)	137(3)	-3907(2)	25(1)
C(1)	-8856(3)	533(4)	-7010(4)	46(1)
C(2)	-8885(3)	-1295(4)	-6018(4)	48(1)
C(3)	-6843(3)	636(4)	-7462(3)	41(1)
C(4)	-5978(3)	-1056(4)	-6722(3)	41(1)
C(5)	-6395(3)	2294(3)	-4539(3)	35(1)
C(6)	-7421(3)	1951(4)	-6143(3)	36(1)
C(7)	-7823(3)	-931(4)	-7184(3)	42(1)
C(8)	-5924(3)	759(3)	-5569(3)	29(1)
C(9)	-6399(2)	-833(3)	-4095(3)	26(1)
C(10)	-5905(3)	-1523(3)	-3476(3)	32(1)
C(11)	-5454(3)	-1181(3)	-2649(3)	37(1)
C(12)	-5538(3)	-162(3)	-2387(3)	30(1)
C(13)	-5098(3)	217(4)	-1483(3)	38(1)
C(14)	-5254(3)	1172(4)	-1237(3)	47(1)
C(15)	-5849(3)	1743(4)	-1838(3)	41(1)
C(16)	-6263(3)	1420(3)	-2716(3)	33(1)
C(17)	-6081(2)	463(3)	-3013(3)	26(1)
C(18)	-7011(3)	-2550(3)	-5242(3)	33(1)
C(19)	-6677(3)	-3144(4)	-5786(4)	47(1)
C(20)	-6720(3)	-4191(4)	-5761(4)	54(1)

Table 3.15 (continued)

C(21)	-7078(3)	-4676(4)	-5205(4)	56(1)
C(22)	-7414(4)	-4101(4)	-4649(4)	59(2)
C(23)	-7387(4)	-3033(4)	-4700(4)	51(1)
C(24)	-8412(3)	466(4)	-3890(3)	34(1)
C(25)	-8777(3)	1079(4)	-3401(4)	51(1)
C(26)	-8932(4)	695(5)	-2612(4)	65(2)
C(27)	-8716(4)	-250(5)	-2308(4)	63(2)
C(28)	-8333(4)	-860(5)	-2758(4)	61(2)
C(29)	-8180(3)	-512(4)	-3567(4)	47(1)
C(30)	-8912(3)	1959(3)	-5266(3)	36(1)
C(31)	-9709(3)	1810(4)	-5708(4)	54(1)
C(32)	-10221(3)	2635(5)	-5936(5)	66(2)
C(33)	-9945(4)	3598(5)	-5707(4)	62(2)
C(34)	-9158(4)	3756(4)	-5257(5)	63(2)
C(35)	-8623(3)	2946(4)	-5047(4)	51(1)

Table 3.16

ANISOTROPIC THERMAL FACTORS ($Å^2$, X10^3) FOR

$[Ru_3\{\mu_3-\eta^2-P(C_6H_5)(C_9H_6N)\}(\mu-PPh_2)(\mu-CO)_2(CO)_6]$ (11)
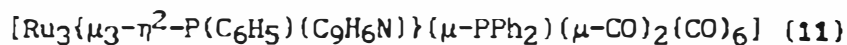
	U(11)	U(22)	U(33)	U(23)	U(13)	U(12)
Ru(1)	25(1)	31(1)	27(1)	-2(1)	7(1)	-2(1)
Ru(2)	32(1)	28(1)	26(1)	0(1)	13(1)	0(1)
Ru(3)	24(1)	22(1)	26(1)	1(1)	7(1)	2(1)
P(1)	33(1)	22(1)	27(1)	-1(1)	11(1)	1(1)
P(2)	26(1)	33(1)	30(1)	1(1)	9(1)	3(1)
O(1)	74(3)	90(3)	63(3)	19(3)	-6(2)	20(3)
O(2)	65(3)	93(4)	150(5)	18(4)	34(3)	-31(3)
O(3)	127(4)	62(3)	45(2)	15(2)	25(3)	-17(3)
O(4)	70(3)	53(2)	111(4)	-12(2)	63(3)	7(2)
O(5)	69(3)	37(2)	65(2)	-11(2)	16(2)	-20(2)
O(6)	64(2)	66(3)	53(2)	31(2)	17(2)	16(2)
O(7)	58(2)	85(3)	46(2)	-35(2)	20(2)	-26(2)
O(8)	32(2)	47(2)	50(2)	-4(2)	15(2)	-4(2)
N	25(2)	26(2)	25(2)	-3(1)	7(2)	-1(1)
C(1)	36(3)	58(3)	38(3)	1(3)	4(2)	9(3)
C(2)	38(3)	45(3)	59(3)	1(3)	14(2)	-11(2)
C(3)	53(3)	36(3)	34(3)	2(2)	14(2)	-8(2)
C(4)	45(3)	42(3)	42(3)	-10(2)	22(2)	-15(2)
C(5)	39(3)	30(3)	34(2)	1(2)	9(2)	4(2)
C(6)	33(3)	37(3)	39(3)	9(2)	10(2)	6(2)
C(7)	55(3)	38(3)	32(3)	-3(2)	11(2)	-6(2)
C(8)	25(2)	29(2)	31(2)	2(2)	6(2)	-3(2)
C(9)	26(2)	27(2)	28(2)	1(2)	10(2)	-1(2)
C(10)	34(2)	27(2)	36(3)	2(2)	9(2)	3(2)
C(11)	37(3)	39(3)	37(3)	6(2)	13(2)	0(2)
C(12)	37(3)	25(2)	30(2)	6(2)	14(2)	-1(2)
C(13)	39(3)	38(3)	33(3)	5(2)	7(2)	-3(2)
C(14)	51(3)	56(4)	33(3)	-3(2)	10(2)	-17(3)
C(15)	51(3)	32(3)	41(3)	-9(2)	14(2)	-5(2)
C(16)	36(3)	31(2)	36(3)	-2(2)	15(2)	2(2)
C(17)	26(2)	31(2)	24(2)	-1(2)	12(2)	-5(2)
C(18)	37(2)	28(3)	32(2)	0(2)	10(2)	-2(2)
C(19)	58(3)	35(3)	52(3)	-4(2)	23(3)	7(2)
C(20)	56(3)	39(3)	67(4)	-9(3)	21(3)	9(3)
C(21)	62(4)	28(3)	67(4)	7(3)	4(3)	-7(2)

Table 3.16 (continued)

C(22)	89(5)	37(3)	55(3)	3(3)	29(3)	3(3)
C(23)	73(4)	33(3)	56(3)	-7(2)	35(3)	-11(3)
C(24)	24(2)	46(3)	31(2)	0(2)	9(2)	-3(2)
C(25)	59(3)	62(4)	40(3)	-12(3)	27(3)	0(3)
C(26)	78(4)	76(5)	48(3)	-3(3)	30(3)	0(4)
C(27)	65(4)	91(5)	36(3)	0(3)	21(3)	-17(3)
C(28)	64(4)	69(4)	45(3)	8(3)	8(3)	-9(3)
C(29)	50(3)	46(3)	48(3)	8(2)	20(3)	-2(3)
C(30)	34(3)	37(3)	35(2)	0(2)	9(2)	5(2)
C(31)	34(3)	55(3)	71(4)	-5(3)	12(3)	8(3)
C(32)	38(3)	62(4)	92(5)	11(4)	12(3)	19(3)
C(33)	53(4)	61(4)	70(4)	10(3)	15(3)	25(3)
C(34)	74(4)	36(3)	85(5)	6(3)	35(4)	16(3)
C(35)	44(3)	43(3)	66(3)	-3(3)	17(3)	10(2)

TABLE 3.17

INFRARED SPECTROSCOPIC DATA

	COMPOUND	$\nu(CO)$ (cm^{-1})			MEDIUM
(2)	$[Ru_3(\eta^1\text{-}Ph_2Pquin)(CO)_{11}]$	2096w	2044s	2029s	CH_2Cl_2
		2015vs	1996w		
(3)	$[Ru_3\{\mu\text{-}\eta^2\text{-}C(O)(C_6H_5)\}\{\mu_3\text{-}\eta^2\text{-}P(C_6H_5)(C_9H_6N)\}(CO)_9]$	2073w	2048vs	2012vs	CH_2Cl_2
		1996m	1978m	1951sh	
(4)	$[Ru_3(\eta^1\text{-}Ph_2Pquin)_2(CO)_{10}]$	2071w	2050w	2036m	CH_2Cl_2
		2035s	1998vs,br		
(5)	$[Ru_3(\mu\text{-}\eta^2\text{-}Ph_2Pquin)_2(CO)_8]$	2059s	2009vs	1998m,br	CH_2Cl_2
		1934w,br			
(6)	$[Ru_3\{\mu\text{-}\eta^2\text{-}C(O)(C_6H_5)\}\{\mu_3\text{-}\eta^2\text{-}P(C_6H_5)(C_9H_6N)\}(\eta^1\text{-}Ph_2Pquin)(CO)_8]$	2054s	2023vs	1992m,br	CH_2Cl_2
		1959m,br	1994sh		
(7)	$[Ru_3(\mu\text{-}H)\{\mu_3\text{-}\eta^2\text{-}P(C_6H_5)(C_9H_6N)\}(CO)_9]$	2079m	2050vs	2025vs	CH_2Cl_2
		2007s	1988s	1967vw	
(8)	$[PPN][Ru_3\{\mu_3\text{-}\eta^2\text{-}P(C_6H_5)(C_9H_6N)\}(CO)_9]$	2027s	1971vs,br	1942m,br	KBr disc
		1913m,br			

Table 3.17 (continued)

COMPOUND	ν(CO) (cm^{-1})				MEDIUM
(9) [Ru$_3$(μ-H){μ_3-η^2-P(C$_6$H$_5$)(C$_9$H$_6$N)}(η^1-Ph$_2$Pquin)(CO)$_8$]	2056vs	2019vs	1998s		CH$_2$Cl$_2$
	1975w	1965w	1939w		
(10) [Ru$_3${μ-η^2-C(O)(C$_6$H$_5$)}{μ_3-η^2-P(C$_6$H$_5$)(C$_9$H$_6$N)}(PPh$_2$H)(CO)$_8$]	2052s	2019vs	1990s,br		CH$_2$Cl$_2$
	1955w,br	1944sh			
(11) [Ru$_3${μ_3-η^2-P(C$_6$H$_5$)(C$_9$H$_6$N)}(μ-PPh$_2$)(μ-CO)$_2$(CO)$_6$]	2052vs	2017vs	1998s	1969w	CH$_2$Cl$_2$
	1953m,br	1869vw	1830m,br		
(12) [Ru$_3${μ_3-η^2-P(C$_6$H$_5$)(C$_9$H$_6$N)}(μ-PPh$_2$)(CO)$_9$]	2067s	2042vs	2013s		CH$_2$Cl$_2$
	2000s	1975w,br	1953w,br		
(13) [Ru$_3${μ_3-η^2-P(C$_6$H$_5$)(C$_9$H$_6$N)}(μ-PPh$_2$)$_2$(μ-H)(CO)$_6$] Isomer (13a)	2032s	2000s	1988vs		KBr Disc
	1951m	1932s	1913vs		
(13) Isomer (13b)	2025s	1998vs	1982m		KBr Disc
	1975w	1936m	1924m		

vs = very strong, s = strong, m = medium, w = weak, vw = very weak, br = broad.

TABLE 3.18

$^{31}P\{^1H\}$ NMR SPECTROSCOPIC DATA

(ppm relative to 85% H_3PO_4 external standard;   solvent is CH_2Cl_2)

	COMPOUND	δ(ppm)	Multiplicity	Assignment
(2)	$[Ru_3(\eta^1\text{-}Ph_2Pquin)(CO)_{11}]$	38.58	s	$\eta^1\text{-}Ph_2Pquin$
(3)	$[Ru_3\{\mu\text{-}\eta^2\text{-}C(O)(C_6H_5)\}\{\mu_3\text{-}\eta^2\text{-}P(C_6H_5)(C_9H_6N)\}(CO)_9]$	48.05	s	$\mu_3\text{-}\eta^2\text{-}P(C_6H_5)(C_9H_6N)$
(4)	$[Ru_3(\eta^1\text{-}Ph_2Pquin)_2(CO)_{10}]$	35.94	s	$2\ \eta^1\text{-}Ph_2Pquin$
(5)	$[Ru_3(\mu\text{-}\eta^2\text{-}Ph_2Pquin)_2(CO)_8]$	9.06	s	$2\ \mu\text{-}\eta^2\text{-}Ph_2Pquin$
(6)	$[Ru_3\{\mu\text{-}\eta^2\text{-}C(O)(C_6H_5)\}\{\mu_3\text{-}\eta^2\text{-}P(C_6H_5)(C_9H_6N)\}\text{-}$	48.09	$d(J_{(P-P)}15.7\ Hz)$	$\mu_3\text{-}\eta^2\text{-}P(C_6H_5)(C_9H_6N)$
	$(\eta^1\text{-}Ph_2Pquin)(CO)_8]$	27.24	$d(J_{(P-P)}15.7\ Hz)$	Ph_2Pquin
(7)	$[Ru_3(\mu\text{-}H)\{\mu_3\text{-}\eta^2\text{-}P(C_6H_5)(C_9H_6N)\}(CO)_9]$	114.57	s	$\mu_3\text{-}\eta^2\text{-}P(C_6H_5)(C_9H_6N)$
(8)	$[PPN][Ru_3\{\mu_3\text{-}\eta^2\text{-}P(C_6H_5)(C_9H_6N)\}(CO)_9]$	136.64	s	$\mu_3\text{-}\eta^2\text{-}P(C_6H_5)(C_9H_6N)$
		20.04	s	$[PPN]^+$
(9)	$[Ru_3(\mu\text{-}H)\{\mu_3\text{-}\eta^2\text{-}P(C_6H_5)(C_9H_6N)\}(\eta^1\text{-}Ph_2Pquin)(CO)_8]$	129.47	$d(J_{(P-P)}13.4\ Hz)$	$\mu_3\text{-}\eta^2\text{-}P(C_6H_5)(C_9H_6N)$
		36.43	$d(J_{(P-P)}13.4\ Hz)$	Ph_2Pquin
(10)	$[Ru_3\{\mu\text{-}\eta^2\text{-}C(O)(C_6H_5)\}\{\mu_3\text{-}\eta^2\text{-}P(C_6H_5)(C_9H_6N)\}$	48.24	$d(J_{(P-P)}17.0\ Hz)$	$\mu_3\text{-}\eta^2\text{-}P(C_6H_5)(C_9H_6N)$
	$(PPh_2H)(CO)_8]$ *cis* isomer	16.88	$d(J_{(P-P)}17.0\ Hz)$	Ph_2PH

Table 3.18 (continued)

	COMPOUND	δ)ppm)	Multiplicity	Assignment
(10)	$[Ru_3\{\mu-\eta^2-C(O)(C_6H_5)\}\{\mu_3-\eta^2-P(C_6H_5)(C_9H_6N)\}-$	50.48	d($J_{(P-P)}$233.6 Hz)	$\mu_3-\eta^2-P(C_6H_5)(C_9H_6N)$
	$(PPh_2H)(CO)_8]$ trans isomer	24.10	d($J_{(P-P)}$23.64 Hz)	Ph_2PH
(11)	$[Ru_3\{\mu_3-\eta^2-P(C_6H_5)(C_9H_6N)\}(\mu-PPh_2)(\mu-CO)_2(CO)_6]$	369.0	d($J_{(P-P)}$15.1 Hz)	$\mu-Ph_2P$
		41.03	d($J_{(P-P)}$15.1 Hz)	$\mu_3-\eta^2-P(C_6H_5)(C_9H_6N)$
(12)	$[Ru_3\{\mu_3-\eta^2-P(C_6H_5)(C_9H_6N)\}(\mu-PPh_2)(CO)_9]$	122.43	d($J_{(P-P)}$19.1 Hz)	$\mu_3-\eta^2-P(C_6H_5)(C_9H_6N)$
		-14.99	d($J_{(P-P)}$19.1 Hz)	$\mu-Ph_2P$
(13)	$[Ru_3\{\mu_3-\eta^2-P(C_6H_5)(C_9H_6N)\}(\mu-PPh_2)_2(\mu-H)(CO)_6]$	247.72	d($J_{(P-P)}$13.9 Hz)	2 $\mu-Ph_2P$
	Isomer (13a)	68.83	d($J_{(P-P)}$13.9 Hz)	$\mu_3-\eta^2-P(C_6H_5)(C_9H_6N)$
(13)	Isomer (13b)	263.75	dd($J_{(P-P)}$131.4 Hz 13.0 Hz)	$\mu-Ph_2P$
		200.28	dd($J_{(P-P)}$131.4 Hz 73.2 Hz)	$\mu-Ph_2P$
		47.62	dd($J_{(P-P)}$13.0 Hz 73.2 Hz)	$\mu_3-\eta^2-P(C_6H_5)(C_9H_6N)$

s = singlet, d = doublet, dd = doublet of doublets, t = triplet.

TABLE 3.19

^{1}H NMR SPECTROSCOPIC DATA

(ppm, solvent is $CDCl_3$)

	COMPOUND	δ(ppm)	Multiplicity	Assignment
(7)	$[Ru_3(\mu\text{-H})\{\mu_3\text{-}\eta^2\text{-P}(C_6H_5)(C_9H_6N)\}(CO)_9]$	-15.31	d($J_{(P-H)}$24.6 Hz)	μ-H
(9)	$[Ru_3(\mu\text{-H})\{\mu_3\text{-}\eta^2\text{-P}(C_6H_5)(C_9H_6N)\}(\eta^1\text{-Ph}_2\text{Pquin})(CO)_8]$	14.50	d($J_{(P-H)}$15.0 Hz, 21.1 Hz)	μ-H
(13)	$[Ru_3\{\mu_3\text{-}\eta^2\text{-P}(C_6H_5)(C_9H_6N)\}(\mu\text{-PPh}_2)_2(\mu\text{-H})(CO)_6]$	-11.24	d($J_{(P-H)}$19.4 Hz, 37.5 Hz)	μ-H
	Isomer (13a)			
(13)	Isomer (13b)	-10.33	ddd($J_{(P-P)}$9.1 Hz, 18.1 Hz, 32.9 Hz)	μ-H

d = doublet, dd = doublet of doublets, t = triplet.

TABLE 3.20

^{13}C NMR SPECTROSCOPIC DATA

(ppm, solvent is $CDCl_3$)

	COMPOUND	δ(ppm)	Multiplicity	Assignment
(3)	$[Ru_3\{\mu-\eta^2-C(O)(C_6H_5)\}\{\mu_3-\eta^2-P(C_6H_5)(C_9H_6N)\}(CO)_9]$	303.69	$d(J_{(P-C)}5.7$ Hz)	$\mu-\eta^1-C(O)(C_6H_5)$
(6)	$\{Ru_3\{\mu-\eta^2-C(O)(C_6H_5)\}\{\mu_3-\eta^2-P(C_6H_5)(C_9H_6N)\}-$	302.56	$t(J_{(P-C)}3.9$ Hz)	$\mu-\eta^1-C(O)(C_6H_5)$
	$(\eta^1-Ph_2Pquin)(CO)_8]$			
(10)	$[Ru_3\{\mu-\eta^2-C(O)(C_6H_5)\}\{\mu_3-\eta^2-P(C_6H_5)(C_9H_6N)\}(PPh_2H)(CO)_8]$			
	cis isomer	301.60	$dd(J_{(P-C)}6.0$ Hz, 3.0 Hz)	$\mu-\eta^1-C(O)(C_6H_5)$
	trans isomer	302.13	$t(J_{(P-C)}5.5$ Hz, 5.6 Hz)	$\mu-\eta^1-C(O)(C_6H_5)$

d = doublet, dd = doublet of doublets, t = triplet.

TABLE 3.21

MICROANALYTICAL DATA FOR C, H AND N CONTENT (%)

COMPOUND		Molecular formula (mass)	ANALYSIS	%C	%H	%N
			Found / Required	%C	%H	%N
(3)	$[Ru_3\{\mu\text{-}\eta^2\text{-}C(O)(C_6H_5)\}\{\mu_3\text{-}\eta^2\text{-}P(C_6H_5)(C_9H_6N)\}(CO)_9]$	$C_{31}H_{16}NO_{10}Ru_3$ (896.66)	Found	41.13	1.96	1.45
			Required	41.53	1.80	1.56
(4)	$[Ru_3(\eta^1\text{-}Ph_2Pquin)_2(CO)_{10}]$	$C_{52}H_{32}N_2O_{10}P_2Ru_3(1209.99)$		51.25	2.62	2.43
				51.62	2.67	2.31
(5)	$[Ru_3\{\mu\text{-}\eta^2\text{-}Ph_2Pquin)_2(CO)_8]$	$C_{50}H_{32}N_2O_{80}P_2Ru_3(1153.97)$		52.63	2.57	2.42
				52.05	2.79	2.48
(6)	$[Ru_3\{\mu\text{-}\eta^2\text{-}C(O)(C_6H_5)\}\{\mu_3\text{-}\eta^2\text{-}P(C_6H_5)(C_9H_6N)\}(\eta^1\text{-}$ $Ph_2Pquin)(CO)_8]$	$C_{51}H_{32}N_2O_9P_2Ru_3(1181.98)$		51.47	2.70	2.34
				51.82	2.73	2.37
(7)	$[Ru_3(\mu\text{-}H)\{\mu_3\text{-}\eta^2\text{-}P(C_6H_5)(C_9H_6N)\}(CO)_9]$	$C_{24}H_{12}NO_9PRu_3(792.54)$		35.97	1.78	1.78
				36.37	1.53	1.78
(8)	$[PPN][Ru_3\{\mu_3\text{-}\eta^2\text{-}P(C_6H_5)(C_9H_6N)\}(CO)_9]$	$C_{60}H_{41}N_2O_9P_3Ru_3(1330.12)$		54.45	3.13	2.00
				54.18	3.11	2.11
(9)	$[Ru_3(\mu\text{-}H)\{\mu_3\text{-}\eta^2\text{-}P(C_6H_5)(C_9H_6N)\}(\eta^1\text{-}Ph_2Pquin)(CO)_8]$	$C_{49}H_{28}N_2O_8P_2Ru_3(1077.87)$		49.11	2.88	2.43
				49.03	2.62	2.60
(10)	$[Ru_3\{\mu\text{-}\eta^2\text{-}C(O)(C_6H_5)\}\{\mu_3\text{-}\eta^2\text{-}P(C_6H_5)(C_9H_6N)\}(PPh_2H)(CO)_8]$	$C_{42}H_{27}NO_9P_2Ru_3(1054.86)$		47.56	3.14	1.13
				47.82	2.58	1.32
(11)	$[Ru_3\{\mu_3\text{-}\eta^2\text{-}P(C_6H_5)(C_9H_6N)\}(\mu\text{-}PPh_2)(\mu\text{-}CO)_2(CO)_6]$	$C_{35}H_{21}NO_8P_2Ru_3(948.73)$		44.40	2.21	1.64
				44.31	2.23	1.48
(13)	$[Ru_3\{\mu_3\text{-}\eta^2\text{-}P(C_6H_5)(C_9H_6N)\}(\mu\text{-}PPh_2)_2(\mu\text{-}H)(CO)_6]$ Isomer (13a)	$C_{42}H_{32}NO_6P_3Ru_3(1078.89)$		49.95	3.16	1.46
				50.10	2.99	1.30
(13)	Isomer (13b)	$C_{42}H_{32}NO_6P_3Ru_3(1078.89)$		50.42	3.10	1.47
				50.10	2.99	1.30

APPENDIX I

GENERAL EXPERIMENTAL

(a) ANALYSES

The infrared spectra were recorded on a Shimadzu FTIR-4300 spectrometer. The $^{31}P\{^1H\}$ NMR spectra were recorded on a Varian FT-80A spectrometer. The ^1H and $^{13}C\{^1H\}$ NMR spectra were recorded on a Varian Gemini-200 spectrometer. The elemental analyses were carried out in the micro-analytical laboratory, University of Natal, Pietermaritzburg, using Perkin-Elmer 240B and Perkin-Elmer 2400 elemental analyzers and at the Council for Scientific and Industrial Research in Pretoria.

(b) TECHNIQUES

All reactions were carried out under a dry nitrogen or a dry argon (ligand synthesis only) atmosphere using standard Schlenk techniques.

i) Solvents

The solvents were freshly dried and distilled according to standard procedures except for petroleum ether (40-60) and hexane which were used in Analar and CP Grade purity respectively.

ii) Starting Materials

Ruthenium dodecacarbonyl (Strem) was purified by extracting it into dichloromethane and filtering the extract through neutral aluminum oxide, followed by crystallization from the dichloromethane at -30°C. Trimethylamine-N-oxide (Aldrich) was recrystallized from acetonitrile.

The sodium benzophenoneketyl catalyst was prepared according to published procedure.[7] Diphenylphosphine (Strem), bis(triphenylphosphine)imminium borohydride ([PPN][BH$_4$], Strem) and trifluoroacetic acid (Aldrich) were used without further purification. The Ph$_2$Pquin ligand was prepared as described in Chapter Two. All the TLC plates used were 1 mm thick silica gel (Kieselgel 60, Merck) on glass.

APPENDIX II
CRYSTAL STRUCTURE DETERMINATIONS

a) Data Collection

The intensities of the reflections were measured at 22°C with an Enraf-Nonius CAD-4 diffractometer using graphite monochromated Mo-K_α radiation.

Cell constants were obtained by fitting the setting angles of 25 high-order reflections. Three standard reflections were measured every hour to check on any possible decomposition of the crystal. An ω-2θ scan with a variable speed up to a maximum of 5.49° min^{-1} was used. The ω-angle changed as $a_\omega + b_\omega \tan \theta$ (°), the horizontal aperture as $a_h + b_h \tan \theta$ (mm), but was limited to the range 1.3-5.9 mm. The vertical slit was fixed at 4 mm. Optimal values of a_ω, b_ω, a_h and b_h were determined for each crystal by a critical evaluation of peak shape for several reflections with different values of θ using the program OTPLOT[94]. Data were corrected for Lorentz and polarisation effects, and for absorption by the psi-scan (empirical) method.[95]

b) <u>Structural solution and refinement</u>

Direct methods were used to solve the phase problem. Once a suitable phasing model was found successive applications of Fourier and difference Fourier techniques allowed the location of the remaining non-hydrogen atoms. Hydrogen atoms were not located. Weighted full-matrix least-squares methods were always used to refine the structure; the weighting scheme was chosen so as to find the smallest variation of the mean value of $\omega(F_oO-F_c)^{96}$ as a function of the magnitude of F_o. Scattering factor data were taken from reference 96. For all these calculations, the programs SHELX-76[97] and SHELX-86[98] were employed. Plotting of the structure was performed using the program ORTEP-II[99] while the tabulation of interatomic distances interatomic angles, fractional co-ordinates and thermal parameters was achieved using the program TABLES.[100]

REFERENCES

1. M.A. Bennett, M.I. Bruce and T.W. Matheson, in E.W. Abel, F.G.A. Stone and G.W. Wilkinson (Eds), "Comprehensive Organo-metallic Chemistry", Pergamon, Oxford (1982), Ch. 32.

2. G.J. Bezems, P.H. Rieger and S.J. Vicco, *J. Chem. Soc., Chem. Commun.*, (1981), **6**, 265; M. Arwegoda, P.H. Rieger, B.H. Robinson, J. Simpson and S.J. Visco, *J. Am. Chem. Soc.*, (1982), **104(21)**, 5633.

3. M.I. Bruce, D.C. Kehoe, J.G. Matisons, B.K.Nicholson, P.H. Reiger and M.L. Williams, *J. Chem. Soc., Chem. Commun.*, (1982), 442.

4. M.I. Bruce, G. Shaw and F.G.A. Stone, *J. Chem. Soc., Dalton Trans.*, (1972), 2094.

5. M.I. Bruce, C.W. Gibbs and F.G.A. Stone, *Z. Naturforsch., B,* (1968), **23**, 1543.

6. G. Lavigne and J.-J. Bonnet, *Inorg. Chem.*, (1981), **20**, 2713.

7. M.I. Bruce, J.G. Matisons and B.K. Nicholson, *J. Organomet. Chem.*, (1983), **247**, 321.

8. M.O. Albers and N.J. Coville, *Coord. Chem. Rev.*, (1984), **53**, 227.

9. J.W. Herschberger and J.K. Kochi, *J. Chem. Soc., Chem. Commun.*, (1982), 212.

10. M. Arwegoda, B.H. Robinson and J. Simpson, *J. Am. Chem. Soc.*, (1983), **105(7)**, 1893.

11. R.W. Alder, *J. Chem. Soc., Chem. Commun.*, (1980), 1184.

12. A.M. Bond, P.A. Dawson, B.H. Robinson and J. Simpson, *Inorg. Chem.*, (1977), **16**, 2199.

13. C.E. Kampe, H.D. Kaesz, *Inorg. Chem.*, (1984), **23**, 1390.

14. G. Lavigne and H.D. Kaesz, *J. Am. Chem. Soc.*, (1984), **106**, 4647.

15. R.E.Stevens and W.L. Gladfelter, *Inorg. Chem.*, (1983), **22**, 2034.

16. D.J. Darensbourg, M. Pala and J. Waller, *Organometallics*, (1983), **2**, 1285.

17. A. Mayr, V.C. Lin, N.M Boag and H.D. Kaesz, *Inorg. Chem.*, (1982), **21**, 1704.

18. C. Jensen, C.M. Knobler and H.D. Kaesz, *J. Am. Chem. Soc.*, (1984), **106(20)**, 5926.

19. M. Anstock, D. Taube and P.C. Ford, personal communication.

20. B.F.G. Johnson, J. Lewis and D.A. Pippard, *J. Chem. Soc., Dalton*, (1982), 407.

21. G.A. Foulds, B.F.G. Johnson and J. Lewis, *J. Organomet. Chem.*, (1985), **296**, 147.

22. G.A. Foulds, B.F.G. Johnson and J. Lewis, *J. Organomet. Chem.*, (1985), **294**, 123.

23. N. Lugan, G. Lavigne and J.-J. Bonnet, *Inorg. Chem.*, (1987), **26**, 585.

24. (a) F.A. Cotton, B.E. Hanson and J.D. Jamerson, *J. Am. Chem. Soc.*, (1977), **998**, 6588.

    (b) C.C. Yin and A.J. Deeming, *J. Chem. Soc., Dalton Trans.*, (1975), 2091.

    (c) A. Eisenstadt, C.M. Giadomenico, M.F. Frederick and R.M. Laine, *Organometallics*, (1985), **4**, 2033.

25. C. Bergounhou, J.-J. Bonnet, P. Fompeyrine, G. Lavigne, N. Lugan and F. Mansilla, *Organometallics*, (1986), 5, 60.

26. P.E. Garrou, *Chem. Rev.*, (1985), 85, 171.

27. M.N. Harding, B.S. Nicholls and A.K. Smith, *J. Chem. Soc., Dalton Trans.*, (1983), 1479.

28. B. Delavaux, B. Chaudert, F. Dahan and R. Poilblanc, *Organometallics*, (1985), **4**, 935.

29. A.R. Siedle, R.A. Newmark and W.B. Gleason, *J. Am. Chem. Soc.*, (1986), **108**, 767.

30. G. Lavigne, N. Lugan and J.-J. Bonnet, *Organometallics.* (1982), **1**, 1040.

31. (a) J.R. Blickensderfer and H.D. Kaesz. *J. Am. Chem. Soc.*, (1975), **97**, 2681.

    (b) J.R. Blickensderfer, C.B. Knobler and H.D. Kaesz, *J. Am. Chem. Soc.*, (1975), **97**, 2686.

32. G.R. Doel, N.D. Feasey, S.A.R. Knox, A.G. Orpen and J. Webster, *J. Chem. Soc., Chem. Commun.*, (1986), 542.

33. A. Mayr, Y.C. Lin, N.M. Boag, C.E. Kampe, C.B. Knobler and H.D. Kaesz, *Inorg. Chem.*, (1984), **23**, 4640.

34. C.E. Kampe and H.D. Kaesz, *Inorg. Chem.*, (1984), **23**, 4646.

35. N. Lugan, G. Lavigne, J.-J. Bonnet, R. Réau, D. Neibecker and I. Ikatchenko, *J. Am. Chem. Soc.*, (1988), **110**, 5369.

36. G. Lavigne and H.D. Kaesz, "Metal Clusters in Catalysis", H. Knözinger, B.C. Gates and L. Guczi, Eds., Elsevier: New York, (1986), Chapter 4, pp 43-88.

37. (a) J.C. Jeffery and L.G. Lawrence-Smith, *J. Chem. Soc., Chem. Commun.*, (1985), 275.

    (b) J.C. Jeffery and L.G. Lawrence-Smith, *J. Chem. Soc., Chem. Commun.*, (1986), 17.

    (c) K. Kwek, N.J. Taylor and A.J. Carty, *J. Am. Chem. Soc.*, (1984), **106**, 4636.

38. (a) L.M. Bavaro, P. Montagero and J.B. Keister, *J. Am. Chem. Soc.*, (1983), **105**, 4977.

    (b) D.M. Dalton, D.J. Burnett, T.P. Duggan, J.B. Keister, P.T. Malik, S.P. Modi, M.R. Shaffer and S.A. Smesko, *Organometallics*, (1985), **4**, 1854.

39. B.F.G. Johnson, J. Lewis and T.I. Odiaka, *J. Organomet. Chem.*, (1985), **294**, 75.

40. A.J. Carty, S.A. McLaughlin and N.J. Taylor *J. Organomet. Chem.,* (1981), **204**, C27.

41. G. Huttner, J. Schneider, H.D. Müller, G. Mohr, J. Von Seyerl and L. Wohlfahrt, *Angew. Chem., Int. Ed. Engl.,* (1979), **18**, 76.

42. J. Schneider, M. Minelli and G. Huttner, *J. Organomet. Chem.,* (1985), **294**, 75.

43. K. Knol, G. Huttner, L. Solnai, I. Jibril and M. Wasiucionek, *J. Organomet. Chem.,* (1985), **294**, 91.

44. R.P. Planalp and H. Vahrenkamp, *Organometallics,* (1987), **6**, 492.

45. G. Huttner and K. Knoll, *Angew. Chem., Int. Ed. Engl.,* (1987), **26**, 743.

46. A.L. Pedro, J.A. Cabeza and V. Riera, *J. Chem. Soc., Dalton Trans.,* (1990), **7**, 2201.

47. (a) M.I. Bruce, "Comprehensive Organometallic Chemistry,"
    G. Wilkinson, F.G.A. Stone and E.W. Abel, Pergamon, Oxford (1982), **4**, 843.

    (b) M.I. Bruce, *Coord, Chem. Rev.,* (1987), **76**, 1.

48. L.H. Staal, L.H. Polm, R.W. Balk, G. Van Koten, K. Vrieze and A.M.F. Brouwers, *Inorg. Chem.,* (1972), **76**, 1

49. F. Calderazzo, C. Floriani, R. Henzi and F. L'Eplattenier, *J. Chem. Soc. A,* (1969), 1378.

50. (a) J.A. Cabeza, C. Landázuri, L.A. Cro, A. Tiripicchio and
    M. Tiripicchio-Camellini, *J. Organomet. Chem.,* (1987), **322**, C16.

    (b) J.A. Cabeza, C. Landázuri, L.A. Cro, D. Bellett, A. Tiripicchio and M. Tiripicchio-Camellini, *J. Chem. Soc., Dalton Trans.,* (1989), 1093.

    (c) F. Neumann and G. Süss-Fink, *J. Organomet. Chem.,* (1989), **367**, 175.

51. S.F. Coloson, S.D. Robinson, M. Motevalli and M.D. Hursthouse, *Polyhedron*, (1988), 7, 1919.

52. (a) D.P. Maddern, A.J. Carty and T. Birchall, *Inorg. Chem.*, (1972), 11, 1453.

     (b) J.A. Cabeza, V. Rlera, M.A. Pellinghelli and A. Tiripicchio, *J. Organomet. Chem.*, (1989), 376, C23.

53. M.I. Bruce, M.G. Humphrey, M.R. Snow, E.R.T. Tiekink and R.C. Wallis, *J. Organomet. Chem.*, (1986), 314, 311.

54. A Eisenstadt, C.M. Giandomenico, M.F. Frederick and R.M. Laine, *Organometallics*, (1985), 4, 311.

55. R.H. Fish, T.-J. Kim, J.L. Stewart, J.H. Bushweller, R.K. Rosen and J.W. Dupon, *Organometallics*, (1986), 5, 2193.

56. G.A. Foulds, B.F.G. Johnson and J. Lewis, *J. Organomet. Chem.*, (1985), 294, 123.

57. (a) J.A. Cabeza, L.A. Oro, A. Tiripicchio and M. Tiripicchio-Camellini, *J. Chem. Soc., Dalton Trans.*, (1988), 1437.

     (b) M.A. Pellinghelli, A. Tiripicchio, J.A. Cabeza and L.A. Oro, *J. Chem. Soc., Dalton Trans.*, (1990), 1509.

58. F.A. Cotton and D.J. Jamerson, *J. Am. Chem. Soc.*, (1976), 98, 5396.

59. T.V. Vanäläinen, J. Pursiainen and T.A. Pakkanen, *J. Chem. Soc., Chem. Commun.*, (1985), 1348.

60. P.L. Andrea, J.A. Cabeza, V. Riera, C. Bois and Y. Jeannin, *J. Organomet. Chem.*, (1990), 384, C25.

61. P.L. Andrea, J.A. Cabeza, V. Riera, C. Bois and Y. Jeannin, *J. Chem. Soc., Dalton Trans.*, (1990), 11, 3347.

62. P.L. Andrea, J.A. Cabeza and V. Riera, *J. Organomet. Chem.*, (1990), 393, C30.

63. P.L. Andrea, J.A. Cabeza, J.M. Fernández-Colinas and V. Riera, *J. Chem. Soc., Dalton Trans.*, (1990), 9, 2927.

64. N. Lugan, F. Laurent, G. Lavigne, T.P. Newcombe, E.W. Liimatta and J.-J. Bonnet, *J. Am. Chem. Soc.*, (1990), **112**, 8607.

65. A.J. Deeming, K.I. Hardcastle and M. Karim, *Inorg. Chem.*, (1992), 31, 4792.

66. P.E. Fanwick, J. Qi and R.A. Walton, *Inorg. Chem.*, (1990), 29, 3787.

67. R.B. Hannan Jr, J.H. Lieblich and A.G.Renfrew, *J. Am. Chem. Soc.*, (1949), 71, 3733.

68. J.A. Van Doorn and P.W.N.M. Van Leeuwen, *J. Organomet. Chem.*, (1981), 222, 299.

69. A.M. Saleem and H.A. Modali, *Inorg. Chim. Acta*, (1990), **174**, 223.

70. F.G. Mann and J. Watson, *J. Organomet. Chem.*, (1948), **13**, 502.

71. J. Overhoff and W. Proost, *Recl. Trav. Chim. Pays-Bas*, (1938), 57, 179.

72. (a) W.C. Davies and F.G. Mann *J. Chem. Soc.*, (1944), 276.

    (b) E. Plazek and R. Tyka, *Zesz. Nauk. Politech. Wroclaw Chem.*, **4** (1957), 79; *Chem. Abstr.*, (1958), 52, 20156c.

    (c) G.E. Griffin and W.A. Thomas, *J. Chem. Soc. B*, (1970), 477.

    (d) H.G. Ang, W.E. Kow and K.F. Mok, *Inorg. Nucl. Chem.*, (1972), 829.

    (e) H.J. Jakobsen, *J. Mol. Spectrosc.*, (1970), 34, 245.

    (f) E. Larson, G.N. La Mar, B.E. Wagner, J.E. Parks and R.H. Holm, *Inorg. Chem.*, (1972), 11, 2652.

    (g) J.E. Parks, B.E. Wagner and R.H. Holm *J. Organomet. Chem.*, (1973), 56, 53.

    (h) J.E. Parks, B.E. Wagner and R.H. Holm *J. Am. Chem. Soc.*, (1970), 92, 3500.

73. H. Schmidbaur and Y. Inoguchi, *Z. Naturforsch. B: Anorg. Chem., Org. Chem.*, (1980), 35B(11), 1329.

74. P.G.R. Newkome and D.C. Hager, *J. Organomet. Chem.*, (1978), **43**, No 5, 947.

75. (a) A. Burger, J.B. Clements, N.D. Dawson and R.B. Henderson, *J. Organomet. Chem.*, (1965), **20**, 1383.

     (b) D. Redmore, *Chem. Rev.*, (1971), **71**, 315.

76. D. Redmore, *Top. Phosphorus Chem.*, (1976), **8**, 515.

77. R.G. Shepherd and J.L. Fedrick, *Adv. Heterocycl. Chem.*, (1965), **4**, 942.

78. A.M. Aguiar and Z.G. Archibald, *Tetrahedron Lett.*, (1966), 5541.

79. K. Issleib and A. Tzschach, *Chem. Ber.*, (1959), **92**, 1118.

80. A.M. Aguiar, J. Beisler and A. Mills. *J. Organomet. Chem.*, (1962), **27**, 1001.

81. A.M. Aguiar, H.G. Greenberg and K.E. Rubenstein, *ibid*, (1963), **28**, 2091.

82. V. Hewertson, R.A. Shaw and B.C. Smith, *J. Chem. Soc.*, (1964), 1020.

83. K. Issleib and L. Brüsehaber, *Z. Naturforsch. B*, (1965), **206**, 181.

84. A. Maisonnet, J.P. Farr, M.M. Olmstead, C.T. Hunt and A.L. Balch, *Inorg. Chem.*, (1982), **21**, 3961.

85. G.W. Luther and G. Beyerle, *Inorganic Synthesis*, (1977), **17**, 187.

86. W.J. Mahn, "Academic Laboratory Chemical Hazards Guidebook," 203.

87. M.M. Olmstead, A. Maisonnet, J.P. Farr and A.L. Balch, *Inorg. Chem.*, (1981), 20, 4060.

88. A.J. Carty, S.A. McLaughlin and D. Nucciarone, "Phosphorus-31 NMR Spectroscopy in Stereochemical Analysis," J.G. Verkade and L.D.Quin, Eds. VCH Publishers Inc., Deerfield Beach, Florida, (1987), Chapter 16, pp. 559-619.

89. Structure Determination Package, Program Plane, B.A. Frenz and Associates Inc., College Station, Texas 77840 and Enraf-Nonius, Holland, (1985).

90. A.S. Pregosin and R.W. Kunz, "^{31}P and ^{13}C NMR of Transition Metal Phosphine Complexes," Springer-Verlag, Berlin, (1979).

91. J.S. Field, R.J. Haines and F. Mulla, *J. Organomet. Chem.*, (1992), **439**, C56.

92. G. Huttner, A. Frank and G. Mohr, *Z. Naturforsch., Teil B*, (1976), **31**, 1161; G. Huttner, G. Mohr and A. Frank, *Angew. Chem., Int. Ed. Engl.*, (1976), **15**, 682; G. Huttner, G. Mohr, P. Friedrich and H.-G. Schmid, *J. Organomet. Chem.*, (1978), **160**, 59; G. Huttner, J. Schneider, H.-D. Muller, G. Mohr, J. von Seyerl and L. Wohlfahrt, *Angew. Chem., Int. Ed. Engl.*, (1979), **18**, 76.

93. J.S. Field, R.J. Haines and D.N. Smit, *J. Organomet. Chem.*, (1982), **240**, C23.

94. Omega-Theta Plot, Enraf-Nonius Diffractometer Control Program, (1988).

95. A.C.T. North, D.C. Philips and F.S. Mathews, *Acta Crystallogr., Sect. A.*, (1968), **24**, 351.

96. "International Tables for X-ray crystallography", Kynoch Press, Birmingham, Vol 4 (1974), pp 99, 149.

97. G.M. Sheldrick, SHELX-76, Program for Crystal Structure Determination, University of Cambridge, (1976).

98. G.M. Sheldrick, SHELX-86, Program for Crystal Structure Determination, University of Göttingen, (1986).

99. C.K. Johnson, ORTEP-II, A Fortran Thermal-Ellipsoid Plot Program for Crystal Structure Illustrations, Oak Ridge National Laboratory, Tennessee, (1976).

100. D.C. Liles, TABLES, Program for Tabulation of Crystallographic Data, Council for Scientific and Industrial Research (Pretoria), (1988).